The Impact of London Dispersion Interactions in Solution

- Bring [a Molecular] Balance to the [LD] Force! -

Inaugural-Dissertation
zur Erlangung des Doktorgrades
der Naturwissenschaftlichen Fachbereiche
im Fachgebiet Organische Chemie (Fachbereich 08)
an der Justus-Liebig-Universität Gießen

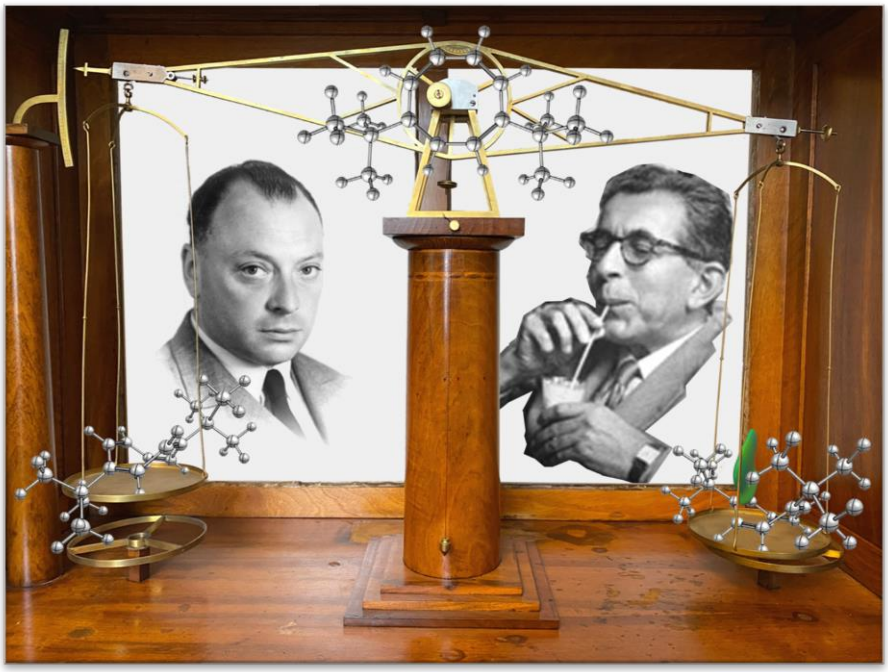

vorgelegt von Jan Michael Schümann, M.Sc.
aus Staufenberg-Daubringen

Angefertigt am
Institut für Organische Chemie
Justus-Liebig-Universität Gießen
im Zeitraum von Juli 2015- März 2021

Betreuer: Prof. Dr. Peter R. Schreiner, Ph.D.

...

Da steh' ich nun, ich armer Tor,

Und bin so klug als wie zuvor!

Heiße "Bachelor", heiße "Master" gar,

Und ziehe schon an die "sechs" Jahr'

Herauf, herab und quer und krumm

Meine "Studenten" an der Nase herum –

Und sehe, daß wir nichts wissen können!

...

Bilde mir nicht ein, was Rechts zu wissen,

Bilde mir nicht ein, ich könnte was lehren,

Die Menschen zu bessern und zu bekehren.

Auch hab' ich weder Gut noch Geld,

Noch Ehr' und Herrlichkeit der Welt;

Es möchte kein Hund so länger leben!

Drum hab' ich mich der "Chemie" ergeben,

Ob mir durch Geistes Kraft und Mund

Nicht manch Geheimnis würde kund;

Dass ich nicht mehr mit saurem Schweiß

Zu sagen brauche, was ich nicht weiß;

Dass ich erkenne, was die Welt

Im Innersten zusammenhält,

Schau' alle Wirkenskraft und Samen,

Und tu' nicht mehr in Worten kramen.

...

- Auszug aus Johann Wolfgang von Goethes Faust,
  frei abgewandelt von Jan M. Schümann

Im Gedenken an Lieselotte "Lotti" Schäfer

Sowie Heinz und Liselotte "Lisi" Dreja

Selbstständigkeitserklärung

Hiermit versichere ich, die vorgelegte Thesis selbstständig und ohne unerlaubte fremde Hilfe und nur mit den Hilfen angefertigt zu haben, die ich in der Thesis angegeben habe. Alle Textstellen, die wörtlich oder sinngemäß aus veröffentlichten Schriften entnommen sind, und alle Angaben, die auf mündlichen Auskünften beruhen, sind als solche kenntlich gemacht. Bei den von mir durchgeführten und in der Thesis erwähnten Untersuchungen habe ich die Grundsätze guter wissenschaftlicher Praxis, wie sie in der ‚Satzung der Justus-Liebig-Universität zur Sicherung guter wissenschaftlicher Praxis' niedergelegt sind, eingehalten. Gemäß § 25 Abs. 6 der Allgemeinen Bestimmungen für modularisierte Studiengänge dulde ich eine Überprüfung der Thesis mittels Anti-Plagiatssoftware.

Ort, Datum Unterschrift

Dekan: Prof. Dr. Holger Zorn

Prodekan: Prof. Dr. Volker Wissemann

Studiendekan: Prof. Dr. Reinhard Dammann

Erstgutachter: Prof. Dr. Peter R. Schreiner, PhD

Zweitgutachter: Prof. Dr. Hermann A. Wegner

Eingereicht: 20. Dezember 2024

Zusammenfassung

Der Beitrag der London Dispersion[1] (LD) zum intermolekularen Faltverhalten von Molekularwaagen auf Cyclooctatetraen(COT)-Basis wurde in einer Vielzahl an Lösungsmitteln untersucht. Im Rahmen dieser Untersuchung wurde ein wohl definiertes System mit einen intramolekularen Abstand von 2,44 Å zwischen zwei *tert*-butyl Gruppen synthetisiert. Diese Molekularwaage wurde anschließend in diversen Lösungsmitteln mit aufsteigender Solvent Polarisierbarkeit (SP) auf dessen Faltverhalten hinsichtlich Londonscher dispersiver Wechselwirkungen untersucht. Es konnte aufgezeigt werden, dass der freie enthalpische Beitrag zu der Isomerisierungsreaktion in jedem Lösungsmittel einem annähernd gleichen Wert folgt. Die freie Gibbs Energie kann hierbei direkt durch das Verhältnis von 1,4- zu 1,6-Isomeren bestimmt werden. Es wurde ersichtlich, dass die unterschiedlich starken entropischen Einflüsse jedes Lösungsmittels für die stärker variierenden Gibbs Enthalpien ausschlaggebend ist. Die Antwort auf die von Yang *et al.* gestellte Frage "How much does LD contribute to molecular recognition in solution?"[2] lautet daher: "Es kommt darauf an!"[3]. Das niedrigste Verhältnis von 1,4- und 1,6-COT konnte in rein aliphatischen Lösungsmitteln festgestellt werden, dies kann auf einen kompensierenden Effekt von dispersiven Wechselwirkungen zwischen dem Lösungsmittel und der Waage hindeuten, wohin polare Lösungsmittel wie DMSO und Chloroform deutlich eine Bevorzugung des 1,6-Isomers zeigen. Zusätzliche computerchemische "Energy Decomposition Analysis" (EDAs) haben gezeigt, dass LD definitiv die vorherrschende Kraft ist, welche für die Faltung verantwortlich ist. Das Konzept wurde durch die Synthese von Adamantyl und Diamantyl-Derivaten erweitert. Die molekularen Waagen haben weiterhin den für Dispersion attraktiven Abstand von 2,4 Å, jedoch werden die Polarisierbarkeiten und die Ausdehnung der Solvent Accessible Surface (SAS) der Substituenten signifikant größer, welches mehr Interaktion mit dem umgebenden Lösungsmittel zulassen müsste. Als Lösungsmittel wurden daher passend zum Wachstum der Derivate längerkettige aliphatische Kohlenwasserstoffe (*n*-Hexan, *n*-Octan und *n*-Dodecan) gewählt. In Zusammenarbeit mit dem Max-Planck Institut für Kohlenforschung konnten computerchemische Rechnungen auf höchstem Niveau mit sowohl expliziten also auch impliziten Lösungsmittel Modellen durchgeführt werden. Sowohl die computerchemischen als auch die experimentellen Daten zeigen, dass eine Art des Anschmiegens durch das Lösungsmittel stattfindet und, dass durch die „rigiden Rotatoren" der Adamantanderivate ein essentieller Beitrag zur Entropie geleistet wird. In jeder bisherigen Studie war stets das gefaltete Derivat das Bevorzugte.

Abstract

The contribution of London Dispersion (LD) to the intramolecular folding behavior of a cyclooctatetraene (COT)-based molecular balances in a variety of solvents was investigated. As part of this investigation, a well-defined system, represented by a *tert*-butyl dimer with an intramolecular distance of 2.44 Å was synthesized. The folding behavior of this molecular balance was then investigated in various solvents with increasing solvent polarizability (SP) to examine the contribution of London interactions. We showed that the free enthalpy of the isomerization reaction in each solvent follows approximately the same value. Gibbs free energy can be readily measured by determination of the ratio of 1,4- to 1,6-isomers. It was found that the entropy in each solvent system is responsible for the diminishing effect on ΔG values. The answer to the question of Yang *et al.* "How much does LD contribute to molecular recognition in solution?" is that "It depends!" The lowest ratio of 1,4- and 1,6-isomers was found in purely aliphatic solvents, this may indicate a compensating effect of dispersion interactions between the solvent and the balance. DMSO and chloroform clearly showed a preference for the 1,6-isomer. However, it became clear through additional energy decomposition analyzes (EDAs) that LD is the predominant force responsible for folding. The extension of the concept was investigated by the synthesis of adamantyl and diamantyl COT derivatives. The molecular balances still have an attractive distance of 2.4 Å for dispersion, but the polarizabilities and the expansion regarding the solvent accessible surface (SAS) of the substituents become significantly larger, which allows more interaction with the surrounding solvent. Longer aliphatic chain hydrocarbons (*n*-hexane, *n*-octane and *n*-dodecane) were therefore chosen as solvents to suit the growth of the derivatives. In collaboration with the Max-Planck Institute for Coal Research, computations at the highest level were carried out using implicit and explicit solvent models to determine the influence of the solvents on the folding behavior. The computational and experimental results lead to the conclusion that an adhesion occurs through the solvent and that the "rigid rotors" of the diamondoid derivatives make an exclusive contribution to the entropy. In every study, the folded derivative is always preferred.

Danksagung

An dieser Stelle möchte ich allen Menschen danken, welche mich auf meinem Weg zur Promotion begleitet und unterstützt haben. Besonderer Dank gilt:

Prof. Dr. Peter R. Schreiner, Ph.D., der mir nicht nur die Möglichkeit der Promotion eröffnete, sondern mir auch erlaubte an der Leitung eines Schwerpunkt Programms der DFG mitzuwirken und in der Funktion als "Scientifc Secretary" menschlich sowie wissenschaftlich zu wachsen.

Prof. Giovanni Bistoni und seiner Gruppe aus Mülheim für die hervorragende Unterstützung bei der computerchemischen Analyse der Adamantan und Diamantan COT Derivate.

Dr. J. Philip Wagner für die Worte, "Jan - mach die Dispersion nicht kaputt.", welche nur einen "leichten" Druck ausübten.

Dr. André K. Eckhardt für sein Interesse an jeglicher Form von Chemie und den daraus resultierenden Diskussionen. Vor allem aber für die gute Zeit während der zahlreichen Konferenzen zu Physikalisch Organischen Themen.

Dr. Heike Hausmann für ihre Geduld und die Durchführung unzähliger temperaturabhängiger NMR-Experimente, um das Cyclooctatetraen Verhalten zu verstehen und reproduzierbare Messreihen zu generieren.

Dr. Dennis Gerbig für die Wartung der Rechencluster und Ratschläge hinsichtlich des Computational Parts der Dissertation. Sowie Dr. Henrik Quanz für die Unterstützung bei der Implementierung von XTb, Crest, Enso sowie der Durchführung der SAPT Analysen des *t*Bu Dimers.

Michaela Richter, Doris Verch und Dr. Jörg Neudert für ihre organisatorische und administrative Unterstützung.

Meinen Bachelorstudenten im Bereich der Organokatalyse Bianca Helm und Dr. Lars Rummel und der wissenschaftlichen Hilfskraft Mitja Lubotta für die Synthese und den Einbau der Adamantyl-Alanin Aminosäure in den CEM Cat und die Erweiterung des Substratesscopes der kinetischen Racematspaltung von 1,2-*trans*-Diolen.

Besonderer Dank an dieser Stelle gilt Dr. Lars Rummel der in seiner Zeit als Student nicht nur ein guter Freund geworden ist, sondern auch meine Nachfolge als wissenschaftlicher Sekretär des SPP1807 übernahm und gemeinsam mit Dr. Henrik F. König nicht nur meine angefangenen Projekte vollendete, sondern auch die Konzepte um mehrere Systeme und Reaktionen erweiterte. Die wissenschaftlichen Diskussionen mit Herrn Dr. Rummel und Herrn Dr. König werden mir in Zukunft sehr fehlen.

Meinem Liebig College Studenten Shuhei Maeda, für die Durchführung der Literatursynthese von 1,4-*di*-methyl-Cyclooctatetraen innerhalb seines drei-monatigen Aufenthaltes in Deutschland.

Meinem ehemaligen Mitbewohner und Abzugsnachbarn Dr. Dominik Niedek für wissenschaftliche und zwischenmenschliche Diskussionen in guten sowie schlechten Zeiten der Promotionszeit.

Meinem Labor B205 in seiner originalen Erstbesetzung mit Dr. Jan-Philipp Berndt, Dr. Dominik Niedek und Dr. Christian Eschmann für gute Musik, Kaffee und Diskussionen, den "Catwalk" und funktionierende Laborabläufe.

Meiner "Kochen & Trinken" Gruppe bestehend aus Jean-Marie Pohl und Dr. Christian Eschmann als Ausgleich neben dem "Uni-Wahnsinn", für tiefgründige Gespräche, leckeres Essen und Wein.

Der PRS Darts Runde bestehend aus Dr. Markus Schauermann, Dr. Finn Marian Wilming, Dr. Lukas Ochmann, Dr. Frederick Ricardo Erb, Dr. Dominik Niedek, Dr. Jan-Philipp Berndt, Alexander Seitz und Dr. Christian Eschmann.

Der AG Wegner in Form von Dr. Sebastian Ahles, Dr. Andreas Hans Heindl, Dr. Marcel André Strauß, Sebastian Beeck, Dr. Anne Kunz und Dr. Julia Ruhl für schöne Kaffeepausen und synthetischem Rat und den Diskussionen Rund um die Dispersion.

Der permanenten Lunch Gruppe bestehend aus Dr. Lijuan Song, Dr. Henrik Quanz, Dr. Felix Keul, Dr. Lars Rummel und den zahllosen "visiting Liebig College students" für einen wunderbaren kulturellen Austausch und unterhaltsame Mittagszeit.

Dr. Marta Larrosa-Ferreiro und Alexander Seitz für ihre unbezahlbaren Einladungen zum Essen und zahlreiche wunderschöne Abende in Gießen.

Vladislav V. Bakhonskyi für seine Freundschaft, aufmunternde Worte und Korrektur dieser Thesis.

Zu guter Letzt möchte ich meiner Familie danken ohne deren Unterstützung das Studium und erst recht die Promotion an mehreren Punkten vorzeitig abgebrochen worden wäre.

Abkürzungsverzeichnis

Abkürzung	Bedeutung
Ad	adamantyl
BJ	Becke-Johnson
***n*-Bu**	butyl
ced	cohesive energy density
COD	cycloocta-1,5-diene
COT	Cycloocta-1,3,5,7-tetraene
CRE	conformer-rotamer-ensembles
CyHex	cyclohexyl
CyPr	cyclopropyl
DBS	double bond shift
DED	Dispersion Energy Donor
Dia	diamantyl
DMF	dimethylformamide
DMSO	dimethylsulfoxide
EDA	Energy Decomposition Analysis
Et	ethyl
HPE	hexaphenyl ethane
***i*Pr**	iso-propyl
LD	London Dispersion
LED	Local Energy Decomposition
Me	methyl
***n*-Bu**	butyl
NCI	non-covalent interactions
***n*-Dec**	decyl
NMR	nuclear magnetic resonance
***n*-Non**	nonyl
***n*-Pen**	pentyl
***n*-Pr**	propyl
***n*-Und**	undecyl
pFPh	pentaflouro phenyl
Ph	phenyl
Py	pyridine
RI	ring inversion
SAPT	Symmetry Adapted Pertubation Theory
sas	solvent accessible surface
SP	solvent polarizability
TBDMS	tertiarybutyldimethylsilyl
***t*Bu**	tertiary butyl
TCE	tetrachlorethane

Abkürzung	Bedeutung
TES	triethylsilyl
THF	tetrahydrofurane
TIBS	triisobutylsilyl
TIPS	triisopropylsilyl
TMEDA	tetramethylethylendiamine
TMS	trimethylsilyl
TPM	triphenylmethyl
TPyP	tetrapyridine porphyrine
TS	transition state
vdW	van der Waals
VRI	valley ridge inflection point

Publizierte Anteile der Thesis

Publications in Peer-Reviewed Journals

1. Schümann, J. M.; Wagner, J. P.; Eckhardt, A. K.; Quanz, H. and Schreiner, P. R., Intramolecular London Dispersion Interactions Do Not Cancel in Solution. *J. Am. Chem. Soc.* **2021,** *143* (1), 41-45.
2. Schümann, J. M.; Ochmann, L.; Becker, J.; Altun, A.; Harden I.; Bistoni G. and Schreiner, P. R., Exploring the limits of intramolecular London dispersion with bulky dispersion energy donors in alkane solution. *J. Am. Chem. Soc.* **2023**, *145* (4), 2093-2097.

Further Scientific Contributions in Peer-Reviewed Journals

1. Hofmann, C.; Schümann, J. M.; Schreiner, P. R., Alcohol Cross-Coupling for the Kinetic Resolution of Diols via Oxidative Esterification. *J. Org. Chem.* **2015**, *80* (3), 1972-1978.
2. Rummel, L., Schümann, J. M. and Schreiner, P. R., Hexaphenylditetrels – When Longer Bonds Provide Higher Stability. *Chem. Eur. J.* **2021**, *27*, 13699-13702.
3. König, H. F.; Rummel, L.; Becker, J.; Hausmann, H.; Schümann, J. M. and Schreiner, P. R., Gauging the Steric Effects of Silyl Groups with a Molecular Balance. *J. Org. Chem.* **2022**, *87*, 7, 4670-4679.

Poster Presentations

Schümann, J. M. and Schreiner, P. R., "GRC POC" –Holderness School, New Hampshire, USA, **2019**.
Schümann, J. M.; Eckhardt, A. K.; Maeda, S.; Hausmann, H.; and Schreiner, P. R., "3rd Workshop" of the SPP1807 – To what degree is London dispersion solvent dependent? Friedrich Alexander Universität, Erlangen, Bavaria, Germany, February 25 & 26, **2019**.
Schümann, J. M. and Schreiner, P. R., "Physical-Organic Chemistry at its Best: The Art of Chemical Problem Solving – Leopoldina Symposium" – Halle (Saale), Saxony-Anhalt, Germany, **2018**.
Schümann, J. M. and Schreiner, P. R., "ICPOC24" – A synthetical approach to 1,4-di-substituted-cyclooctatetraene based dispersion balances via 3,6-substituted pyrocatechol derivatives. Faro, Algarve, Portugal, **2018**.
Schümann, J. M.; Maeda, S.; Hausmann H. and Schreiner, P. R., "GRC POC" – To what degree is London dispersion solvent dependent? Holderness School, New Hampshire, USA, **2017**.
Schümann, J. M.; Maeda, S.; Hausmann H. and Schreiner, P. R., "2nd Workshop" of the SPP1807 – Universität zu Köln, Cologne, North Rhine-Westphalia, Germany, **2016**.
Schümann, J. M.; Maeda, S.; Hausmann H. and Schreiner, P. R., "ORCHEM"-Weimar, Thuringia, Germany, **2016**.

Oral Presentations

The Impact of London Dispersion in Solution – Reconsidering "Steric" Effects
CECAM Workshop on Modeling Noncovalent Interactions in Supra/Bio Catalysis, Sorbonne University, Paris, France, August 27th, **2019**.

Quantifying London Dispersion with 1,4-Substituted Cyclooctatetraene Based Balances
"4th Summer School" of the SPP1807, Universität Paderborn, Paderborn, North Rhine-Westphalia, Germany, July 16-19, **2019**.

Quantifying London Dispersion with 1,4-Substituted Cyclooctatetraene Based Balances
"3rd Summer School" of the SPP1807, DESY, City of Hamburg, Hamburg, Germany, July 22-25, **2018**.

"Dispersion Driven Peptide Folding?" – The Leucine-Zipper Protein!
20 Years PRS Group anniversary, Schloss Hornberg, Baden-Wuerttemberg, Germany, **2017**.

To what degree is London dispersion solvent dependent?
"2nd Summer School" of the SPP1807, Universität Rostock, Rostock, Mecklenburg-Western Pomerania, Germany, July 9-12, **2017**.

To what degree is London dispersion solvent dependent? Re-vitalizing an old molecular balance "1st Summer School" of the SPP1807, Jacobs University, City of Bremen, Bremen, Germany, May 29 - June 1, **2016**.

Acknowledged Scientific Contributions/Discussions in Peer-Review Journals

1. Strauss, M. A.; Wegner, H. A., Exploring London Dispersion and Solvent Interactions at Alkyl–Alkyl Interfaces Using Azobenzene Switches. *Angew. Chem. Int. Ed.* **2019,** *58* (51), 18552-18556.
2. Strauss, M. A.; Wegner, H. A., Molecular Systems for the Quantification of London Dispersion Interactions. *Eur. J. Org. Chem.* **2019,** *2019* (2-3), 295-302.
3. Strauss, M. A.; Wegner, H. A., London Dispersion in Alkane Solvents. *Angew. Chem. Int. Ed. Engl.* **2021,** *60* (2), 779-786.
4. Bernhardt, B.; Ruth, M.; Eckhardt, A. K.; Schreiner, P. R., Ethynylhydroxycarbene (H–C≡C–C̈–OH). *J. Am. Chem. Soc.* **2021,** *143* (10), 3741-3746.
5. Eschmann, C.; Song, L.; Schreiner, P. R., London Dispersion Interactions Rather than Steric Hindrance Determine the Enantioselectivity of the Corey–Bakshi–Shibata Reduction. *Angew. Chem. Int. Ed.* **2021,** *60* (9), 4823-4832.
6. König, H. F.; Hausmann, H.; Schreiner, P. R., Assessing the Experimental Hydrogen Bonding Energy of the Cyclic Water Dimer Transition State with a Cyclooctatetraene-Based Molecular Balance. *J. Am. Chem. Soc.* **2022,** *144* (37), 16965-16973.
7. Rummel, L.; König, H. F.; Hausmann, H.; Schreiner, P. R., Silyl Groups Are Strong Dispersion Energy Donors. *J. Org. Chem.* **2022**, *87* (19), 13168-13177.
8. Rummel, L.; Domanski, M. H. J.; Hausmann, H.; Becker, J.; Schreiner, P. R., London Dispersion Favors Sterically Hindered Diarylthiourea Conformers in Solution. *Angew. Chem. Int. Ed. Engl.* **2022**, *61* (29), e202204393.
9. Rummel, L.; Hanke, K.; Becker, J.; Schreiner, P. R., London Dispersion Stabilizes Chloro-Substituted cis-Double Bonds. *Synlett* **2022**, *34* (10), 1129-1134.
10. Wilming, F. M.; Becker, J.; Schreiner, P. R., Quantifying Solvophobic Effects in Organic Solvents Using a Hydrocarbon Molecular Balance. *J. Org. Chem.* **2022**, *87* (3), 1874-1878.
11. Wilming, F. M.; Marazzi, B.; Debes, P. P.; Becker, J.; Schreiner, P. R., Probing the Size Limit of Dispersion Energy Donors with a Bifluorenylidene Balance: Magic Cyclohexyl. *J. Org. Chem.* **2022**, *88* (2), 1024-1035.
12. Rummel, L.; Schreiner, P. R., Advances and Prospects in Understanding London Dispersion Interactions in Molecular Chemistry. *Angew. Chem. Int. Ed. Engl.* **2024**, *63*, e202316364.

Table of Contents

1. Introduction

1.1 Motivation and Goals

At the beginning of my undergraduate studies a new/old question arose due to the increasing number of high-quality computations showing the importance of NCI's (non-covalent interactions) in molecular chemistry.[4] A priority program (*dt.* Schwerpunktprogramm – SPP 1807) was launched to tackle those deepened questions arguing with already well accepted concepts of steric repulsion, especially in organic chemistry. Back in 2015, experimental trends in reaction enantioselectivity or the orientation of molecules in crystals were ascribed largely to Pauli repulsion/steric hinderance by experimentalists. Although, the fact that the properties of organic matter are indeed governed by the strange and hidden quantum realms was acknowledged at the time. However, state-of-the-art computational models like B3LYP neglected dispersion forces. The unintentional outcome was that it reinforced the idea of a world dominated by Pauli exchange repulsion. On the other hand, empirical dispersion corrections, especially the models developed by Grimme *et al.*, already delivered results better agreeing with experimental data sets for small additional computational cost.[5] A highly debated question at that time and still is, does dispersion exist in solution and why do we rarely argue about it in a productive way or use it for the benefit and guidance of molecular reactions?

Fritz London's famous London equation (Eq. I) gives chemists the tool to correlate distance dependence (r) and relations due to polarizabilities (α) and ionization potentials (I) of molecule dimers (A & B).[1,6]

$$E_{AB}^{disp} = -\frac{3}{2}\frac{\alpha_A \alpha_B}{r^6}\frac{I_A I_B}{I_A + I_B} = -\frac{C_{disp}}{r^6} \quad \text{(I)}$$

While figuring out a descent topic to work on in the field of London Dispersion (LD), talking to the first scientific secretary of SPP1807, J. Philip Wagner and my supervisor Prof. P. R. Schreiner was crucial.[4,7,8] Their advice on how to impact on the field was rather simple: "Jan, if you would like to contribute, synthesize a molecular balance and show the community hard numbers." Digging deep into literature and keeping in mind the question asked by NCI chemists—like Schneider, [9,10] Cockroft, [2,3,11,12] Hunter,[13–15] and Shimizu[16,17]—"How much do van der Waals dispersion forces contribute to molecular interactions in solution?"

1.2 Van der Waals Forces

The direct manifestation of attractive forces were described by van der Waals equation of state.[18] Together with Keesom interactions (dipole-dipole, electrostatic/orientational)

and Debye interactions (dipole–induced dipole, induction), London dispersion interaction (induced dipole–induced dipole) is a key contributor to van der Waals forces,[19] especially in gases without a permanent dipole moment, e.g. noble gases.[1,6,20] A common example is taught in organic chemistry undergraduate studies on the difference in boiling points of linear and branched alkanes. The boiling point decreases with increased branching due to the reduced surface area reducing intermolecular dispersion interactions.[21,22]

London dispersion also stabilizes molecules, particularly with bulky groups like *tert*-butyl (*t*Bu). This is demonstrated in the hexaphenylethane (**HPE**) riddle (Figure 1).[23–25] While parent **HPE** is unstable due to the steric repulsion between the six phenyl groups of the corresponding triphenylmethyl radical (**TPM**), introducing a dozen bulky *t*Bu groups stabilizes the dimerization, allowing it to crystallize.[23,26] The *t*Bu groups create a "corset effect"[27] by holding the molecule together (Figure 1)[28] with London dispersion interactions leading to an increased bond dissociation energy, which is the reason for the observable crystal structure of the heavily substituted ***t*Bu-HPE** whereas the unsubstituted derivative remains elusive.

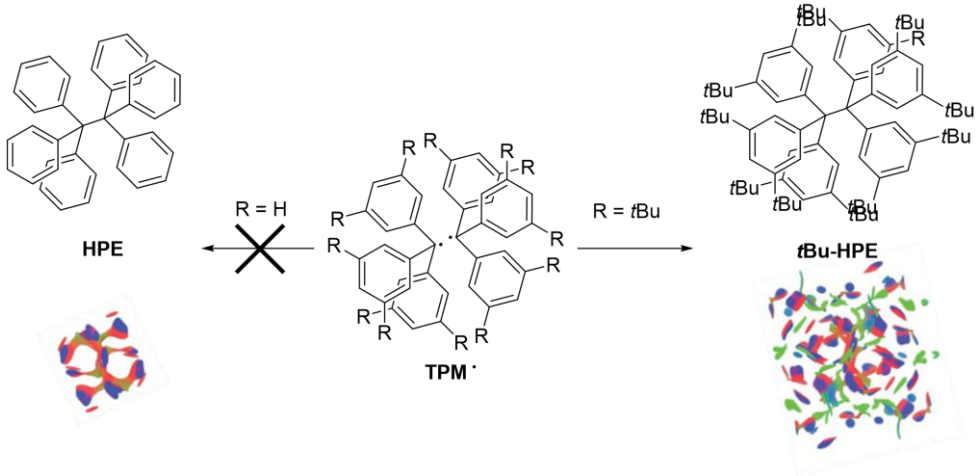

Figure 1. Bulky substituted **tBu-HPE** forms due to the attractive NCI interactions (green belts on the NCI plots shown below structures) while less bulky unsubstituted **HPE** does not. Adapted with permission from Schreiner et al. Copyright 2017 Royal Chemical Society[24].

Heitler and London[29] were the first to characterize the long-range distance (r^{-6}) dependent attractive interactions in molecular dimers, which are now known as LD interactions in honor of Fritz London. Despite these forces contributing significantly to the overall interactions in bulk materials, they are often perceived as the weakest component of van der Waals (vdW) forces. Dispersion forces may be overshadowed by the stronger interactions (Figure 2) such as electrostatic[30] and induction forces.[31] LD forces contribute theoretically to 100% of the interaction energy of the methane dimer in vacuum at 293 K. Looking at the dimer of water and methane the inductive interaction has only a small effect on the overall Energy, LD forces contribute here up to 87%.

C [10^{-79} Jm^6]	Keesom Force	Debeye Force	London Dispersion Force
C_{ind}	10	9	0
C_{orient}	96	0	0
C_{disp}	33	58	102
Total C_{vdW}	139	67	102

Figure 2. A comparison of van der Waals force contributions in water–methane interaction through the theoretical van der Waals Coefficients (C_{ind}, C_{orient}, and C_{disp}) at 293 K in vacuum. Numbers are taken from Chapter 6 Table 6.3 of Israelachvili's Intermolecular and Surface Forces[19]

Looking at the (dipole–dipole) water dimer, electrostatics take over as the main contributor to the overall energy, here LD is further diminished and contributes roughly to 24% of the overall energy. However, it is clear that all those forces are stabilizing the dimerization process and can only be dissected by modern energy decomposition analysis (EDA) such as SAPT[32] (symmetry adapted perturbation theory) and LED[33–36] (local energy decomposition). Such analysis conducted for two "*t*Bu" moieties approaching each other (Figure 3) illustrates how LD can be a very strong contributor in comparison to the electrostatic and induction forces.

In view of London's approximate equation for quantifying the attractive interactions (Eq. I) one can grasp why LD interactions are commonly rationalized by means of fluctuating dipole–induced dipole interactions. Especially the correlation with ionization potentials and polarizabilities gives a notion of charge separation and subsequent polarization being

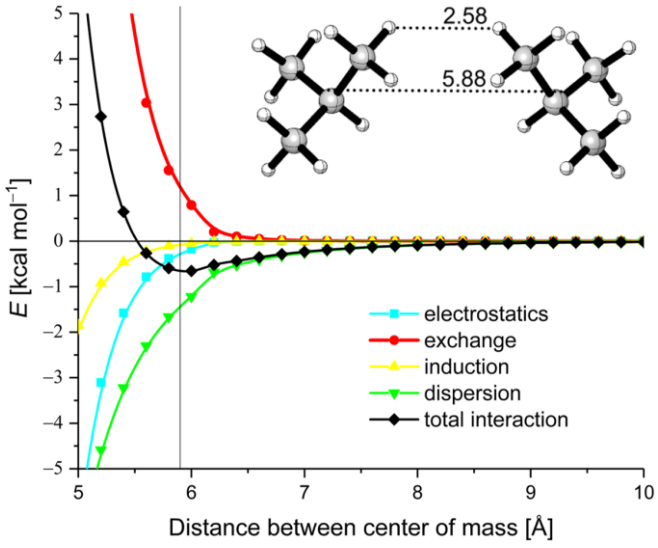

Figure 3. SAPT Scan of an isobutyl dimer showing the greater contribution of dispersion forces compared to the electrostatic and induction forces at the energy minimum.

relevant for the interaction. However, this leads to the wrongful picture of classical electrostatics somehow being involved in an interaction that can only be rationalized properly by quantum theory, as originally shown by London. In fact, London's original description of LD interactions is much closer to the "modern" view of LD, which involves seemingly enigmatic fluctuations due to zero-point energy, which lead to the engagement of "virtual" excited electronic states in interacting atoms or molecules.[1,37]

When two interacting systems have different polarizabilities, the dispersion interaction can be expressed in terms of the polarizabilities α_A and α_B of the respective systems. Additionally, the zero-point energy ($h\nu_0$) can be approximated using the ionization potentials I_A and I_B of the two systems. This approximation provides an upper bound for the intermolecular dispersion interaction between two atoms. Empirical results have shown that this upper bound performs better than a similar lower bound based on electronic excitation energies. Consequently, the well-known London dispersion formula is derived (Eq. I).[20]

Obtaining reasonably accurate correlation energies, defined as the energy difference between the Hartree-Fock method with an infinite basis set and the exact electronic energy derived from the Schrödinger equation, has previously been a major bottleneck for theoretical methods.[38] In this regard, substantial progress has been made by introducing approximate treatments for costly correlation energy terms. For example, empirical dispersion correction terms have been developed for density functionals,[39] and local approximations for high-end wavefunction methods are now widely available, so that chemically accurate computations are obtainable for systems comprising hundreds of atoms including heavy elements.[40–42] Moreover, developments in computational chemistry have popularized energy decomposition methods derived from both wavefunction theory and computationally cheap DFT.[36,43] Consequently, through a myriad of decomposition studies[36], we now have a much broader understanding of the true quantum chemical character of most non-covalent interactions systems, which is based on hard numbers, rather than "chemical intuition". Only seldom the outcome of such studies fits well with the chemical intuition[44,45] of general synthetic organic chemists.

1.3 What is Molecular Balance?

1.3.1 Quantifying non-covalent interactions

Molecular balances are model systems developed to isolate a specific interaction in an attempt to measure it.[46,47] Chemists can use their advanced synthetic knowledge to define distance and substitution pattern in a model system to mimic natural occurring effects by enhancing them.[13,47] In principle, moieties are forced to interact with each other by bringing them in close proximity or leave enough space to circumvent the intramolecular

interaction.[17] Intramolecular or intermolecular complexes/dimers are prime examples to investigate attractive interactions.[48] The design of the balance backbone needs to address observable force of interest.[11,49–52] The limitations of molecular balances in providing insights towards LD forces in solution include:

- **Sensitivity:** LD interactions are rather small due to their nature being enforced by induced dipole-induced dipole interactions. This usually results in ΔG values around -0.1 to -0.5 kcal mol^{-1}. This energetic difference is within the error range of NMR studies.[9,47,53]
- **Complexity:** LD forces are influenced by a number of factors, such as the size,[21] shape,[54] and polarizability[20] of the molecules in question, making it difficult to isolate and measure their effects. Moreover, LD never comes alone when dimers interact with each other. Keesom and Debye forces always also favor dimerization processes.[19]

Therefore, molecular balances alone may not provide sufficient information about LD forces in solution via spectroscopic measures, other techniques such computational methods are needed to complement the information obtained by molecular balances to provide a more complete understanding of these interactions.[5,8]

London dispersion effects are counteracted primarily by entropy and secondarily solvation.[19,55] While these mechanisms do not reduce the strength of dispersion itself, they provide compensating energy contributions.[56] Entropy increases with molecular size and floppiness of the systems, leading to a greater penalty for intermolecular complexes partially offsetting dispersion interactions.[9] In solution, dissociation of intermolecular complexes frees surface area, enhancing solute-solvent interactions, which further compensates for dispersion. However, the relative importance of these effects remains poorly understood due to limited experimental data and computational complexity.

Folding molecules serve as an effective platform for studying non-covalent interactions (Figure 4), with the relative stabilities of conformational states being influenced by

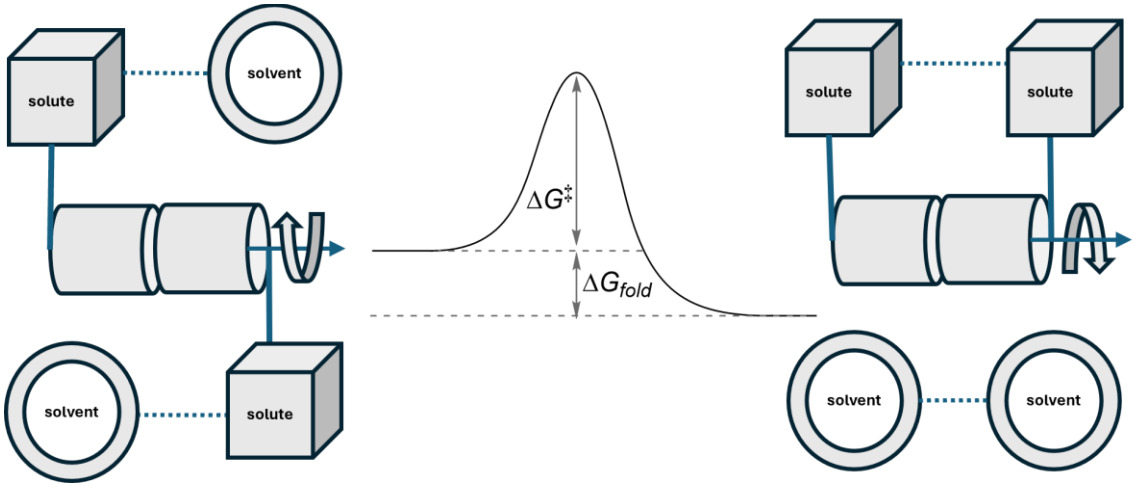

Figure 4. Schematic representation of molecular balances with solvent interactions.

intramolecular contacts and solvent interactions unique to each conformation.[13–15]

However, experimentally assessing the relative stabilities of all possible conformations, particularly in highly flexible molecules such as long alkyl chains, is not feasible via nuclear magnetic resonance (NMR) spectroscopy as the signals will broaden and overlap with each other at a wide range of temperature. Instead, thermodynamic data should be derived from simpler model systems with constrained conformational freedom.[57] To minimize the impact of steric effects, solvation, and secondary intramolecular interactions on folding behavior, molecular balances with high symmetry are preferred, as they reduce these background contributions.[3,47,58,59]

1.3.2 Determination of the Gibbs energy of activation

Ioulia K. Mati described in 2013 very suitably in her thesis[58] on "Molecular torsion balances for quantifying non-covalent interactions" following statements on the determination of Gibbs Free Energies which also applies for all further balance systems. Though not all foldable molecules have the desired properties to permit ΔG^{T}_{fold} determination, numerous molecular systems have been successfully applied to the quantitative study of non-covalent interactions.[58] Molecular torsion balances[58] with rotational bonds (e.g., triypticenes,[60–62] Trögers base,[2,11,14,46,52,63–65] *N*-arylamides,[16,17,66–68] and thioureas[69]), general dimerization of compounds (e.g., pyridine dimers,[70,71] and triphenylmethane dimers[72]), double bond switching compounds (e.g., azobenzenes,[53,73–75] and bifluoronilidienes[76–79]) or general ring inversion driven balances (e.g., cylooctatetraene[44,45,56,57,80–85] based balances, cyclohexyl[50,51] axial values[86,87]) have all one thing in common, their low barrier heights ($\Delta G^{\ddagger}_{fold}$). The barrier prone to the switch or folding ($\Delta G^{\ddagger}_{fold}$) quantifies the free energy difference between a ground-state conformation and the transition state, and can provide insight into the strength of non-covalent interactions.[47,53,74] $\Delta G^{\ddagger}_{fold}$ values (Eq. II) can be readily determined using variable-temperature NMR spectroscopy[58] or UV/Vis spectroscopy in case of some model compounds like azobenzenes.[48]

$$\Delta G^{\ddagger}_{fold} = \Delta H^{\ddagger}_{fold} - \mathrm{T}\,\Delta S^{\ddagger}_{fold} \quad \text{(II)}$$

Even though the interpretation of the attractive interactions in transition states is complicated itself, the knowledge about the barrier height gives valuable insights for the experimental set up.[47,56,78,84] In general the folding needs to be observable at a reasonable time scale to determine true thermodynamic data.[58] For example, for room temperature analysis using ^{1}H-NMR this typically requires a transition barrier $\Delta G^{\ddagger}_{fold}$ larger than 16 kcal mol^{-1} but smaller than 26 kcal mol^{-1}.[66,82] This numbers translate to half-lives of minutes to hours.

1.3.3 Determination of Gibbs free energy

However, the free energy difference between ground-state conformers (ΔG^{T}_{fold}) is more easily interpreted than $\Delta G^{\ddagger}_{fold}$ barrier measurements because the interactions present in the ground-state conformations can often be calculated with a high degree of certainty (Eq. III) or observed experimentally (equilibrium constant in NMR solution studies).[47,58,86,87] Nevertheless, interaction energies should always be interpreted with care; the role of the solvent in determining molecular conformation should never be overlooked.[2,14,88] The foremost requirement for ΔG^{T}_{fold} measurement using folding molecules is that the relative populations of each distinct conformer must be quantifiable.[58] NMR spectroscopy is a powerful technique for assessing the conformation of small molecules in solution.[47,58,88]

One approach to quantifying ground-state non-covalent interactions is to use molecules featuring a slow rotation or inversion around a bond or cycle for distinct conformational populations to be directly quantified by NMR, but rapid enough for conformational equilibrium to be reached within a reasonable timescale.[58]

$$\Delta G^{T}_{fold} = -\mathrm{RT}\ln\frac{\int(folded)}{\int(unfolded)} = -\mathrm{RT}\ln \mathrm{K}_{eq.} \quad \text{(III)}$$

The advantage is that time-consuming variable-temperature experiments are not required to extract thermodynamic information from the system.[47,58]

1.3.4 Determination of the reaction enthalpy

LD by first approximation is temperature independent as (Eq. I) indicates, so it is necessary to get insights via the determination of $\Delta H^{\ominus}_{fold}$ to gain further knowledge on the strength of its nature. It is known that entropy, namely Pauli-repulsion acts as a counterpart to any attractive forces.[19]

$$\Delta G^{\ominus}_{fold} = \Delta H^{\ominus}_{fold} - \mathrm{T}\,\Delta S^{\ominus}_{fold} \quad \text{(IV)}$$

Taking Eq. III into account and combining it with Eq. IV divided by the temperature we form the following Van 't Hoff equation (Eq. V).

$$\ln K_{eq.} R = -\Delta H^{\ominus}_{fold}\,\frac{1}{T} + \Delta S^{\ominus}_{fold} \quad \text{(V)}$$

Provided that the system under investigation is sufficiently geometrically well-defined, the approach allows both attractive and repulsive interactions to be measured with a high degree of accuracy (often ±0.1 kcal mol^{-1}).[48] The precise range and accuracy of the approach depends upon the sensitivity of the spectroscopic technique employed. In

general, Van 't Hoff data derived enthalpies are highly dependent on the number of datapoints as even a slight change has a huge influence on the slope.[89,90]

1.3.5 The beauty of cyclooctatetraene

Since the first synthesis (Figure 5) of cyclooctatetraene **5** on the pursuit of investigating benzene type molecules by Willstätter and Waser, the understanding of [8]annulenes became much more advanced. They synthesized **5** by extracting the natural substance pseudopelletierine (**1**) from the pomegranate tree bark. Four subsequent elimination steps yielded only 4% of **5** in regard of the starting material **1** in 1911.[91]

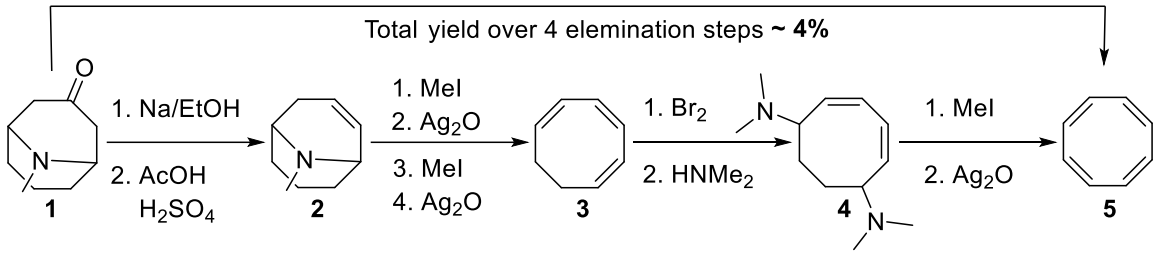

Figure 5. Willstätter's first synthesis of COT.[91]

Willstätter noted almost disappointedly that the properties of the new found eight membered ring with the formula C_8H_8 does not possess any comparable properties to benzene (e.g., hydrogen uptake, addition of bromine).[91,92]

"*Vom Benzol ist das Cyclooctatetraen im chemischen Verhalten vollkommen verschieden; wie folgende Reaktionen zeigen, ist es ein wahres Cycloolefin:*

1. *Das Tetraen addiert bei Gegenwart von Platin rasch vier Mole Wasserstoff, während Benzol unter den gleichen Bedingungen keinen Wasserstoff aufnimmt.*
2. *Das Tetraen reduziert heftig Permanganat und addiert Brom sofort.*
3. *Es ist nicht leicht subsituierbar, mit Salpeterschwefelsäure gibt es keine Nitroverbindungen, sondern es verharzt.*
4. *Das Tetraen stabilisiert sich durch Umlagerung in Isomere mit Brückenbindungen."*

However, his findings showed clearly that the yellow fluid with the pungent smell possessed more interesting properties, as many following publications showed. The double bond characteristics and simple ability to be substituted kept chemists busy for decades.[92,93]

The synthetic pathway towards **5** was unfortunately not efficient until Walter Reppe's group developed a method of cyclizing acetylene gas with a Nickel cyanide in THF solution under high pressure (Figure 6) during the Second World War.[94] The turmoil of the war led to a delayed, incomplete publication in 1947. The since then easy access of **5**

in huge quantities led to an explosion of **COT** related chemistry in the 70s and 80s of the 20th century.[93]

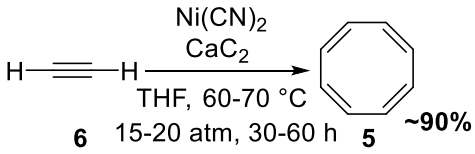

Figure 6. Reppe's synthesis of COT.[94]

The work of Leo A. Paquette[80,95] and Andrew Streitwieser Jr.[44,96] focused on substituting COT und understanding its properties as uranocene ligand. They were also the first to describe the synthesis and unusual properties of the molecular balance chosen of in this work to investigate LD interactions in solution.[44,80] Computational studies in the late 90s and early 2000s explained the iconic properties and its folding ability by a bifurcating pathway.[97,98] The at room temperature occurring double-bond shift[99] (**DBS**) and the synthetic accessibility to its 1,4-substitution pattern makes **5** a prime example of a molecular balance backbone.[44,45,56,57,80,82,100–103] The fine works of Leo A. Paquette,[80] Andrew Streitwieser Jr.[44] and Peter A. Kirsch[82] granted a great start for a success-oriented study on LD interactions in solution.

The now widely agreed upon mechanistic pathway (Figure 7), which has been verified computationally[97,98] and spectroscopically,[99] first proceeds through the planar ring inversion (**RI**) transition state (**TS**) structures **RI TS' (1,4)** and **RI TS' (1,6)** in which the double bonds are localized. Over this pathway marked with a green dotted line the minima (**MIN**) of the 1,4- and 1,6-isomers are interconverted into their mirror images. One of the peculiarities of such substituted **COT** is that due to the C_2-symmetry 1,4-isomers are interconverted into their enantiomers, which is, however, irrelevant for the

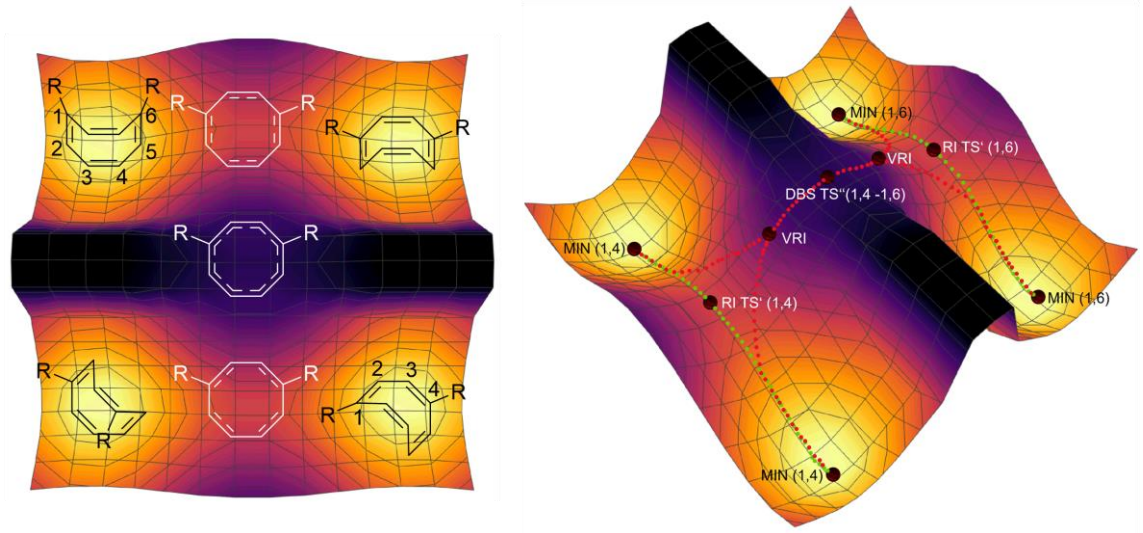

Figure 7. Schematic depiction of bifurcation[98] pathway of substituted COT. R = H, Me, Et, *i*Pr, *t*Bu, Ad, Dia, and all possible functional groups.

use of such a system to quantify NCIs in an achiral environment as well as that enantiomers are not distinguishable via NMR spectroscopy. The 1,6-isomers **MIN (1,6)** on the other hand belong to the C_s point group, with an intramolecular plane of symmetry so that the inversion leads to the exact compound again. Both isomers are readily distinguishable via NMR spectroscopy (Figure 8). The difference in symmetry between the 1,4- and 1,6-isomers is reflected in their respective NMR spectra as well, with the 1,4-isomer exhibiting a singlet and two AB-quartet signals, while the 1,6-isomer shows three distinct signals in the olefinic area.

All 1,4-disubstituted cyclooctatetraenes follow this multiplicity and only vary the shift hence the electronic properties of the substituent. Transition state structures **RI TS' (1,4/1,6)** cannot undergo direct double-bond shift to **DBS TS"** but proceed via a similar structural pathway over the valley ridge inflection points (VRIs) and vice versa, passing through the antiaromatic, C_S symmetric planar transition structure **DBS TS"**, in which the double bounds are truly delocalized. Naturally, as **DBS TS"** is higher in energy than **RI TS'**, it resembles the rate determining transition state. Estimates for the activation barrier for the **DBS** have been deduced experimentally for various di- substituted derivatives, with typical $\boldsymbol{\Delta G^{\ddagger}_{DBS}}$ values being in the range of 13–23 kcal mol^{-1} (Figure 9).

Thus, **COT** molecular balance systems should reach equilibrium within a few hours at near ambient temperatures following the approximations of transition state theory. It is important to note that with the increasing size of the substituents the barrier also increases drastically. So far, no solvent dependence on the transition state has been investigated. For all kinetic measurements, either benzene or chloroform has been used.

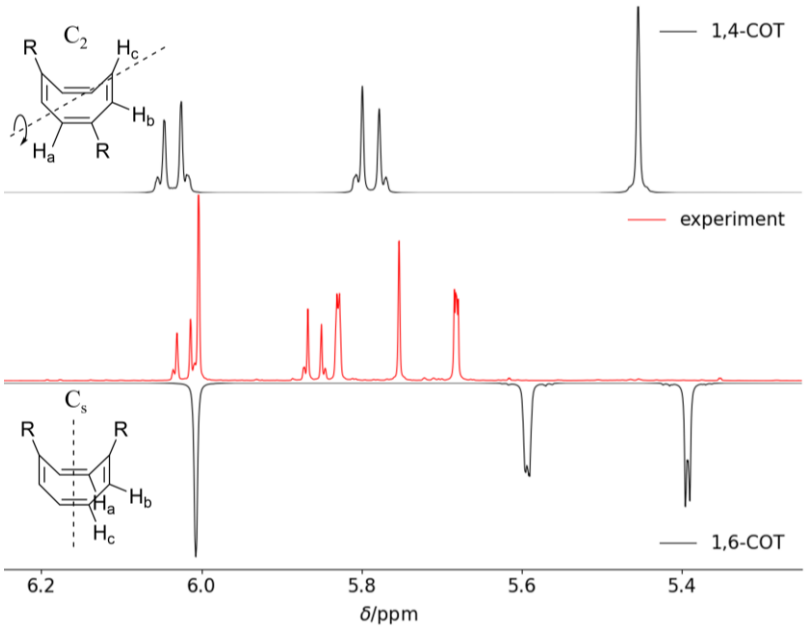

Figure 8. *Exemplified experimental 1,4-and 1,6-di-tBu-COT spectra in deuterated benzene and the corresponding computed spectra (in black). Adapted with permission from Schreiner et al. Supporting information. Copyright 2021 American Chemical Society.*[56]

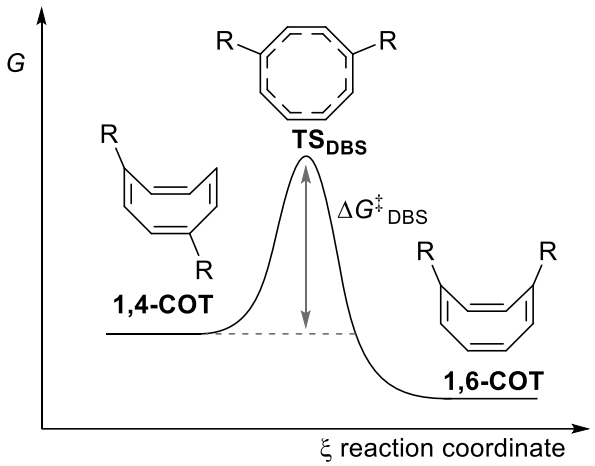

R	$\Delta G^{\ddagger}_{DBS}$ (T) [kcal mol^{-1}]
H[99]	13.7 (263 K)
Me[102]	17.3 (325 K)
Et[82]	17.8 (322 K)
*i*Pr[82]	19.0 (359 K)
*t*Bu[44]	22.6 (298 K)

Figure 9. Simplified depiction of the activation barrier red dotted line of Figure 7 and the experimentally determined barriers for the substituted COT through kinetic measurements and the use of Eyring equation.

A simple DF-SAPT2/aug-cc-pVTZ energy decomposition analysis of isobutane dimers gave first insights into the prominence of LD interactions within the range of the COT system. We took the B3LYP–D3(BJ)/def2–QZVPP optimized geometries, removed the COT moiety, and saturated the resulting radicals with hydrogen atoms. This evaluates the "isolated" interactions of the two isobutane moieties at the distance of the full COT isomer as shown in Figure 10.[56] Nowadays, there are now several routes for the functionalization of 1,4-derivatives (see Figures 11, 12, and 13).

The most promising approach to the synthesis of 1,4-disubstituted cyclooctatetraenes **9** lays within the deprotonation of the readily available bridged sulfone **7** and its

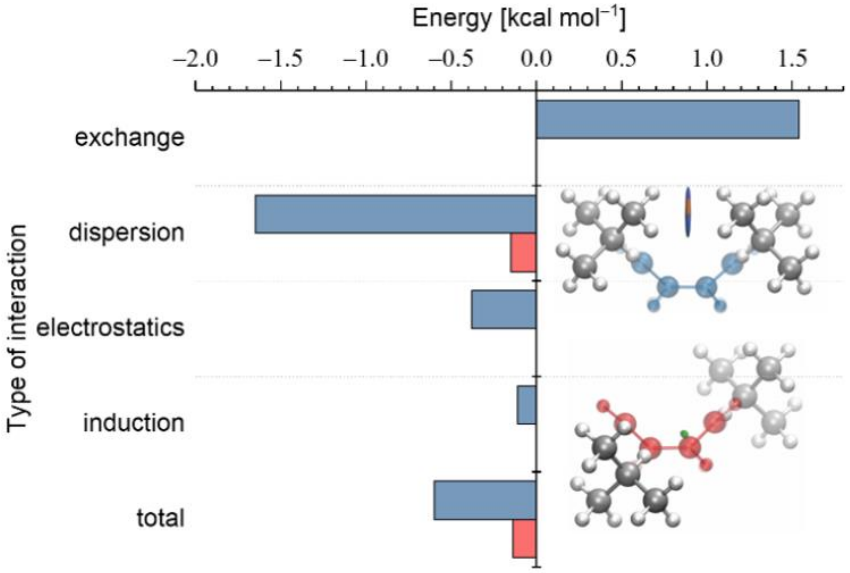

Figure 10. DF–SAPT2/aug–cc–pVTZ energy decomposition of isobutane dimers based on the optimized geometry of the spatial 1,4-(red) and 1,6-(blue) COT arrangement. Adapted with permission from Schreiner et al.[56] Supporting information. Copyright 2021 American Chemical Society.[56]

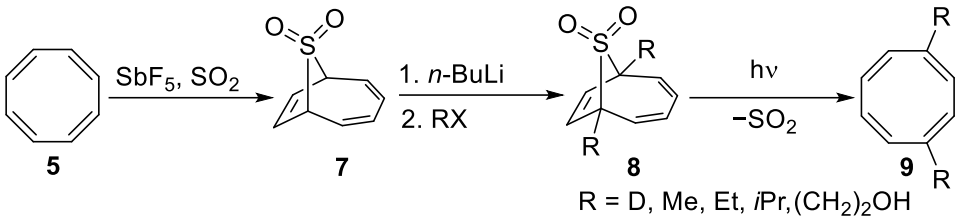

Figure 11. Applicable synthesis route towards primary and secondary alkane 1,4-substituted **9** via bridged sulfone **7**.[82,95,102,104,105]

electrophilic substitution with alkyl halides. Photolysis of **8** provides the pure polyolefins **9** in high yields. Ejection of sulfur dioxide with white LEDs (Xenon) is so rapid that possible photorearrangement of the COT products has not been encountered.

However, this method is limited to unbranched alkyl derivatives and their availability as electrophiles. The synthetic approach developed by Hanzawa and Paquette via Diels-Alder reaction and following Strating Zwanenburg Photodecarboxylation[80] lead to tertiary alkyl balances such as *t*Bu, Ad, Dia (Figure 12). The main disadvantage of this approach is that cyclobutadiene precursor **10** is not commercially available and needs to be synthesized first from **5** over several steps, **11** is synthesized via methods of Ershov *et al.* and Ochmann *et al.*.[106,57]

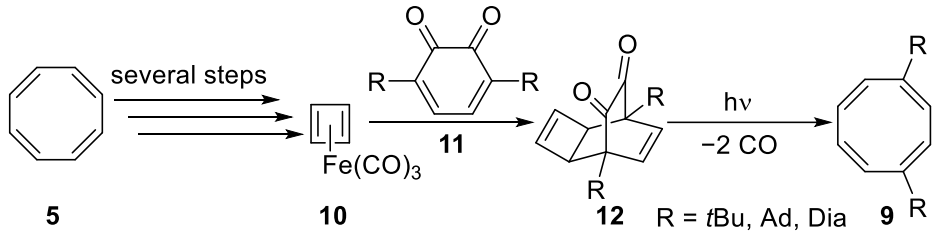

Figure 12. Applicable synthesis route towards tertiary alkane 1,4-substituted **9** via bridged dione **12**[56,57,80]

Later a way cheaper approach for 1,4-di-substitutions was developed, employing readily available cyclooctadiene (COD, **13)**, which is initially deprotonated to form a TMEDA stabilized dark red di-anion complex, which can easily be used to form triene **14** by addition of tetrel chlorides. Said triene **14** is further deprotonated and oxidized to form the desired compounds. This method (Figure 13) has been used and further optimized by König & Rummel *et al.*[83,84]

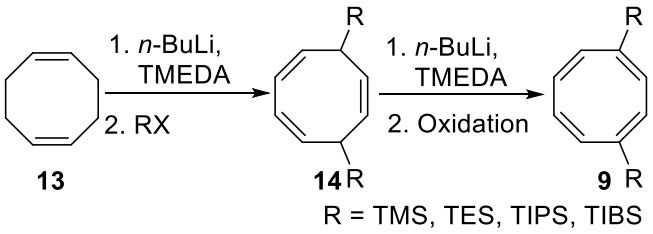

Figure 13. Applicable synthesis route towards tetrel 1,4-substituted **9**.[84,103]

1.4 Quantifying London Dispersion in Solution

1.4.1 Current state of the art

The earliest extensive work on LD in solution is the life's work of Schneider on the studies on porphyrin interactions in water (Figure 14).[9]

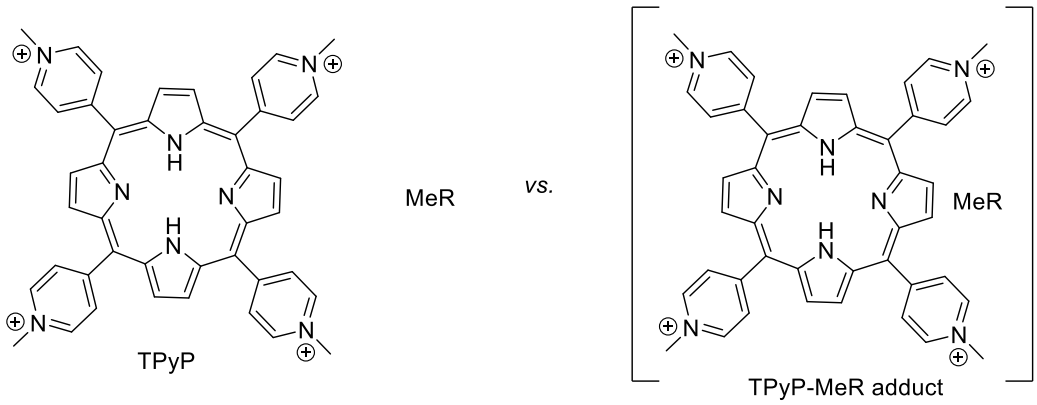

Figure 14. Schneider's system of choice MeR adducts on porphyrins in water.

His studies show that the $T\Delta S$ term contributes 10% to 80% of the total ΔG, depending on the interaction mechanisms, such as hydrogen bonding and ion pairing. Analysis of over 90 equilibrium measurements of porphyrin receptors in water reveals that small alkanes do not bind to hydrophobic flat surfaces ($\Delta G \approx \pm 0.1$ kcal mol^{-1}), while 20 heteroatom-bearing functions interact via dispersive forces, with ΔG values up to 1.9 kcal mol^{-1}, correlating with polarizability. Aromatic systems exhibit size-dependent binding affinities, which are linearly related to the number of π-electrons.

Cockroft *et al.* started in 2013 the hunt for dispersion interactions in solution by asking the question "How much do van der Waals dispersion forces contribute to molecular recognition in solution?"[2] They chose a Tröger's base "Wilcox torsion balance"[46] derived balance (Figure 15) with linear alkyl chains to describe the folding behavior in a variety of polar (water/THF) and nonpolar solvents (linear alkanes). The conclusion lead to a huge uproar in the molecular balance and attractive interactions investigative community as it suggested a rather low contribution meant to be neglectable as the ratios from the folded to unfolded state remain very small.[2] Shimizu mediated the situation by publishing a further explanatory statement.[107] As linear alkanes within this balance may actually never really have the chance of interacting strongly with each other due to their floppiness at elevated temperatures. The studies were further extended towards solvophobic effects.[63] Only at considerably low temperatures alkanes remain in their all *trans* conformation, while increasing their chain length at C17 they start to predominantly form an intrinsic foldamer.[108]

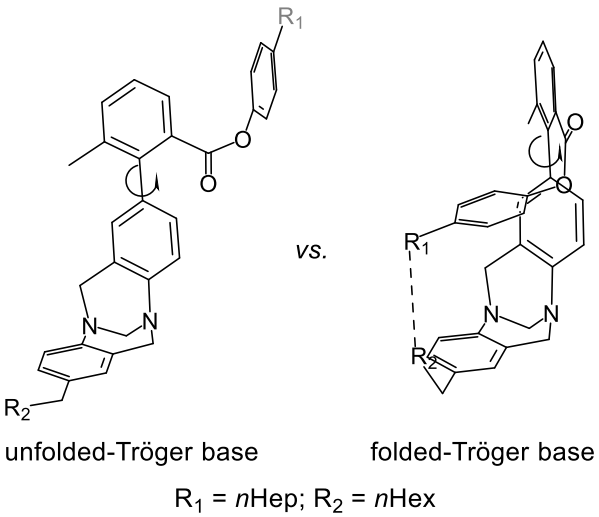

Figure 15. Cockroft's system of choice linear alkane residues on a Tröger's base backbone.

As the famous quote of Johann Diderik van der Waals "matter will always display attraction" remains a stronghold being observable in boiling points of organic liquids and nowadays prime examples of enantioenriched molecules due to catalysis in solution, Tröger's balance with long alkane chains might not have the best design to unravel the importance of LD in solution.[54]

In 2019 Chen *et al.* chose proton bound pyridine dimers with larger substituents to determine (Figure 16) their binding via their dissociation energy in dichloromethane solutions via NMR as well as in the gas phase with ESI-MS/MS. They found that LD forces are largely attenuated in dichloromethane compared to the gas phase by up to 70%.[70] Further developments in aprotic solvents (perfluoro-*n*-hexane, 1-flouro-*n*-hexane, 1,2-difloruobenzene, dichloromethane, cyclohexylbromide and 1-bromobenzene) underlined their finding of a diminishing effect.[71]

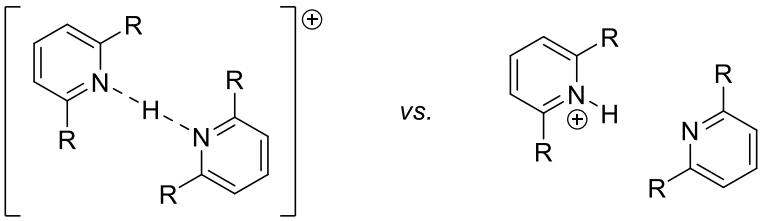

Figure 16. Chen's system of choice, dissociation of proton bound pyridine dimers.

From 2015 onwards the studies of Wegner *et al*. were focused on the determination of the *Z*/*E* isomerization rates of all *meta* substituted alkylated azobenzenes in DMSO and *n*-octane (Figure 17).[73] The system is no traditional molecular balance as over time only the E isomer is observable – so the balance is already tilted on one site. The *Z*/*E* isomerization could be rather considered a dissociation event.[48] The isomerization rate is conveniently followed by UV/Vis and NMR spectroscopy. With increasing size of the substituent, the half-life of the *Z* isomer is steadily increasing. They noted the same trend of increasing

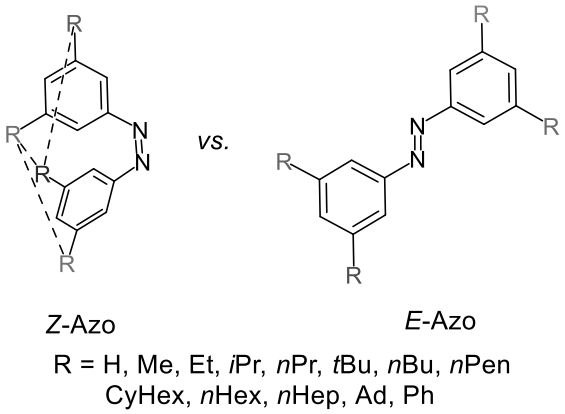

Figure 17: Wegner's system of choice *E*/*Z* isomerization of azo switches.

half-lives with increasing polarizability of substituents are observed in both solvents, stating that the effect is largely solvent independent.[73] Computational investigations showed that the impact of LD forces in TS of the *Z*/*E* isomerization is rather neglectable.[73] The second study focused on linear alkanes, with increasing chain length, as all *meta* substituents to harness a possible compensation effect on the isomerization rate in n-octane and DMSO.[74] Solvents used for their third study ranged from linear, to branched as well as cyclic aliphatic solvents. (e.g., *n*-heptane, *iso*-octane, *n*-octane, *n*-decane, *n*-undecane, *n*-dodecane towards cyclooctane). Hence the interactions between the (solute-solute) intra molecular interactions, the (solute-solvent) and (solvent-solvent) intermolecular interactions will range in the same area. The findings of the first study were underlined as the change in solvent only changed marginally the tendency of the half-lives. However, solvents with low surface tension resulted in a destabilizing contribution of solvent-solvent interactions (±0.1 kcal mol^{-1}) leading to an half-life increase of up to 20%.[53]

The main solvent studies performed between 2019 and 2023 within Schreiner's group based on the cyclooctatetraene backbone (Figure 18) is described in the next chapters.

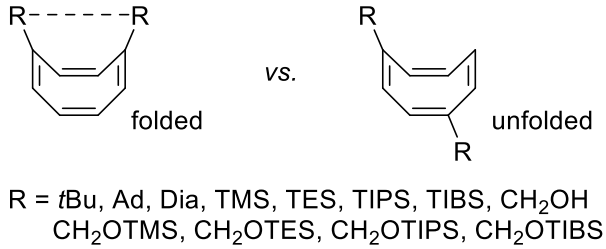

Figure 18. Schreiner's system of choice, balances on the cyclooctatetraene backbone.

Schreiner *et al.* used strained bifluorenylidene[78,79] balances (Figure 19) to investigate the limits of close contacts in terms of London forces by showing that the unfolded conformer with R = *t*Bu and Dia being the most stable in all solvents. All other substituted derivatives favored the *Z*-bifluorenylidene. Furthermore, they showed in an additional

study that the folding of the famous thiourea catalyst framework is also highly dependent on LD interactions.[69] Substituents with increasing size from H to *t*Bu have been measured in THF solution at –70 °C.

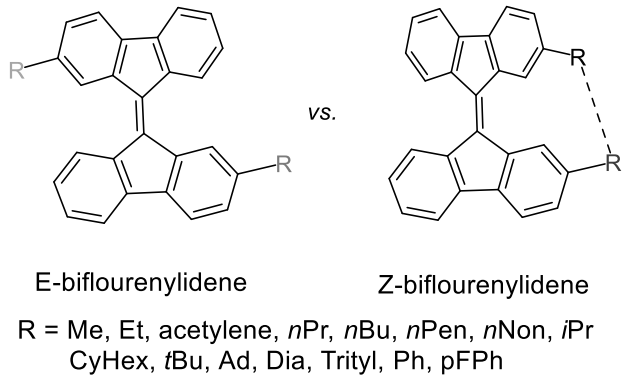

Figure 19. Schreiner's choice for the determination of solvophobic effects.

In 2024 Shimizu *et al*. developed molecular torsional balances (Figure 20) to measure and model the organic solvophobic effect across 46 solvent systems with varying alkyl surface lengths (ethyl, hexyl, undecyl).[109] By using ^{19}F NMR spectroscopy to assess folding ratios and incorporating a control balance to isolate alkyl surface effects, the study quantified solvophobic interactions. The analysis, based on solvent parameters and surface area differences between folded and unfolded conformers, led to a predictive model for association energies of alkane dimers.

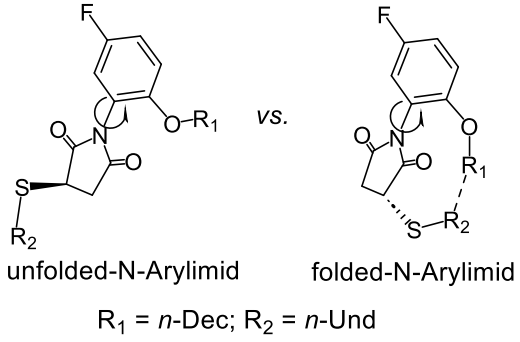

Figure 20. Shimizu's system of choice, alkane chains on N-Arylamide backbones.

These findings were summarized in a review by Cockroft *et al*.[3] showing "a context-dependent" significance of LD in solution by noting that alkyl-alkyl interactions in proximity result in the observation of stronger LD interactions. Moreover, perfluorinated alkanes or very rigid and close contacts in balances are more likely to contribute to the investigation of solvophopic effects rather than intramolecular LD forces.

1.4.2 Interactions in 1,4-substituted cyclooctatetraenes

While still heavily discussed, LD seems to be readily measurable in cyclooctatetraene derivatives (Figure 21) due to their close contact and high symmetry.[56,82] The balances have already been extended to silyl groups,[84] silyl protected alcohols,[83] and even to a water

mimicking tracking of a transition state.[85] All of those recent enhancements found dispersion forces to be a very well measurable force which might only be attenuated due to respect of the expectations due to "not that precise" computations.[70,55] As a matter of fact, the recent investigations find that while in close contact and under the right conditions (in respect of floppiness – entropy diminishing, and close proximity to each other) LD forces are always dominant and never vanish.

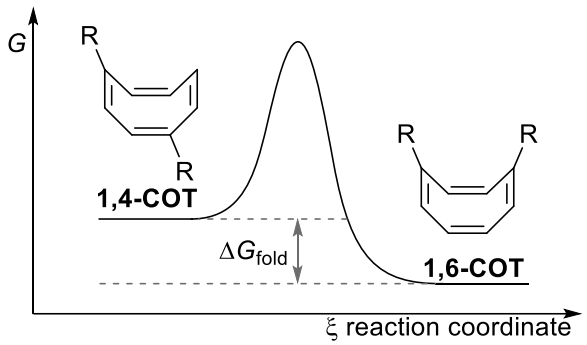

Figure 21. Simplified equilibrium of 1,4- and 1,6-R-COT.

Table 1 shows a broad overview of 1,4-COT derivatives where the equilibrium was determined, solvents and temperature vary strongly so that no direct comparison between all derivatives can be made. However, all moieties ranging from pure aliphatic to highly polar groups such as nitrosyl show a preference for the folded isomer. For R = CH_2OH, water as solvent was chosen to outline the strong electrostatic influence which diminished the intramolecular LD interaction almost completely. Furthermore, solvents are discussed in Table 2.

So far, no extensive investigation on solvent effects on the most prominent example for a molecular balance di-*t*Bu-COT (Figure 22) has been performed. The main study of this thesis focused on this topic. The resulting Table 2 of different equilibrium constants in 15 solvents with the same balance shows clearly that a solvent effect on folding does exist.

Table 1: A brief overview of all known COT derivatives with determined Gibbs free Energy.

R	solvent	$\Delta H^{\ominus}_{fold}$ [kcal mol^{-1}]	$\Delta S^{\ominus}_{fold}$ [cal mol^{-1} K^{-1}]	ΔG^{T}_{fold} [kcal mol^{-1}]	$K_{eq.}$ [1,6]/[1,4]
H[91,94,56]	$CHCl_3$	n.a.	n.a.	0.00 (298 K)	1.00
Me[95,102]	benzene	−0.05	−0.3	−0.08 (293 K)	1.15
Et[82,105]	benzene	−0.52	1.0	−0.24 (293 K)	1.52
*i*Pr[82,105]	benzene	−0.61	1.0	−0.36 (293 K)	1.84
*t*Bu[44,80]	$CHCl_3$	−1.14	2.5	−0.39 (298 K)	1.93
Ad[57]	*n*-hexane	−0.26	−0.36	−0.14 (333 K)	1.29
Dia[57]	*n*-hexane	−0.79	−1.81	−0.19 (333 K)	1.34
Ph[110]	$CHCl_3$	n.d.	n.d.	−0.18 (298 K)	1.35
CH_2OH[85]	water	n.d.	n.d.	+0.02 (298 K)	0.97
$(CH_2)_2OH$[45]	water	n.d.	n.d.	−0.25 (273 K)	1.60
NO_2[81,100,111]	$CHCl_3$	−1.98	4.5	−0.61 (293 K)	2.86

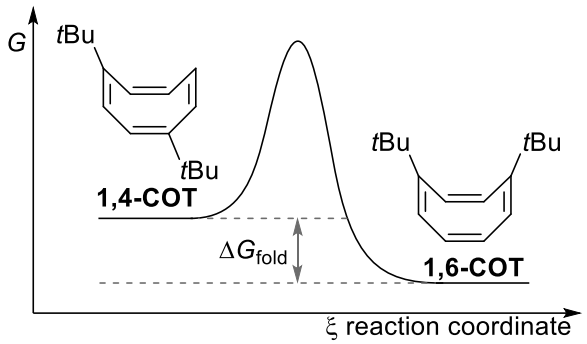

Figure 22. Simplified equilibrium of 1,4- and 1,6-*t*Bu-COT.

However, this must not and cannot be only attributed to a cancelation effect on LD as many publications suggest. Solvophobic effects as well as strong electrostatics in more polar solvents are making the interpretation of data harder the more data are produced. As already stated, the enthalpic energy stays very similar in each solvent and is countered by entropy.

The second focus of this thesis was to rule those effects out. From the first study it was clear that *t*Bu-COT shows the smallest preference for the folded isomer in a pure aliphatic solvent like cyclohexane or *n*-hexane. So, the concept of matching solvent type with balance type as both are purely hydrocarbon based was born. Using increasing polarizable aliphatic solvents representing size increase as the molecular balances to diminish or attenuate possible intramolecular interactions versus solvent-solute intermolecular interactions.

Table 2. Determination of the folding behavior of 1,4-*t*Bu-COT in various solvents.[56] The solvents are listed according to their solvent polarizability (SP) value. The SP value is an empirical value of LD for each solvent by Hopf and Catalan.[112]

solvent	SP	$\Delta H^{\ominus}_{fold}$ [kcal mol^{-1}]	$\Delta S^{\ominus}_{fold}$ [cal mol^{-1} K^{-1}]	$\Delta G^{303\ K}_{fold}$ [kcal mol^{-1}]	$K_{eq.}$ [1,6]/[1,4]
n-hexane	0.6164	−0.39±0.02	−0.75±0.06	−0.16±0.03	1.31
ethanol	0.6334	−0.42±0.02	−0.53±0.05	−0.26±0.03	1.54
acetonitrile	0.6448	−0.74±0.03	−1.06±0.10	−0.42±0.03	2.01
acetone	0.6510	−0.49±0.01	−0.47±0.04	−0.35±0.03	1.78
acetic acid	0.6513	−0.55±0.01	−0.62±0.04	−0.36±0.03	1.83
cyclohexane	0.6830	−0.50±0.04	−1.14±0.12	−0.15±0.03	1.29
DMF	0.7589	−0.65±0.01	−0.76±0.04	−0.42±0.03	2.01
CH_2Cl_2	0.7612	−0.64±0.02	−0.72±0.09	−0.42±0.03	2.02
CCl_4	0.7677	−0.57±0.03	−1.02±0.10	−0.26±0.03	1.54
toluene	0.7816	−0.65±0.03	−1.17±0.09	−0.30±0.03	1.63
$CHCl_3$	0.7833	−0.80±0.02	−1.33±0.05	−0.40±0.03	1.93
benzene	0.7929	−0.88±0.03	−1.92±0.10	−0.30±0.03	1.64
DMSO	0.8295	−0.63±0.03	−0.61±0.10	−0.45±0.03	2.10
pyridine	0.8416	−0.78±0.02	−1.27±0.07	−0.40±0.03	1.93
CS_2	1.0000	−0.65±0.06	−1.02±0.20	−0.34±0.03	1.76

The effects of silyl groups as direct Dispersion Energy Donors (DEDs), focusing on their steric size and polarizability have been investigated. Silyl groups, being larger and more polarizable than alkyl groups, were found to be effective DEDs. However, the bulkiness in proximity of these groups was correlated with established steric parameters, such as *A*-values, solvolysis rates, and Tolman's θ. Internal strain within the COT backbone was identified as the main factor favoring the unfolded isomer (Figure 23). For all derivatives larger than TMS, the unfolded isomer is favored as seen in Table 3.

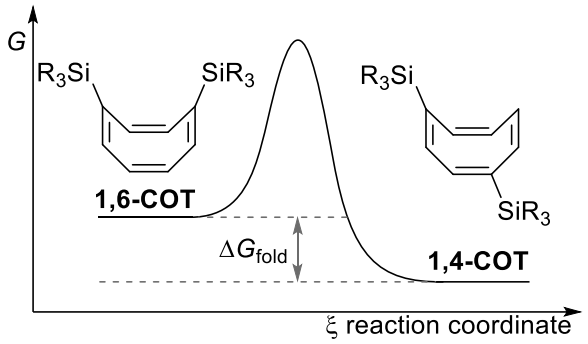

Figure 23. Simplified equilibrium of substituted 1,4- and 1,6-SiR_3-COT.

Table 3. Overview of all Silyl COT derivatives in toluene.[84]

SiR_3	$\Delta G_{fold}^{313\,K}$ [kcal mol^{-1}]	$K_{eq.}$ [1,6]/[1,4]
TMS	−0.19±0.03	1.36
TBDMS	+0.64±0.03	0.36
TES	+0.49±0.02	0.46
TIBS	+0.97±0.05	0.21
TIPS	+1.75±0.09	0.06

This negative trend can be reversed when a CH_2O spacer group is placed between COT and the silyl groups (Figure 24). The NMR measurements reveal that the bulky TIPS group shifts the equilibrium furthest towards the folded and more crowded valence isomer. However, flexibility due to the CH_2O spacer comes at the cost of unfavorable folding entropy. The result is a 1:1 ratio of all derivatives as seen in Table 4.

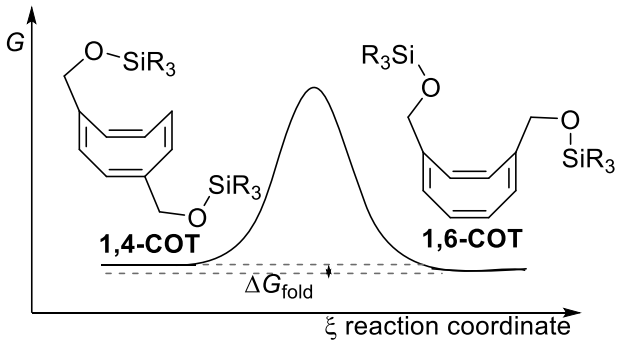

Figure 24: Simplified equilibrium of 1,4- and 1,6-CH_2O-SiR_3-COT.

Table 4. Overview of Gibbs Free Energy in toluene of 1,4- and 1,6-CH_2O-SiR_3-COT.[83]

SiR_3	$\Delta G_{fold}^{313\,K}$ [kcal mol^{-1}]	$K_{eq.}$ [1,6]/[1,4]
TMS	−0.01±0.03	1.01±0.05
TBDMS	−0.08±0.03	1.14±0.06
TES	−0.03±0.03	1.05±0.05
TIPS	−0.14±0.03	1.26±0.05
TBDPS	−0.10±0.03	1.18±0.06
TTMSS	+0.13±0.03	0.81±0.06

The COT molecular backbone was also used to study hydrogen bonding via a model system (Figure 25) resembling the cyclic water dimer transition structure.[85] Energy decomposition analysis showed that electrostatic interactions dominate the hydrogen bonding (65% of the total energy), with London dispersion (LD) interactions contributing 25%. Similar contributions have been noted in the theoretical vdW Coefficients in Figure 2. As visible in Table 5, the highest proportion of the folded isomer was observed in apolar

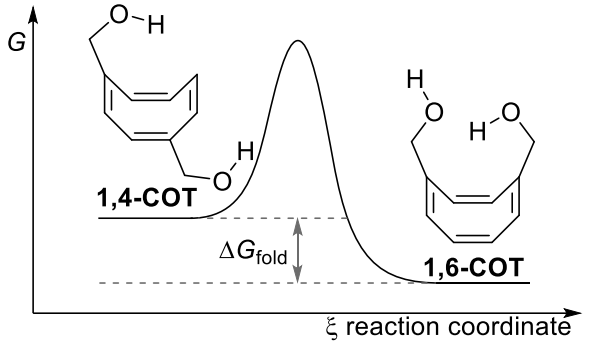

Figure 25. Simplified equilibrium of 1,4- and 1,6-CH_2O-H-COT.

Table 5. Folding ratios of CH_2OH COT in various solvents ranked according to their SP value.[85]

solvent	SP	$\Delta G_{fold}^{298\,K}$ [kcal mol^{-1}]	$K_{eq.}$ [1,6]/[1,4]
cyclohexane	0.6830	−0.90±0.03	4.66±0.23
CH_2Cl_2	0.7612	−0.28±0.03	1.61±0.08
CCl_4	0.7677	−1.03±0.03	5.80±0.29
toluene	0.7816	−0.43±0.03	2.09±0.10
benzene	0.7929	−0.33±0.03	1.74±0.09
$CHCl_3$	0.7833	−0.39±0.03	1.95±0.10
DMSO	0.8295	−0.03±0.03	1.05±0.05
pyridine	0.8416	−0.12±0.02	1.23±0.06
TCE	0.8870	−0.12±0.03	1.22±0.06
nitrobenzene	0.8910	−0.07±0.03	1.12±0.06
water	n.a.	+0.02±0.02	0.97±0.05

solvents (cyclohexane, tetrachloromethane), while a 1:1 ratio was found in polar and polar-protic solvents (DMSO, water). This emphasizes the significant role of solubility and the solvophobic effect in stabilizing strong hydrogen bonds between heterogeneous atoms.

Performing a Local Energy Decomposition[34] analysis with the ORCA program[113] on the simple water dimer results (part of the LED training session of the 2017 Orca user meeting) in an overall stabilizing energy of the dimer of –4.5 kcal mol^{-1} with a powerful increment of stabilization energy of –1.1 kcal mol^{-1} of pure LD energy. Comparing the –1.1 kcal mol^{-1} computed value with the ΔG of the measured value of 1,4-di-CH_2OH-COT in cyclohexane or tetrachloromethane results in –0.9 to –1.03±0.03 kcal mol which is a strong indicator of the absence of further water molecules in the hydrophobic environment. Hence, the balance mimics the water dimer almost perfectly. The solvation of the balance in pure water completely resolves the observable ratio of 1,6 being the most prominent isomer. This is easily explained by the compensation effect of surrounding water molecules being able to form dimers with the hydroxy moiety. This is the most prominent example that even in hydrogen bonds there is a significant portion of LD interactions at play and cannot be neglected.

1.5 Outlook

1.5.1 Gedankenexperiment I: H, D, F

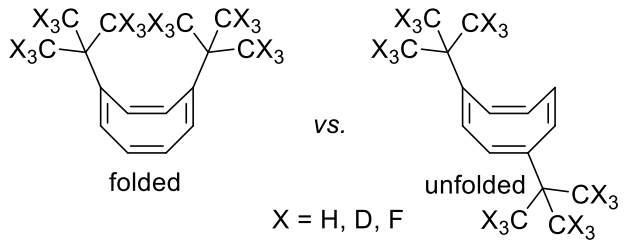

Figure 26. Proposed Gedankenexperiment of perfluorinated, perdeuterated *t*Bu substituents.

As we have shown, COT with *t*Bu substituents is already the prime example to determine LD interactions whether complete deuteration or fluorination changes the equilibrium. Hence deuterated D–C bonds are shorter than H–C bonds, the perfect distance for LD might be diminished. A similar comparison of fluorine and hydrogen (F–C and H–C) will have a huge difference in polarizability, which might also be an interesting option worth investigation. However, since the changes in the equilibrium constant will be rather small a purely computational investigation is recommended.

1.5.2 Gedankenexperiment II: C, Si, Ge, Sn, Pb

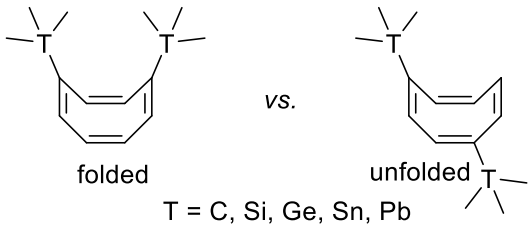

Figure 27: Proposed Gedankenexperiment on increasing polarizability by varying the tetrel (T) in the COT environment.

As we have shown in "Hexaphenylditetrels-When longer bonds provide higher stability" (see Chapter 3.2) the effect of elongated bonds[114] might be worthwhile to check on the cyclooctatetraene backbone. Since the synthesis route of the silica COT is known it might also be applicable for other trimethyltetrelchlorides. The increasing bond length towards the lead compound might result in further repulsive effects.

1.6 Concluding remarks

Our studies clearly show the abundance and availability of LD forces by computational investigations and spectroscopic measurements. By using Fritz London's formula, we were able to determine a direct influence of the size of substituents as well as their distance relationship on dispersive attraction between them. The claim that LD forces are negligible in solution does not hold true demonstrated on multiple model systems. However, Shimizu's,[109] Cockroft's,[63] Chen's,[70] and Wegner's[74] studies of attractive interactions in solutions using models with long alkyl chains lead to predominantly solvophobic-driven attraction between these alkyl chains, whereas our molecular balances behave in a similar fashion in gas phase and solvent model computations as well as experimental investigations showing much higher degree of actual dispersive interactions over solvophobic effect. Additionally, our balances are modular and can be refined to further isolate the dispersion interactions or adapted to accommodate ions to study other vdW forces.

1.7 Bibliography

(1) London, F. Zur Theorie und Systematik der Molekularkräfte. *Z. Phys.* **1930**, *63* (3), 245–279.

(2) Yang, L.; Adam, C.; Nichol, G. S.; Cockroft, S. L. How Much Do van Der Waals Dispersion Forces Contribute to Molecular Recognition in Solution? *Nat. Chem.* **2013**, *5* (12), 1006–1010.

(3) Gravillier, L.-A.; Cockroft, S. L. Context-Dependent Significance of London Dispersion. *Acc. Chem. Res.* **2023**, *56* (23), 3535–3544.

(4) Wagner, J. P.; Schreiner, P. R. London Dispersion in Molecular Chemistry—Reconsidering Steric Effects. *Angew. Chem. Int. Ed.* **2015**, *54* (42), 12274–12296.

(5) Grimme, S.; Huenerbein, R.; Ehrlich, S. On the Importance of the Dispersion Energy for the Thermodynamic Stability of Molecules. *ChemPhysChem* **2011**, *12* (7), 1258–1261.

(6) Eisenschitz, R.; London, F. Über das Verhältnis der van der Waalsschen Kräfte zu den homöopolaren Bindungskräften. *Z. Phys.* **1930**, *60* (7), 491–527.

(7) Rummel, L.; Schreiner, P. R. Advances and Prospects in Understanding London Dispersion Interactions in Molecular Chemistry. *Angew. Chem. Int. Ed.* **2024**, *63*, e202316364.

(8) Grimme, S.; Schreiner, P. R. The Role of London Dispersion Interactions in Modern Chemistry. *Acc. Chem. Res.* **2024**, *57* (16), 2233–2233.

(9) Schneider, H.-J. Dispersive Interactions in Solution Complexes. *Acc. Chem. Res.* **2015**, *48* (7), 1815–1822.

(10) Schneider, H.-J. Distinction and Quantification of Noncovalent Dispersive and Hydrophobic Effects. *Molecules* **2024**, *29* (7), 1591.

(11) Yang, L.; Adam, C.; Cockroft, S. L. Quantifying Solvophobic Effects in Nonpolar Cohesive Interactions. *J. Am. Chem. Soc.* **2015**, *137* (32), 10084–10087.

(12) Elmi, A.; Cockroft, S. L. Quantifying Interactions and Solvent Effects Using Molecular Balances and Model Complexes. *Acc. Chem. Res.* **2021**, *54* (1), 92–103.

(13) Hunter, C. A. Quantifying Intermolecular Interactions: Guidelines for the Molecular Recognition Toolbox. *Angew. Chem. Int. Ed.* **2004**, *43* (40), 5310–5324.

(14) Cockroft, S. L.; Hunter, C. A. Desolvation Tips the Balance: Solvent Effects on Aromatic Interactions. *Chem. Commun.* **2006**, No. 36, 3806–3808.

(15) Cockroft, S. L.; Hunter, C. A. Chemical Double-Mutant Cycles: Dissecting Non-Covalent Interactions. *Chem. Soc. Rev.* **2007**, *36* (2), 172–188.

(16) Carroll, W. R.; Pellechia, P.; Shimizu, K. D. A Rigid Molecular Balance for Measuring Face-to-Face Arene−Arene Interactions. *Org. Lett.* **2008**, *10* (16), 3547–3550.

(17) Hwang, J.; Li, P.; Smith, M. D.; Shimizu, K. D. Distance-Dependent Attractive and Repulsive Interactions of Bulky Alkyl Groups. *Angew. Chem. Int. Ed.* **2016**, *55* (28), 8086–8089.

(18) van der Waals, J. D. Over de Continuiteit van den Gas- en Vloeistoftoestand. Ph.D. Thesis, Universität Leiden, Leiden, Netherlands, 1873.

(19) Israelachvili, J. N. *Intermolecular and Surface Forces*; Academic Press, 2011.

(20) London, F. The General Theory of Molecular Forces. *Trans. Faraday Soc.* **1937**, *33* (0), 8b–26.
(21) Ferrighi, L.; Madsen, G. K. H.; Hammer, B. Alkane Dimers Interaction: A Semi-Local MGGA Functional Study. *Chem. Phys. Lett.* **2010**, *492* (1), 183–186.
(22) Pitzer, K. S.; Catalano, E. Electronic Correlation in Molecules. III. The Paraffin Hydrocarbons1. *J. Am. Chem. Soc.* **1956**, *78* (19), 4844–4846.
(23) Kahr, Bart.; Van Engen, Donna.; Mislow, Kurt. Length of the Ethane Bond in Hexaphenylethane and Its Derivatives. *J. Am. Chem. Soc.* **1986**, *108* (26), 8305–8307.
(24) Rösel, S.; Balestrieri, C.; R. Schreiner, P. Sizing the Role of London Dispersion in the Dissociation of All- Meta Tert-Butyl Hexaphenylethane. *Chem. Sci.* **2017**, *8* (1), 405–410.
(25) Rösel, S.; Schreiner, P. R. Computational Chemistry as a Conceptual Game Changer: Understanding the Role of London Dispersion in Hexaphenylethane Derivatives (Gomberg Systems). *Isr. J. Chem.* **2022**, *62* (1–2), e202200002.
(26) Grimme, S.; Schreiner, P. R. Steric Crowding Can Stabilize a Labile Molecule: Solving the Hexaphenylethane Riddle. *Angew. Chem. Int. Ed.* **2011**, *50* (52), 12639–12642.
(27) Maier, G.; Neudert, J.; Wolf, O.; Pappusch, D.; Sekiguchi, A.; Tanaka, M.; Matsuo, T. Tetrakis(Trimethylsilyl)Tetrahedrane. *J. Am. Chem. Soc.* **2002**, *124* (46), 13819–13826.
(28) Contreras-García, J.; Johnson, E. R.; Keinan, S.; Chaudret, R.; Piquemal, J.-P.; Beratan, D. N.; Yang, W. NCIPLOT: A Program for Plotting Noncovalent Interaction Regions. *J. Chem. Theory Comput.* **2011**, *7* (3), 625–632.
(29) Heitler, W.; London, F. Wechselwirkung neutraler Atome und homöopolare Bindung nach der Quantenmechanik. *Z. Phys.* **1927**, *44* (6), 455–472.
(30) Keesom, W. H. The Second Viral Coefficient for Rigid Spherical Molecules, Whose Mutual Attraction Is Equivalent to That of a Quadruplet Placed at Their Centre. *Proc. R. Acad. Sci.* **1915**, No. 18, 636–646.
(31) Debye, P. Reaction Rates in Ionic Solutions. *Trans. Electrochem. Soc.* **1942**, *82* (1), 265.
(32) Jansen, G. Symmetry-Adapted Perturbation Theory Based on Density Functional Theory for Noncovalent Interactions. *WIREs Comput. Mol. Sci.* **2014**, *4* (2), 127–144.
(33) Schneider, W. B.; Bistoni, G.; Sparta, M.; Saitow, M.; Riplinger, C.; Auer, A. A.; Neese, F. Decomposition of Intermolecular Interaction Energies within the Local Pair Natural Orbital Coupled Cluster Framework. *J. Chem. Theory Comput.* **2016**, *12* (10), 4778–4792.
(34) Altun, A.; Neese, F.; Bistoni, G. Local Energy Decomposition Analysis of Hydrogen-Bonded Dimers within a Domain-Based Pair Natural Orbital Coupled Cluster Study. *Beilstein J. Org. Chem.* **2018**, *14* (1), 919–929.
(35) Altun, A.; Saitow, M.; Neese, F.; Bistoni, G. Local Energy Decomposition of Open-Shell Molecular Systems in the Domain-Based Local Pair Natural Orbital Coupled Cluster Framework. *J. Chem. Theory Comput.* **2019**, *15* (3), 1616–1632.
(36) Bistoni, G.; Altun, A.; Wang, Z.; Neese, F. Local Energy Decomposition Analysis of London Dispersion Effects: From Simple Model Dimers to Complex Biomolecular Assemblies. *Acc. Chem. Res.* **2024**, *57* (9), 1411–1420.

(37) Grimme, S.; Hansen, A.; Brandenburg, J. G.; Bannwarth, C. Dispersion-Corrected Mean-Field Electronic Structure Methods. *Chem. Rev.* **2016**, *116* (9), 5105–5154.
(38) Löwdin, P.-O. Quantum Theory of Many-Particle Systems. III. Extension of the Hartree-Fock Scheme to Include Degenerate Systems and Correlation Effects. *Phys. Rev.* **1955**, *97* (6), 1509–1520.
(39) Grimme, S. Density Functional Theory with London Dispersion Corrections. *WIREs Comput. Mol. Sci.* **2011**, *1* (2), 211–228.
(40) Riplinger, C.; Neese, F. An Efficient and near Linear Scaling Pair Natural Orbital Based Local Coupled Cluster Method. *J. Chem. Phys.* **2013**, *138* (3), 034106.
(41) Liakos, D. G.; Sparta, M.; Kesharwani, M. K.; Martin, J. M. L.; Neese, F. Exploring the Accuracy Limits of Local Pair Natural Orbital Coupled-Cluster Theory. *J. Chem. Theory Comput.* **2015**, *11* (4), 1525–1539.
(42) Yepes, D.; Neese, F.; List, B.; Bistoni, G. Unveiling the Delicate Balance of Steric and Dispersion Interactions in Organocatalysis Using High-Level Computational Methods. *J. Am. Chem. Soc.* **2020**, *142* (7), 3613–3625.
(43) Bistoni, G. Finding Chemical Concepts in the Hilbert Space: Coupled Cluster Analyses of Noncovalent Interactions. *WIREs Comput. Mol. Sci.* **2020**, *10* (3), e1442.
(44) Lyttle, M. H.; Streitwieser, A.; Kluttz, R. Q. Unusual Equilibrium between 1,4- and 1,6-Di-Tert-Butylcyclooctatetraenes. *J. Am. Chem. Soc.* **1981**, *103* (11), 3232–3233.
(45) Gottesfeld, M. R.; Masoudi, F. A.; Hansen, D. E. Unusual (but Precedented) Equilibrium between 1,4- and 1,6-Di-(2-Hydroxyethyl)Cyclooctatetraene. *Tetrahedron Lett.* **1992**, *33* (4), 447–450.
(46) Paliwal, S.; Geib, S.; Wilcox, C. S. Molecular Torsion Balance for Weak Molecular Recognition Forces. Effects of "Tilted-T" Edge-to-Face Aromatic Interactions on Conformational Selection and Solid-State Structure. *J. Am. Chem. Soc.* **1994**, *116* (10), 4497–4498.
(47) Mati, I. K.; Cockroft, S. L. Molecular Balances for Quantifying Non-Covalent Interactions. *Chem. Soc. Rev.* **2010**, *39* (11), 4195–4205.
(48) Strauss, M. A.; Wegner, H. A. Molecular Systems for the Quantification of London Dispersion Interactions. *Eur. J. Org. Chem.* **2019**, *2019* (2–3), 295–302.
(49) Jian, J.; Poater, J.; White, P. B.; McKenzie, C. J.; Bickelhaupt, F. M.; Mecinović, J. Probing Halogen–π versus CH–π Interactions in Molecular Balance. *Org. Lett.* **2020**, *22* (20), 7870–7873.
(50) Solel, E.; Ruth, M.; Schreiner, P. R. London Dispersion Helps Refine Steric A-Values: Dispersion Energy Donor Scales. *J. Am. Chem. Soc.* **2021**, *143* (49), 20837–20848.
(51) Solel, E.; Ruth, M.; Schreiner, P. R. London Dispersion Helps Refine Steric A-Values: The Halogens. *J. Org. Chem.* **2021**, *86* (11), 7701–7713.
(52) West, A. M. L.; Dominelli-Whiteley, N.; Smolyar, I. V.; Nichol, G. S.; Cockroft, S. L. Experimental Quantification of Halogen···Arene van Der Waals Contacts. *Angew. Chem. Int. Ed.* **2023**, *135* (38), e202309682.
(53) Strauss, M. A.; Wegner, H. A. London Dispersion in Alkane Solvents. *Angew. Chem. Int. Ed.* **2021**, *60* (2), 779–786.
(54) Ehlert, S.; Grimme, S.; Hansen, A. Conformational Energy Benchmark for Longer N-Alkane Chains. *J. Phys. Chem. A* **2022**, *126* (22), 3521–3535.

(55) Pollice, R. London Dispersion in Molecular Systems. Ph.D. Thesis, ETH Zurich, Zurich, Switzerland, 2019.
(56) Schümann, J. M.; Wagner, J. P.; Eckhardt, A. K.; Quanz, H.; Schreiner, P. R. Intramolecular London Dispersion Interactions Do Not Cancel in Solution. *J. Am. Chem. Soc.* **2021**, *143* (1), 41–45.
(57) Schümann, J. M.; Ochmann, L.; Becker, J.; Altun, A.; Harden, I.; Bistoni, G.; Schreiner, P. R. Exploring the Limits of Intramolecular London Dispersion Stabilization with Bulky Dispersion Energy Donors in Alkane Solution. *J. Am. Chem. Soc.* **2023**, *145* (4), 2093–2097.
(58) Mati, I. K. Molecular Torsion Balances for Quantifying Non-Covalent Interactions. Ph.D. Thesis, University of Edinburgh, Edinburgh, Scottland, 2013.
(59) Garza, A. J. Solvation Entropy Made Simple. *J. Chem. Theory Comput.* **2019**, *15* (5), 3204–3214.
(60) Oki, M. 1,9-Disubstituted Triptycenes: An Excellent Probe for Weak Molecular Interactions. *Acc. Chem. Res.* **1990**, *23* (11), 351–356.
(61) Gung, B. W.; Xue, X.; Reich, H. J. The Strength of Parallel-Displaced Arene−Arene Interactions in Chloroform. *J. Org. Chem.* **2005**, *70* (9), 3641–3644.
(62) Gung, B. W.; Patel, M.; Xue, X. A Threshold for Charge Transfer in Aromatic Interactions? A Quantitative Study of π-Stacking Interactions. *J. Org. Chem.* **2005**, *70* (25), 10532–10537.
(63) Adam, C.; Yang, L.; Cockroft, S. L. Partitioning Solvophobic and Dispersion Forces in Alkyl and Perfluoroalkyl Cohesion. *Angew. Chem. Int. Ed.* **2015**, *54* (4), 1164–1167.
(64) Nakamura, K.; Houk, K. N. Theoretical Studies of the Wilcox Molecular Torsion Balance. Is the Edge-to-Face Aromatic Interaction Important? *Org. Lett.* **1999**, *1* (13), 2049–2051.
(65) Yang, L.; Brazier, J. B.; Hubbard, T. A.; Rogers, D. M.; Cockroft, S. L. Can Dispersion Forces Govern Aromatic Stacking in an Organic Solvent? *Angew. Chem. Int. Ed.* **2016**, *55* (3), 912–916.
(66) Chong, Y. S.; Carroll, W. R.; Burns, W. G.; Smith, M. D.; Shimizu, K. D. A High-Barrier Molecular Balance for Studying Face-to-Face Arene–Arene Interactions in the Solid State and in Solution. *Chem. Eur. J.* **2009**, *15* (36), 9117–9126.
(67) Hwang, J.; E. Dial, B.; Li, P.; E. Kozik, M.; D. Smith, M.; D. Shimizu, K. How Important Are Dispersion Interactions to the Strength of Aromatic Stacking Interactions in Solution? *Chem. Sci.* **2015**, *6* (7), 4358–4364.
(68) Li, P.; Vik, E. C.; Shimizu, K. D. N-Arylimide Molecular Balances: A Comprehensive Platform for Studying Aromatic Interactions in Solution. *Acc. Chem. Res.* **2020**, *53* (11), 2705–2714.
(69) Rummel, L.; Domanski, M. H. J.; Hausmann, H.; Becker, J.; Schreiner, P. R. London Dispersion Favors Sterically Hindered Diarylthiourea Conformers in Solution. *Angew. Chem. Int. Ed.* **2022**, *134* (29), e202204393.
(70) Pollice, R.; Bot, M.; Kobylianskii, I. J.; Shenderovich, I.; Chen, P. Attenuation of London Dispersion in Dichloromethane Solutions. *J. Am. Chem. Soc.* **2017**, *139* (37), 13126–13140.
(71) Pollice, R.; Fleckenstein, F.; Shenderovich, I.; Chen, P. Compensation of London Dispersion in the Gas Phase and in Aprotic Solvents. *Angew. Chem. Int. Ed.* **2019**, *58* (40), 14281–14288.

(72) Rösel, S.; Becker, J.; Allen, W. D.; Schreiner, P. R. Probing the Delicate Balance between Pauli Repulsion and London Dispersion with Triphenylmethyl Derivatives. *J. Am. Chem. Soc.* **2018**, *140* (43), 14421–14432.

(73) Schweighauser, L.; Strauss, M. A.; Bellotto, S.; Wegner, H. A. Attraction or Repulsion? London Dispersion Forces Control Azobenzene Switches. *Angew. Chem. Int. Ed.* **2015**, *54* (45), 13436–13439.

(74) Strauss, M. A.; Wegner, H. A. Exploring London Dispersion and Solvent Interactions at Alkyl–Alkyl Interfaces Using Azobenzene Switches. *Angew. Chem. Int. Ed.* **2019**, *58* (51), 18552–18556.

(75) Di Berardino, C.; Strauss, M. A.; Schatz, D.; Wegner, H. A. An Incremental System To Predict the Effect of Different London Dispersion Donors in All-Meta-Substituted Azobenzenes. *Chem. Eur. J.* **2022**, *28* (12), e202104284.

(76) Minabe, M.; Oba, T.; Tanaka, M.; Kanno, K.; Tsubota, M. Z/E Selectivity on the Formation of 2,2′-Diacyl-9,9′-Bifluorenylidenes Was Controlled by the Length of Acyl Side Chains. *Chem. Lett.* **2000**, *29* (5), 498–499.

(77) Minabe, M.; Yamazaki, A.; Imai, T.; Takanezawa, T.; Karikomi, M. Formation of 2,2′-Diacyl-9,9′-Bifluorenylidene Isomers from 2-Acyl-9-Bromofluorene and Base-Catalyzed Isomerization of the Formed Alkenes. *Bull. Chem. Soc. Jpn.* **2006**, *79* (11), 1758–1765.

(78) Wilming, F. M.; Becker, J.; Schreiner, P. R. Quantifying Solvophobic Effects in Organic Solvents Using a Hydrocarbon Molecular Balance. *J. Org. Chem.* **2022**, *87* (3), 1874–1878.

(79) Wilming, F. M.; Marazzi, B.; Debes, P. P.; Becker, J.; Schreiner, P. R. Probing the Size Limit of Dispersion Energy Donors with a Bifluorenylidene Balance: Magic Cyclohexyl. *J. Org. Chem.* **2023**, *88* (2), 1024–1035.

(80) Paquette, L. A.; Hefferon, G. J.; Samodral, R.; Hanzawa, Y. Bond Fixation in Annulenes. XIV. Synthesis of and Bond Shifting Equilibrium between 1,4- and 1,6-Di-Tert-Butylcyclooctatetraenes. *J. Org. Chem.* **1983**, *48* (8), 1262–1266.

(81) Todres, Z.; Ovsepyan, G. T.; Bakhmutov, V.; Kosnikov, A. Y.; Lindeman, S.; Struchkov, Y. T. Structure of Difunctional Cyclooctatetraene Derivatives in Crystals and Solutions. 1,4-Di-Nitro-, and (2-Nitrobenzenethio)-Cyclooctatetraenes, 1-Nitro-4-(4-Thiocyanogenbenzeneazo)-, and (2-Nitrobenzenetho) Cyclooctatetraenes and 1-Nitro-4-(2-Nitrobenzenethio) Cyclooctatetraene. *Russ. J. Org. Chem.* **1989**, *25* (1), 75–82.

(82) Anderson, J. E.; Kirsch, P. A. Structural Equilibria Determined by Attractive Steric Interactions. 1,6-Dialkylcyclooctatetraenes and Their Bond-Shift and Ring Inversion Investigated by Dynamic NMR Spectroscopy and Molecular Mechanics Calculations. *J. Chem. Soc. Perkin Trans. 2* **1992**, No. 11, 1951–1957.

(83) Rummel, L.; König, H. F.; Hausmann, H.; Schreiner, P. R. Silyl Groups Are Strong Dispersion Energy Donors. *J. Org. Chem.* **2022**, *87* (19), 13168–13177.

(84) König, H. F.; Rummel, L.; Hausmann, H.; Becker, J.; Schümann, J. M.; Schreiner, P. R. Gauging the Steric Effects of Silyl Groups with a Molecular Balance. *J. Org. Chem.* **2022**, *87* (7), 4670–4679.

(85) König, H. F.; Hausmann, H.; Schreiner, P. R. Assessing the Experimental Hydrogen Bonding Energy of the Cyclic Water Dimer Transition State with a

Cyclooctatetraene-Based Molecular Balance. *J. Am. Chem. Soc.* **2022**, *144* (37), 16965–16973.

(86) Squillacote, M.; Sheridan, R. S.; Chapman, O. L.; Anet, F. A. L. Spectroscopic Detection of the Twist-Boat Conformation of Cyclohexane. Direct Measurement of the Free Energy Difference between the Chair and the Twist-Boat. *J. Am. Chem. Soc.* **1975**, *97* (11), 3244–3246.

(87) Booth, H.; Everett, J. R. The Experimental Determination of the Conformational Free Energy, Enthalpy, and Entropy Differences for Alkyl Groups in Alkylcyclohexanes by Low Temperature Carbon-13 Magnetic Resonance Spectroscopy. *J. Chem. Soc. Perkin Trans. 2* **1980**, No. 2, 255–259.

(88) Mati, I. K.; Adam, C.; Cockroft, S. L. Seeing through Solvent Effects Using Molecular Balances. *Chem. Sci.* **2013**, *4* (10), 3965–3972.

(89) Krug, R. R.; Hunter, W. G.; Grieger, R. A. Statistical Interpretation of Enthalpy–Entropy Compensation. *Nature* **1976**, *261* (5561), 566–567.

(90) Bailey, W. F.; Monahan, A. S. Statistical Effects and the Evaluation of Entropy Differences in Equilibrium Processes. Symmetry Corrections and Entropy of Mixing. *J. Chem. Educ.* **1978**, *55* (8), 489.

(91) Willstätter, R.; Waser, E. Über Cyclo-octatetraen. *Berichte Dtsch. Chem. Ges.* **1911**, *44* (3), 3423–3445.

(92) Schröder, G. *Cyclooctatetraen*; Verlag Chemie, 1965.

(93) Paquette, L. A. The Renaissance in Cyclooctatetraene Chemistry. *Tetrahedron* **1975**, *31* (23), 2855–2883.

(94) Reppe, W.; Schlichting, O.; Klager, K.; Toepel, T. Cyclisierende Polymerisation von Acetylen I Über Cyclooctatetraen. *Justus Liebigs Ann. Chem.* **1948**, *560* (1), 1–92.

(95) Paquette, L. A.; Ley, S. V.; Meisinger, R. H.; Russell, R. K.; Oku, M. Directed Syntheses of the Isomeric Dimethylcyclooctatetraenes and a Study of Their Polarographic and Alkali Metal Reduction. *J. Am. Chem. Soc.* **1974**, *96* (18), 5806–5815.

(96) Lyttle, M. H.; Streitwieser, A.; Miller, M. J. 1,5-Disubstituted Cyclooctatetraenes. *J. Org. Chem.* **1989**, *54* (10), 2331–2335.

(97) Andrés, J. L.; Castaño, O.; Morreale, A.; Palmeiro, R.; Gomperts, R. Potential Energy Surface of Cyclooctatetraene. *J. Chem. Phys.* **1998**, *108* (1), 203–207.

(98) Castaño, O.; Palmeiro, R.; Frutos, L. M.; Luisandrés, J. Role of Bifurcation in the Bond Shifting of Cyclooctatetraene. *J. Comput. Chem.* **2002**, *23* (7), 732–736.

(99) Anet, F. A. L. The Rate of Bond Change in Cycloöctatetraene. *J. Am. Chem. Soc.* **1962**, *84* (4), 671–672.

(100) Todres, Z. V.; Ovsepyan, G. Ts. Valence Isomerization of 1,4-Di-Nitrocyclooctatetraene. *Bull. Acad. Sci. USSR Div. Chem. Sci.* **1985**, *34* (8), 1597–1599.

(101) Eaton, P. E.; Stossel, D. Synthesis of Alkynylcyclooctatetraenes and Alkynylcubanes. *J. Org. Chem.* **1991**, *56* (17), 5138–5142.

(102) Anderson, J. E.; Kirsch, P. A. Molecular Structures Determined by Intramolecular Attractive Steric Interactions. Dynamic NMR and Molecular Mechanics Investigation of 1,6-Di-Methylcyclo-Octatetraene. *J. Chem. Soc. Perkin Trans. 2* **1990**, No. 6, 885–889.

(103) Burton, N. C.; Cloke, F. G. N.; Joseph, S. C. P.; Karamallakis, H.; Sameh, A. A. Trimethylsilyl Derivatives of Cyclooctatetraene. *J. Organomet. Chem.* **1993**, *462* (1), 39–43.
(104) Gasteiger, J.; Huisgen, R. 9-Thiabicyclo[4.2.1]Nona-2,4,7-Triene 9,9-Dioxide. *J. Am. Chem. Soc.* **1972**, *94* (18), 6541–6543.
(105) Kirsch, P. A. Molecular Equilibria Determined by van Der Waals' Attraction. Ph.D. Thesis, University College London, London, 1991.
(106) Belostotskaya, I. S.; Komissarova, N. L.; Dzhuaryan, É. V.; Ershov, V. V. The Ortho-Alkylation of Catechol. *Bull. Acad. Sci. USSR Div. Chem. Sci.* **1972**, *21* (7), 1535–1536.
(107) Shimizu, K. D. A Solution to Dispersion Interactions. *Nat. Chem.* **2013**, *5* (12), 989–990.
(108) Lüttschwager, N. O. B.; Wassermann, T. N.; Mata, R. A.; Suhm, M. A. The Last Globally Stable Extended Alkane. *Angew. Chem. Int. Ed.* **2013**, *52* (1), 463–466.
(109) Manzewitsch, A. N.; Liu, H.; Lin, B.; Li, P.; Pellechia, P. J.; Shimizu, K. D. Empirical Model of Solvophobic Interactions in Organic Solvents. *Angew. Chem. Int. Ed.* **2024**, *63* (2), e202314962.
(110) Lyttle, M. H. Ph.D. Thesis, University of California, Berkeley, 1982.
(111) Todres, Z. V.; Ovsepyan, G. Ts.; Garbuzova, I. A.; Stankevich, I. V.; Bakhmutov, V. I. Electronic Structure of Dianion of 1,4-Dinitrocyclo-Octatetraene. *Bull. Acad. Sci. USSR Div. Chem. Sci.* **1987**, *36* (9), 1824–1828.
(112) Catalán, J.; Hopf, H. Empirical Treatment of the Inductive and Dispersive Components of Solute–Solvent Interactions: The Solvent Polarizability (SP) Scale. *Eur. J. Org. Chem.* **2004**, *2004* (22), 4694–4702.
(113) Neese, F. The ORCA Program System. *WIREs Comput. Mol. Sci.* **2012**, *2* (1), 73–78.
(114) Rummel, L.; Schümann, J.; Schreiner, P. Hexaphenylditetrels – When Longer Bonds Provide Higher Stability. *Chem. Eur. J.* **2021**, *27*.

2. Publications

2.1 Intramolecular London Dispersion Interactions Do Not Cancel in Solution

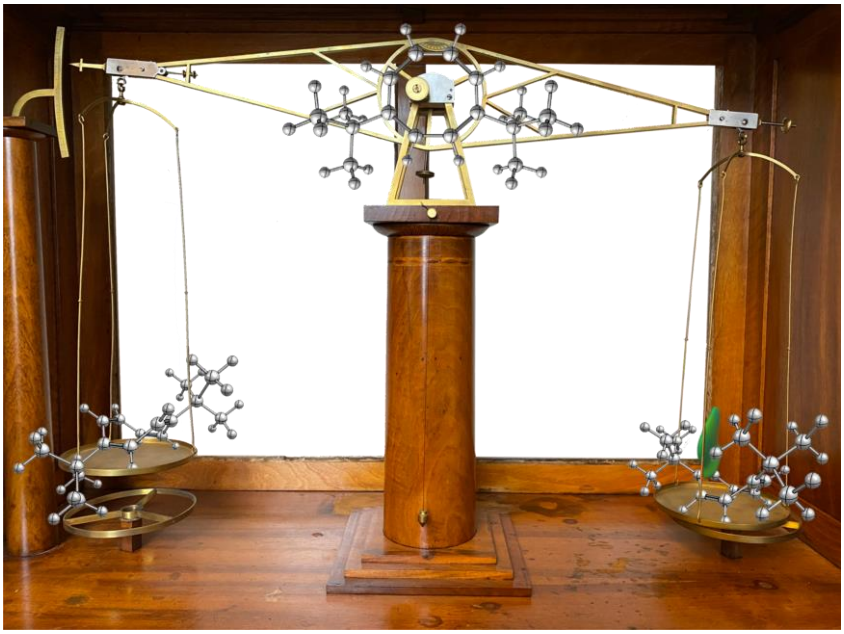

Abstract: We present a comprehensive experimental study of a di-t-butyl-substituted cyclooctatetraene-based molecular balance to measure the effect of 16 different solvents on the equilibrium of folded versus unfolded isomers. In the folded 1,6-isomer, the two t-butyl groups are in close proximity (H···H distance ≈ 2.5 Å), but they are far apart in the unfolded 1,4-isomer (H···H distance ≈ 7 Å). We determined the relative strengths of these noncovalent intramolecular σ−σ interactions via temperature-dependent nuclear magnetic resonance measurements. The origins of the interactions were elucidated with energy decomposition analysis at the density functional and ab initio levels of theory, pinpointing the predominance of London dispersion interactions enthalpically favoring the folded state in any solvent measured.

Reference:

Intramolecular London Dispersion Interactions Do Not Cancel in Solution. - J. M. Schümann, J. P. Wagner, A. K. Eckhardt, H. Quanz, and P. R. Schreiner, *J. Am. Chem. Soc.* **2021**, *143*(*1*), 41–45. **DOI:** 10.1021/jacs.0c09597

JACS
JOURNAL OF THE AMERICAN CHEMICAL SOCIETY
pubs.acs.org/JACS
Communication

Intramolecular London Dispersion Interactions Do Not Cancel in Solution

Jan M. Schümann, J. Philipp Wagner, André K. Eckhardt, Henrik Quanz, and Peter R. Schreiner*

Cite This: J. Am. Chem. Soc. 2021, 143, 41−45
Read Online
ACCESS | Metrics & More | Article Recommendations | Supporting Information

ABSTRACT: We present a comprehensive experimental study of a di-*t*-butyl-substituted cyclooctatetraene-based molecular balance to measure the effect of 16 different solvents on the equilibrium of folded versus unfolded isomers. In the folded 1,6-isomer, the two *t*-butyl groups are in close proximity (H···H distance ≈ 2.5 Å), but they are far apart in the unfolded 1,4-isomer (H···H distance ≈ 7 Å). We determined the relative strengths of these noncovalent intramolecular $\sigma-\sigma$ interactions via temperature-dependent nuclear magnetic resonance measurements. The origins of the interactions were elucidated with energy decomposition analysis at the density functional and *ab initio* levels of theory, pinpointing the predominance of London dispersion interactions enthalpically favoring the folded state in any solvent measured.

London dispersion (LD), the attractive part of the van der Waals potential,[1] is ubiquitously present but often underestimated.[2] This is particularly true for molecules in solution, where it is often assumed that LD is overridden by solvent effects.[3] Recently, this view has been carefully refined,[4−9] but an analysis of a nonpolar molecular balance that avoids additional interactions arising from (local) dipoles is still lacking.[10] Hence, by utilizing a pure hydrocarbon balance, we show here that solvents do affect LD interactions, mostly through changes in the solvent reorganization entropy, but that LD enthalpically remains constant and comparable to gas-phase values. We employ the sterically very different bond shift isomers of 1,4- and 1,6-di-*t*-butyl cycloocta-1,3,5,7-tetraene (**1,4-** and **1,6-COT**, Figure 1) and demonstrate that the thermodynamic preference for LD-stabilized but visually more crowded **1,6-COT** isomer is preserved across 16 solvents ranging from polar to apolar as well as from protic to aprotic.

Highly functionalized molecular balances bearing heteroatoms "fold" (having a preference for the more crowded structure) due to a multitude of interactions (polar, induced dipolar, hydrogen bonding, etc.) and therefore make it difficult to discern these effects from unperturbed LD interactions. A case in point is the often employed "Wilcox−Tröger base-torsion balance" that was initially developed to evaluate nonbonding intramolecular interactions between aromatic rings.[11] Rigid and polar *N*-arylamide balances led to the conclusion that LD is only a small component of the aromatic stacking interaction in solution, in contrast with its dominant role *in vacuo*;[12] the theoretically predicted distance dependence (R^{-6}) of the observed LD stabilization was also confirmed.[13]

Strikingly, the often invoked aryl $\pi-\pi$ interactions are also mimicked by nonaromatic, highly polarizable groups such as cyclohexyl and *t*-butyl ("$\sigma-\sigma$ interactions"[14]) that show the same conformational preference for the chemically less intuitive "folded" state.[15] A pertinent example is the favored all-*cis* conformation of 1,3,5-tribromo-2,4,6-trineopentylbenzene in fluorobenzene.[16] Subsequent investigations suggested based on a comparison of perfluoroalkane versus alkane chain folding that the LD contributions are largely attenuated in solution in reference to computed gas-phase values. Whereas LD was deemed non-negligible, solvophobic effects were found to be dominant in driving the association of apolar chains in aqueous solution.[7]

In choosing an optimal balance to determine solvent effects on LD interactions, we followed the suggested guidelines.[19] Such a balance should display high symmetry, show distinguishable NMR signals at variable temperatures, and have a reasonably low barrier for interconversion of the folded

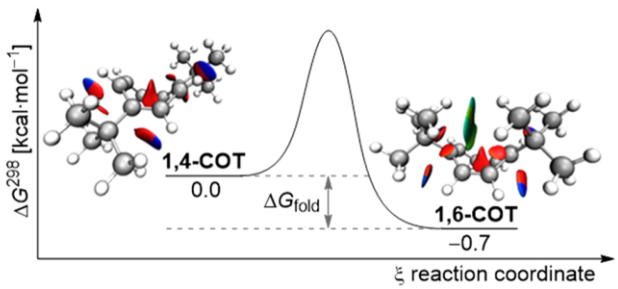

Figure 1. Simplified equilibrium of 1,4- and 1,6-COT. The noncovalent interaction (NCI) surfaces (CCSD(T)/CBS//MP2/cc-pVTZ) are colored on a blue−green−red scale according to an isovalue $s(\rho)$ of 0.35, ranging from $\rho(r)$ −0.025 to 0.025 Å. Blue indicates strong attractive interactions, green corresponds to weak NCIs, and red indicates strong repulsion.[17,18] (See the SI.)

Received: September 7, 2020
Published: December 15, 2020

https://dx.doi.org/10.1021/jacs.0c09597
J. Am. Chem. Soc. 2021, 143, 41−45

Journal of the American Chemical Society pubs.acs.org/JACS Communication

and unfolded states. We found that **1,4-** and **1,6-COT** perfectly fulfill these guidelines and therefore chose this system to determine the effects of LD on its folding preference in a large variety of solvents.[20]

The determination of pure LD interactions in solution is challenging because electrostatic and inductive interactions as well as solvophobic effects favor folding.[21] The energy differences in hydrocarbon configurational isomers are often rather low, and the barriers for their interconversion are high. In most cases, only Gibbs free energies (ΔG) are discussed because they can be determined directly from temperature-dependent equilibrium measurements. Free energies, however, are rather difficult to interpret due to the often encountered enthalpy (ΔH) and entropy (ΔS) compensation.[22] Second, in a first approximation, LD is temperature-independent,[23] so it is instructive to analyze ΔH and ΔS separately. This is important because LD contributes to ΔH, whereas ΔS reflects the disorder of the solute and predominantly solvent reorganization.[24] Our experiments provide the standard isomerization enthalpies ($\Delta_r H^{\ominus}$) and entropies ($\Delta_r S^{\ominus}$) assuming that both are temperature-independent within the chosen experimental window (20−80 °C).

The **COT** isomers considered here were first synthesized by Streitwieser et al.,[20] and a molecular mechanics study helped rationalize the unexpected preference for the apparently more crowded isomer in terms of "intramolecular van der Waals attraction"[25] as early as 1982.[26] Shortly thereafter, Paquette et al. synthesized **1,4-** and **1,6-COT** along a different route, confirming the preference of the more crowded diastereomer in C_6D_6[27] and $CDCl_3$.[25] These results were confirmed and refined in 1992 by Anderson and Kirsch, who demonstrated that with increasing substituent size the preference for the more crowded structure increases on the basis of attractive steric interactions.[28] Early semiempirical[29] and force-field studies[26] on a series of disubstituted COT isomers also suggested that LD might be solely responsible for the observed preference. Remarkably, these pivotal studies have largely been overlooked. The advent of modern computational and improved spectroscopic techniques as well as an improved synthetic approach (*vide infra*) prompted us to study this fascinating system in more detail.

Scheme 1 displays an idealized computed version of the complex valence shift isomerization (VSI) in cyclooctatetraenes;[30] there is spectroscopic evidence of the planar singlet double-bond shift transition state $\mathbf{TS_{DBS}}$ of the parent COT

Scheme 1. Computed Double-Bond Valence Shift (DBS) and Ring Inversion (RI) of Cyclooctatetraene Enthalpies (ΔH_0) at the Level Given[a]

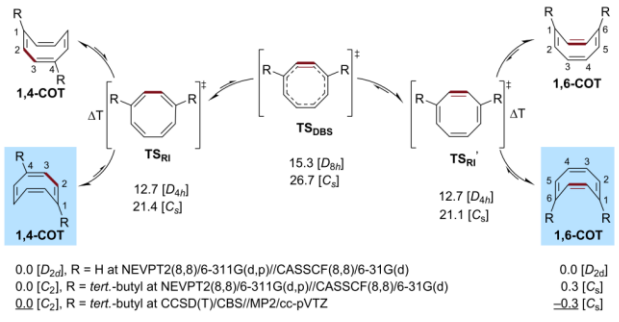

[a]See the SI for details.

that formally violates Hund's rule.[31] Both di-*t*-butyl isomers individually undergo conformational ring isomerization through $\mathbf{TS_{RI}}$ and $\mathbf{TS_{RI}}'$, which are connected via rate-limiting $\mathbf{TS_{DBS}}$, whose description requires multiconfigurational wave functions (such as CASSCF), which do not, however, treat LD in a balanced fashion. The energy of $\mathbf{TS_{DBS}}$ implies that this equilibration will require significant time at ambient temperatures (*vide infra*). The 11.4 kcal mol^{-1} higher energy of the di-*t*-butyl-substituted COT versus the unsubstituted system at TS_{DBS} may be attributed to twice the *t*-butyl strain of ~6 kcal mol^{-1} reported for the axial *t*-butyl ring strain on cyclohexane.[32] Notwithstanding the complexity of the equilibration, only the 1,4- and 1,6-valence bond isomers are observable and can readily be distinguished via NMR spectroscopy (Figure S19). Gratifyingly, the agreement between experimental and computed (enso/xTB) splitting patterns is also in good agreement (Figure S14).

We synthesized **1,4-** and **1,6-COT** utilizing a modification of Paquette's route starting with an ortho-alkylation of **1** using the method of Ershov et al. (Scheme 2).[33] This was followed by a

Scheme 2. Synthesis of the Target Structures[a]

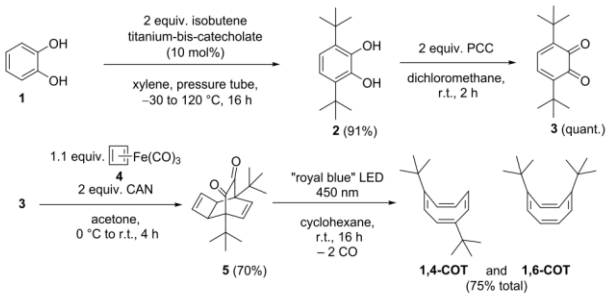

[a]PCC, pyridinium chlorochromate; CAN, ceric(IV) ammonium nitrate; LED, light-emitting diode.

Corey−Suggs oxidation[34] of 3,6-di-*t*-butyl-pyrocatechol (**2**) to 3,6-di-*t*-butyl-*o*-benzochinone (**3**). The Diels−Alder reaction of **3** with cyclobutadiene iron(II) tricarbonyl (**4**), synthesized via Pettit's method,[35] gave 1,6-di-*t*-butyltricyclo[4.2.2.$0^{2,5}$]-deca-3,7-diene-9,10-dione (**5**) as a storable COT precursor from which the target compounds **1,4-** and **1,6-COT** can be prepared cleanly right before the NMR measurements via Strating−Zwanenburg photodecarbonylation.[36] For the synthesis, see the SI.

We decided to take 16 of the most common organic solvents covering most parameters of the empirical solvent polarizability (SP) and solvent polarity−polarizability (SPP) scale established by Catalán and Hopf[37] to estimate their influence on the COT equilibrium. Because **1,4-** and **1,6-COT** are barely soluble in water and hexafluorobenzene, the equilibrium constant (K_{eq}) could not be determined in these.[38] We allowed the isomeric mixtures to equilibrate for at least 1 h at each temperature inside the NMR spectrometer (see details in the SI) by initially warming the sample to the highest possible temperature for a given solvent and decreasing it in 5−10 °C steps immediately thereafter. The resulting experimental data are summarized in Figure 2. Whereas the values of neither Streitwieser et al.[25] nor Paquette et al.[39] (both are different) were reproduced, our results agree well with the most recent measurements of Anderson and Kirsch in the same temperature regime (Figure S1).[28]

https://dx.doi.org/10.1021/jacs.0c09597
J. Am. Chem. Soc. 2021, 143, 41−45

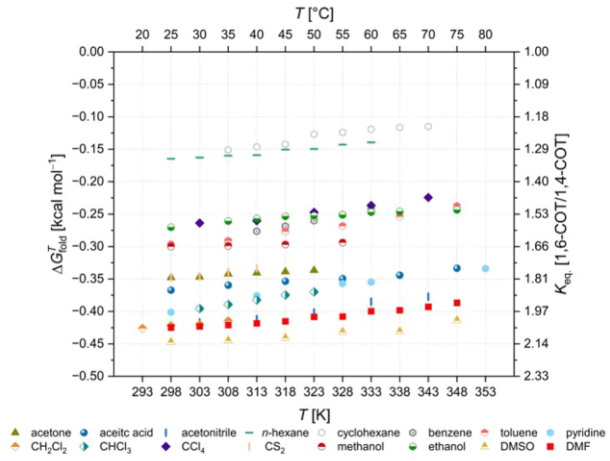

Figure 2. Temperature-dependent Gibbs free energies and equilibrium constants of the **1,4-** and **1,6-COT** equilibrium in various solvents.

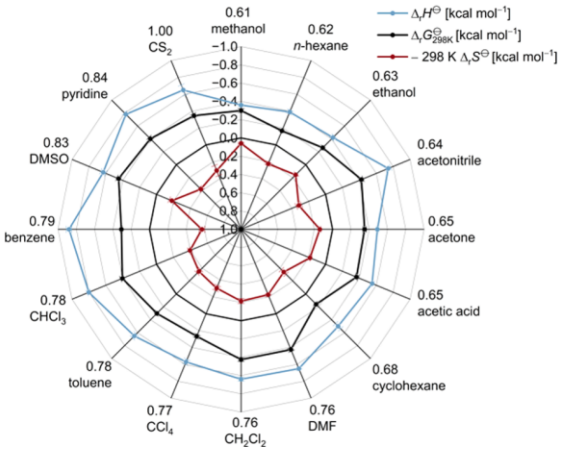

Figure 3. Correlation of thermodynamic quantities at 298 K in kcal mol^{-1} with clockwise increasing relative solvent polarizabilities (min = 0.00 vacuum, max = 1.00 CS_2) (Catalán−Hopf SP scale[37]).

In looking at K_{eq} always being larger than unity, it is clear that **1,6-COT** is *always* favored, just to different degrees depending on the solvent. Whereas solvents of low polarity show the smallest preference for the folded isomer, it is highly favored in polar and chlorinated solvents, which shows that the inductive effect of the dipole moment also is present. Remarkably, the $\Delta_rH^{\ominus}$ values cover a range of only −0.4 to −0.9 kcal mol^{-1} over this wide range of solvents, indicating that the preference for **1,6-COT** is an intrinsic structural property. We therefore conclude that the isomer structures are comparable in different solvents and that the enthalpic intramolecular LD stabilization of **1,6-COT** must be rather similar. The $\Delta_rS^{\ominus}$ values extrapolated from the intercepts with the ordinate vary considerably and thereby have a much larger effect on the $\Delta_rG^{\ominus}$ values. Entropy consistently favors **1,4-COT**, which is at odds with simple symmetry considerations that would favor the C_s over the C_2 symmetric structure due to its reduced rotational symmetry number.[40] Thus we attribute the entropy changes to solvent reorganization. Because of the small changes in enthalpy and the large entropic contributions, we estimate an enthalpy−entropy compensation temperature range of 291 ± 57 K over all 16 solvents (Figure S4). This indicates that only at elevated temperatures, for all solvents above their boiling point, is LD overcome by entropy. We choose 298 K as the temperature for comparing our results for $\Delta_rG^{\ominus}$ (Figure 3).

The $\Delta_rH^{\ominus}$ values increase steadily with increasing solvent polarizabilities, with the exception of a few outliers like DMSO and acetonitrile (Figure 3). This intriguing finding is hard to rationalize and strongly contradicts the importance of competitive dispersive solute−solvent interactions that are thought to diminish LD interactions in solution.[41] Accordingly, comparing the results within solvent groups, we do see trends: In hydrocarbons, the **1,6-COT** preference is proportional to increasing polarizability, hexane < cyclohexane < toluene < benzene. The same is true for chlorinated solvents, CH_2Cl_2 < CCl_4 < $CHCl_3$, and for alcohols with methanol < ethanol. This contradicts the expected simple correlation between solvent polarizability and LD interactions with and within the solute.

Because only LD interactions play a role in solute−solvent interactions, the polar effects of permanent dipole moments have to be taken into account as well. A benchmark study showed that the best results for dipole computations are obtained by the ωB97xD/cc-pVQZ level of theory.[42] The computed gas-phase dipole moments of **1,4-** and **1,6-COT** are rather small (**1,6-COT**, 0.6 D; **1,4-COT**, 0.1 D) but might favor **1,4-COT** in the gas phase and nonpolar solvents. For comparison, the difference in dipole moments between toluene (0.4 D)[43] and benzene (0.0 D)[43] is similar. Taking solvent polarity into account, we find that highly polar solvents indeed favor the population of the higher dipole moment **1,6-COT** isomer. However, this cannot necessarily be traced back to an increased enthalpic interaction but to a favorable entropic origin. One might envision that competition of the solute for dipolar interactions with the solvent disrupts the organized internal structure of the solvent, resulting in a favorable solvent entropy contribution. Because the computed solvent-accessible area of **1,4-COT** (260 Å^2) is even larger than that of **1,6-COT** (256 Å^2), solvent interactions should favor **1,4-COT**.

Having established the given preference for the more crowded isomer irrespective of the environment, we returned to a more detailed molecular analysis and took the B3LYP-D3(BJ)/def2-QZVPP optimized geometries, removed the COT moiety, and saturated the resulting radicals with hydrogen (Figure S18). This should bring the "isolated" interactions of the alkyl groups depicted in the NCI plot in Figure 1 as a green surface to the fore by excluding the COT moiety. To separate electrostatic and inductive effects from the LD, we used symmetry-adapted perturbation theory (DF-SAPT2/aug-cc-pVTZ),[44] which revealed that LD is the largest component of all evaluated interactions, in particular, in **1,6-COT**. Apart from Pauli exchange repulsion, all other contributors (electrostatics and induction together) favor **1,6-COT** by ∼0.5 kcal mol^{-1}, in good agreement with our other energy evaluations (summarized in the SI). In line with this finding, the **1,4-** and **1,6-COT** isomers are almost isoenergetic at the Hartree−Fock level, and the preference for the more crowded structure only comes from the electron correlation, which is the quantum-mechanical origin of LD.

Counterintuitively, intramolecular LD interactions favor the visually sterically more demanding **1,6-COT** isomer in all solvents measured. This preference is assisted by induction and electrostatics, which, in sum, counterbalance the Pauli exchange repulsion. LD is thereby the largest single energy

https://dx.doi.org/10.1021/jacs.0c09597
J. Am. Chem. Soc. 2021, 143, 41−45

contributor. The equilibrium $\Delta_r H^{\ominus}$ values vary from −0.4 to −0.9 kcal mol^{-1}, whereas $\Delta_r G^{\ominus}$ values at 298 K (−0.2 to −0.4 kcal mol^{-1}) attenuate these by a positive entropy contribution arising from solvent reorganization. Even though this partial enthalpy−entropy compensation is apparent, it does not qualitatively change the preference for the more crowed structure that is stabilized through intramolecular LD interactions.

■ ASSOCIATED CONTENT

Supporting Information

The Supporting Information is available free of charge at https://pubs.acs.org/doi/10.1021/jacs.0c09597.

Comparison with previous measurements as well as synthetic and computational details (PDF)

■ AUTHOR INFORMATION

Corresponding Author

Peter R. Schreiner − *Institute of Organic Chemistry, Justus Liebig University, 35392 Giessen, Germany;* orcid.org/0000-0002-3608-5515; Email: prs@uni-giessen.de

Authors

Jan M. Schümann − *Institute of Organic Chemistry, Justus Liebig University, 35392 Giessen, Germany*

J. Philipp Wagner − *Institute of Organic Chemistry, Justus Liebig University, 35392 Giessen, Germany;* orcid.org/0000-0002-1433-0292

André K. Eckhardt − *Institute of Organic Chemistry, Justus Liebig University, 35392 Giessen, Germany;* orcid.org/0000-0003-1029-9272

Henrik Quanz − *Institute of Organic Chemistry, Justus Liebig University, 35392 Giessen, Germany*

Complete contact information is available at: https://pubs.acs.org/10.1021/jacs.0c09597

Notes

The authors declare no competing financial interest.

■ ACKNOWLEDGMENTS

We dedicate this work to Henning Hopf for his seminal contributions to hydrocarbon chemistry and on the occasion of his 80th birthday. This work was supported by the priority program "Control of London Dispersion in Molecular Chemistry" (SPP1807) of the Deutsche Forschungsgemeinschaft. A.K.E. and J.P.W. thank the Fonds der Chemischen Industrie for fellowships. We thank Heike Hausmann for performing the NMR measurements. J.M.S. thanks Marcel A. Strauss and Robert Pollice for fruitful discussions and Sebastian Ahles for synthetic advice.

■ REFERENCES

(1) Israelachvili, J. N. *Intermolecular and Surface Forces*; Academic Press: San Diego, 1991.

(2) Wagner, J. P.; Schreiner, P. R. London Dispersion in Molecular Chemistry—Reconsidering Steric Effects. *Angew. Chem., Int. Ed.* **2015**, *54* (42), 12274−12296.

(3) Yang, L.; Adam, C.; Nichol, G. S.; Cockroft, S. L. How much do van der Waals dispersion forces contribute to molecular recognition in solution? *Nat. Chem.* **2013**, *5* (12), 1006−1010.

(4) Yang, L.; Brazier, J. B.; Hubbard, T. A.; Rogers, D. M.; Cockroft, S. L. Can Dispersion Forces Govern Aromatic Stacking in an Organic Solvent? *Angew. Chem., Int. Ed.* **2016**, *55* (3), 912−916.

(5) Pollice, R.; Bot, M.; Kobylianskii, I. J.; Shenderovich, I.; Chen, P. Attenuation of London Dispersion in Dichloromethane Solutions. *J. Am. Chem. Soc.* **2017**, *139* (37), 13126−13140.

(6) Pollice, R.; Fleckenstein, F.; Shenderovich, I.; Chen, P. Compensation of London Dispersion in the Gas Phase and in Aprotic Solvents. *Angew. Chem., Int. Ed.* **2019**, *58* (40), 14281−14288.

(7) Adam, C.; Yang, L.; Cockroft, S. L. Partitioning Solvophobic and Dispersion Forces in Alkyl and Perfluoroalkyl Cohesion. *Angew. Chem., Int. Ed.* **2015**, *54* (4), 1164−1167.

(8) Strauss, M. A.; Wegner, H. A. London Dispersion in Alkane Solvents. *Angew. Chem., Int. Ed.* **2020**, DOI: 10.1002/anie.202012094.

(9) Giese, M.; Albrecht, M. Alkyl-Alkyl Interactions in the Periphery of Supramolecular Entities: From the Evaluation of Weak Forces to Applications. *ChemPlusChem* **2020**, *85* (4), 715−724.

(10) Mati, I. K.; Adam, C.; Cockroft, S. L. Seeing through solvent effects using molecular balances. *Chem. Sci.* **2013**, *4* (10), 3965−3972.

(11) Paliwal, S.; Geib, S.; Wilcox, C. S. Molecular Torsion Balance for Weak Molecular Recognition Forces. Effects of "Tilted-T" Edge-to-Face Aromatic Interactions on Conformational Selection and Solid-State Structure. *J. Am. Chem. Soc.* **1994**, *116* (10), 4497−4498.

(12) Hwang, J.; Dial, B. E.; Li, P.; Kozik, M. E.; Smith, M. D.; Shimizu, K. D. How important are dispersion interactions to the strength of aromatic stacking interactions in solution? *Chem. Sci.* **2015**, *6* (7), 4358−4364.

(13) Hwang, J.; Li, P.; Smith, M. D.; Shimizu, K. D. Distance-Dependent Attractive and Repulsive Interactions of Bulky Alkyl Groups. *Angew. Chem., Int. Ed.* **2016**, *55* (28), 8086−8089.

(14) Fokin, A. A.; Gerbig, D.; Schreiner, P. R. σ/σ- and π/π-Interactions Are Equally Important: Multilayered Graphanes. *J. Am. Chem. Soc.* **2011**, *133* (50), 20036−20039.

(15) Nakamura, K.; Houk, K. N. Theoretical Studies of the Wilcox Molecular Torsion Balance. Is the Edge-to-Face Aromatic Interaction Important? *Org. Lett.* **1999**, *1* (13), 2049−2051.

(16) Carter, R. E.; Nilsson, B.; Olsson, K. Barriers to internal rotation in 1,3,5-trineopentylbenzenes. VII. Evidence for attractive steric effects. *J. Am. Chem. Soc.* **1975**, *97* (21), 6155−6159.

(17) Johnson, E. R.; Keinan, S.; Mori-Sánchez, P.; Contreras-García, J.; Cohen, A. J.; Yang, W. Revealing Noncovalent Interactions. *J. Am. Chem. Soc.* **2010**, *132* (18), 6498−6506.

(18) Contreras-García, J.; Johnson, E. R.; Keinan, S.; Chaudret, R.; Piquemal, J.-P.; Beratan, D. N.; Yang, W. NCIPLOT: A Program for Plotting Noncovalent Interaction Regions. *J. Chem. Theory Comput.* **2011**, *7* (3), 625−632.

(19) Mati, I. K.; Cockroft, S. L. Molecular balances for quantifying non-covalent interactions. *Chem. Soc. Rev.* **2010**, *39* (11), 4195−4205.

(20) Miller, M. J.; Lyttle, M. H.; Streitwieser, A. tert-Butyl-substituted cyclooctatetraenes. *J. Org. Chem.* **1981**, *46* (10), 1977−1984.

(21) Strauss, M. A.; Wegner, H. A. Molecular Systems for the Quantification of London Dispersion Interactions. *Eur. J. Org. Chem.* **2019**, *2019* (2−3), 295−302.

(22) Liu, L.; Guo, Q.-X. Isokinetic Relationship, Isoequilibrium Relationship, and Enthalpy−Entropy Compensation. *Chem. Rev.* **2001**, *101* (3), 673−696.

(23) London, F. Zur Theorie und Systematik der Molekularkräfte. *Eur. Phys. J. A* **1930**, *63* (3), 245−279.

(24) Garza, A. J. Solvation Entropy Made Simple. *J. Chem. Theory Comput.* **2019**, *15* (5), 3204−3214.

(25) Lyttle, M. H.; Streitwieser, A.; Kluttz, R. Q. Unusual equilibrium between 1,4- and 1,6-di-tert-butylcyclooctatetraenes. *J. Am. Chem. Soc.* **1981**, *103* (11), 3232−3233.

(26) Allinger, N. L.; Frierson, M.; Van-Catledge, F. A. The importance of van der Waals attractions in determining the equilibrium between 1,4- and 1,6-dialkylcyclooctatetraenes. *J. Am. Chem. Soc.* **1982**, *104* (17), 4592−4593.

(27) Paquette, L. A.; Hefferon, G. J.; Samodral, R.; Hanzawa, Y. Bond fixation in annulenes. 14. Synthesis of and bond shifting equilibrium between 1,4- and 1,6-di-tert-butylcyclooctatetraenes. *J. Org. Chem.* **1983**, *48* (8), 1262−1266.

https://dx.doi.org/10.1021/jacs.0c09597
J. Am. Chem. Soc. 2021, 143, 41−45

(28) Anderson, J. E.; Kirsch, P. A. Structural equilibria determined by attractive steric interactions. 1, 6-Dialkylcyclooctatetraenes and their bond-shift and ring inversion investigated by dynamic NMR spectroscopy and molecular mechanics calculations. *J. Chem. Soc., Perkin Trans. 2* **1992**, No. 11, 1951−1957.
(29) Tosi, C. A quantum mechanical study of the equilibrium between 1, 4-and 1, 6-dialkylcyclooctatetraenes. *J. Comput. Chem.* **1984**, *5* (3), 248−251.
(30) Castaño, O.; Palmeiro, R.; Frutos, L. M.; Luisandrés, J. Role of bifurcation in the bond shifting of cyclooctatetraene. *J. Comput. Chem.* **2002**, *23* (7), 732−736.
(31) Wenthold, P. G.; Hrovat, D. A.; Borden, W. T.; Lineberger, W. C. Transition-State Spectroscopy of Cyclooctatetraene. *Science* **1996**, *272* (5267), 1456−1459.
(32) Johnson, F. Allylic strain in six-membered rings. *Chem. Rev.* **1968**, *68* (4), 375−413.
(33) Belostotskaya, I. S.; Komissarova, N. L.; Dzhuaryan, É. V.; Ershov, V. V. The ortho-alkylation of catechol. *Bull. Acad. Sci. USSR, Div. Chem. Sci.* **1972**, *21* (7), 1535−1536.
(34) Corey, E. J.; Suggs, J. W. Pyridinium chlorochromate. An efficient reagent for oxidation of primary and secondary alcohols to carbonyl compounds. *Tetrahedron Lett.* **1975**, *16* (31), 2647−2650.
(35) Emerson, G. F.; Watts, L.; Pettit, R. Cyclobutadiene- and Benzocyclobutadiene-Iron Tricarbonyl Complexes1. *J. Am. Chem. Soc.* **1965**, *87* (1), 131−133.
(36) Strating, J.; Zwanenburg, B.; Wagenaar, A.; Udding, A.C. Evidence for the expulsion of bis-CO from bridged alfa-diketones. *Tetrahedron Lett.* **1969**, *10*, 125−128.
(37) Catalán, J.; Hopf, H. Empirical Treatment of the Inductive and Dispersive Components of Solute−Solvent Interactions: The Solvent Polarizability (SP) Scale. *Eur. J. Org. Chem.* **2004**, *2004* (22), 4694−4702.
(38) Pollice, R.; Chen, P. Origin of the Immiscibility of Alkanes and Perfluoroalkanes. *J. Am. Chem. Soc.* **2019**, *141* (8), 3489−3506.
(39) Paquette, L. A.; Hefferon, G. J.; Samodral, R.; Hanzawa, Y. Bond fixation in annulenes. 14. Synthesis of and bond shifting equilibrium between 1, 4-and 1, 6-di-tert-butylcyclooctatetraenes. *J. Org. Chem.* **1983**, *48* (8), 1262−1266.
(40) Bailey, W. F.; Monahan, A. S. Statistical effects and the evaluation of entropy differences in equilibrium processes. Symmetry corrections and entropy of mixing. *J. Chem. Educ.* **1978**, *55* (8), 489.
(41) Hunter, C. A. Quantifying Intermolecular Interactions: Guidelines for the Molecular Recognition Toolbox. *Angew. Chem., Int. Ed.* **2004**, *43* (40), 5310−5324.
(42) McCarthy, M.; Lee, K. L. K. Molecule Identification with Rotational Spectroscopy and Probabilistic Deep Learning. *J. Phys. Chem. A* **2020**, *124* (15), 3002−3017.
(43) *CRC Handbook of Chemistry and Physics*, 97th ed.; Haynes, W. M., Ed.; CRC Press: Cleveland, OH, 2017.
(44) Hohenstein, E. G.; Sherrill, C. D. Density fitting of intramonomer correlation effects in symmetry-adapted perturbation theory. *J. Chem. Phys.* **2010**, *133* (1), No. 014101.

https://dx.doi.org/10.1021/jacs.0c09597
J. Am. Chem. Soc. 2021, 143, 41−45

2.2 Exploring the Limits of Intramolecular London Dispersion Stabilization with Bulky Dispersion Energy Donors in Solution

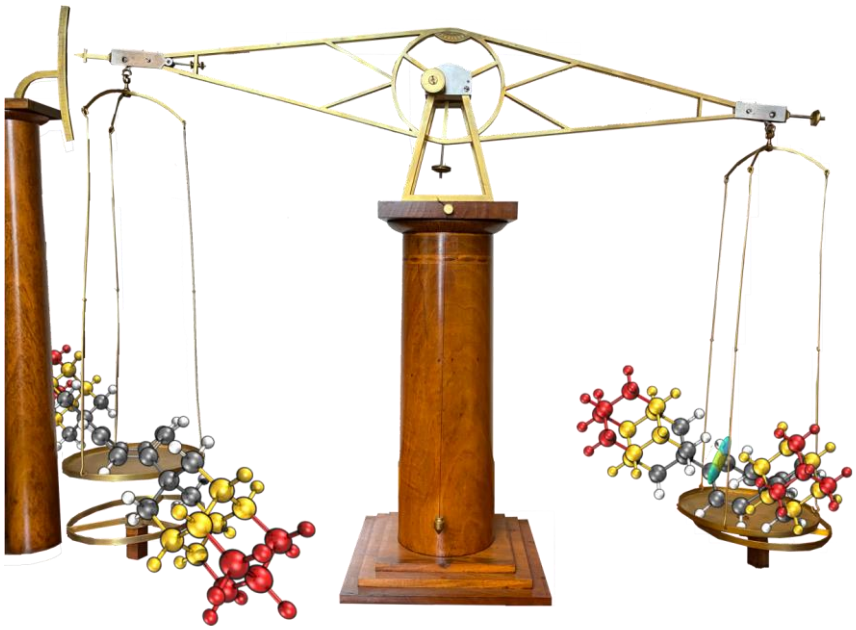

Abstract: *We present an experimental study of a cyclooctatetraene-based molecular balance disubstituted with increasingly bulky t-butyl (tBu), adamantyl (Ad), and diamantyl (Dia) substituents in the 1,4-/1,6-positions and determined the valence-bond shift equilibrium in n-hexane (hex), n-octane (oct), and n-dodecane (dod). Computations including implicit and explicit solvation support our temperature-dependent NMR equilibrium measurements that the more sterically crowded 1,6-isomer is always favored, irrespective of solvent, and that the free energy is quite insensitive to substituent size.*

Reference:

Exploring the Limits of Intramolecular London Dispersion Stabilization with Bulky Dispersion Energy Donors in Solution. - J. M. Schümann, Lukas Ochmann, Jonathan Becker, Ahmet Altun, Ingolf Harden, Giovanni Bistoni, and P. R. Schreiner, *J. Am. Chem. Soc.* **2023**, *145* (4), 2093–2097. **DOI:** 10.1021/jacs.2c13301

JACS
JOURNAL OF THE AMERICAN CHEMICAL SOCIETY
pubs.acs.org/JACS
Communication

Exploring the Limits of Intramolecular London Dispersion Stabilization with Bulky Dispersion Energy Donors in Alkane Solution

Jan M. Schümann, Lukas Ochmann, Jonathan Becker, Ahmet Altun, Ingolf Harden, Giovanni Bistoni,* and Peter R. Schreiner*

Cite This: J. Am. Chem. Soc. 2023, 145, 2093−2097
Read Online
ACCESS | Metrics & More | Article Recommendations | Supporting Information

ABSTRACT: We present an experimental study of a cyclooctatetraene-based molecular balance disubstituted with increasingly bulky *tert*-butyl (*t*Bu), adamantyl (Ad), and diamantyl (Dia) substituents in the 1,4-/1,6-positions for which we determined the valence-bond shift equilibrium in *n*-hexane (hex), *n*-octane (oct), and *n*-dodecane (dod). Computations including implicit and explicit solvation support our temperature-dependent NMR equilibrium measurements indicating that the more sterically crowded 1,6-isomer is always favored, irrespective of solvent, and that the free energy is quite insensitive to substituent size.

Even though our understanding of attractive London dispersion (LD) interactions in solution has much improved,[1−9] there are still open questions regarding the attenuation of LD of hydrocarbons in like-solvents. It is often assumed that if groups are just bulky and solvents similar enough, LD will be very strongly attenuated. Here we show with extreme experimental model compounds that this is not necessarily the case. LD can be a decisive factor in catalyzed reactions[10−18] as well as for the thermodynamic stability of otherwise far more reactive hydrocarbons and some substituted systems.[19−23] Recently, we demonstrated that intramolecular LD does not cancel in solution by using a cyclooctatetraene (COT)-based molecular balance substituted with *t*Bu groups in the 1,4-/1,6-positions. These two isomers are connected through a valence-bond isomerization that sensitively responds to solvent effects. We demonstrated that the apparently more crowded ("folded") 1,6-di-*t*Bu-COT isomer is preferred in any of the 16 solvents (including alkanes) used to determine the equilibrium positions.[24] This has been traced back to the stabilizing LD-driven H···H contact interactions of the *t*Bu substituents that are at just the right distance. But how far can one go with increasing steric bulk? Can the preference for the folded isomer be increased with even larger alkyl groups? How much is LD attenuated in increasingly more polarizable (longer) *n*-alkane solvents? This knowledge is essential for improving our reaction planning and exerting conformational control, e.g., in catalysis, where small differential interactions in transition structures are pivotal for selectivity.

Here we expand the COT balance by substitution with the rigid rotors adamantyl (Ad) and diamantyl (Dia) and compare their folding equilibrium positions with that of 1,6-di-*t*Bu-COT. These so-called dispersion energy donors (DEDs) are known to strongly enhance LD interactions through their high polarizability.[27−31] The three balances are pictorially presented in Figure 1. The shortest computed (*vide infra*) H···H distance between the alkyl substituents (~2.5 Å) does not significantly change with increasing substituent size, but the solvent-accessible surface (SAS) does. Hence, the larger COT derivatives are expected to interact more strongly with the solvent. As in the **1,4-/1,6-di-*t*Bu-COT** balance the preference for the folded 1,6-isomer is the smallest in cyclohexane and *n*-

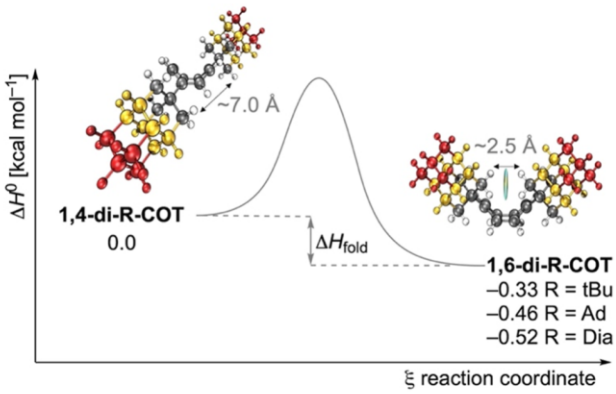

Figure 1. Simplified equilibrium of 1,4- and 1,6-dialkyl-substituted cyclooctatetraene (COT). The non-covalent interaction (NCI)[25,26] surface is colored on a blue-green-red scale according to an isovalue $s(\rho)$ of 0.3, ranging from $\rho(r) = -0.025$ to 0.025 Å. The greenish color corresponds to weak interactions. The NCIs are only computed between *t*Bu (gray), Ad (yellow), and Dia (red). Enthalpies in the gas phase are computed at the r^{2}SCAN-3c level of theory.

Received: December 13, 2022
Published: January 23, 2023

https://doi.org/10.1021/jacs.2c13301
J. Am. Chem. Soc. 2023, 145, 2093−2097

Journal of the American Chemical Society pubs.acs.org/JACS Communication

hexane,[24] one might expect similar if not stronger effects with increasing SAS for the larger balances. When dissolving the diamondoid COT balances in linear alkanes with increasing boiling points and polarizabilities,[32] we will be able to analyze these solvation effects.

We synthesized the new di-adamantyl- and di-diamantyl-COT derivatives utilizing our recently developed method for the preparation of 3,6-dialkyl-substituted *ortho*-hydroquinones (Scheme 1).[34] The yields for the alkylation are generally low

Scheme 1. Synthesis of the 1,4-/1,6-di-Ad-COT and 1,4-/1,6-di-Dia-COT Molecular Balances[33,34]

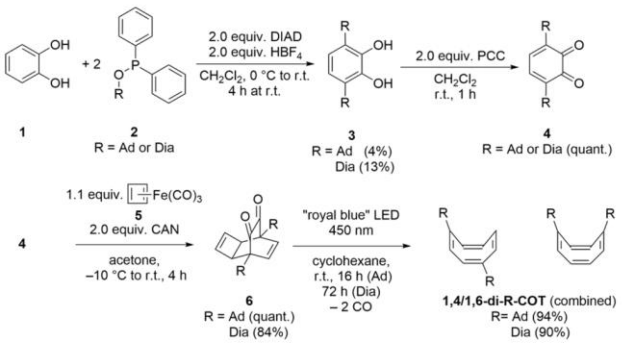

because the 3,5-substitution pattern is thermodynamically preferred. Diones (**6**) are storable COT precursors from which the target compounds can readily be prepared cleanly right before the NMR measurements via photodecarbonylation.[35] For details of the synthesis, see the SI.

We were able to crystallize **1,4-di-Ad-COT** from $CDCl_3$ in a "beehive" structure (Figure 2a); the crystal belongs to the C_2 space group (for details see SI section S5). Even though we find the 1,6-isomer to be preferred in all solvents, the larger intermolecular contact area apparently favors the 1,4-isomer that can pack more tightly in the solid state. The shortest intermolecular H···H contact distances are around 2.5 Å, i.e., essentially the same as the shortest intramolecular contacts shown in Figure 1. This indicates that the large substituents are placed at an optimal distance for LD interactions in the **1,6-di-R-COT** isomers.

Accurate quantum mechanical calculations at the HFLD* level[36,37] were carried out to estimate the magnitude of intermolecular LD interactions in the solid state. With a cluster model of 11 di-adamantyl COT monomers extracted from the experimental crystal structure (Figure 2b), we found that the LD energy between the central monomer and its neighbors amounts to −68.2 kcal mol^{-1}. This is larger in absolute terms than the energy required to remove the central monomer from this system at the same level of theory (48.8 kcal mol^{-1}), which demonstrates that the lattice energy is dominated by the LD energy. Interestingly, the LD interaction density plot (DID)[38] demonstrates that LD is "short-sighted'", i.e., only the shortest intermolecular H···H contacts significantly contribute.

Remarkably, when dissolving crystals of pure **1,4-di-Ad-COT** in *n*-octane at room temperature, we could readily discern the formation of some amount of **1,6-di-Ad-COT** in the NMR spectrum (Figure S1), but full equilibration required heating to about 60 °C, upon which **1,6-di-Ad-COT** dominated. This indicates that the barrier for the adamantane-based balance is higher than that of **1,4-/1,6-di-*t*Bu-COT**. This is in line with the observation that the barrier

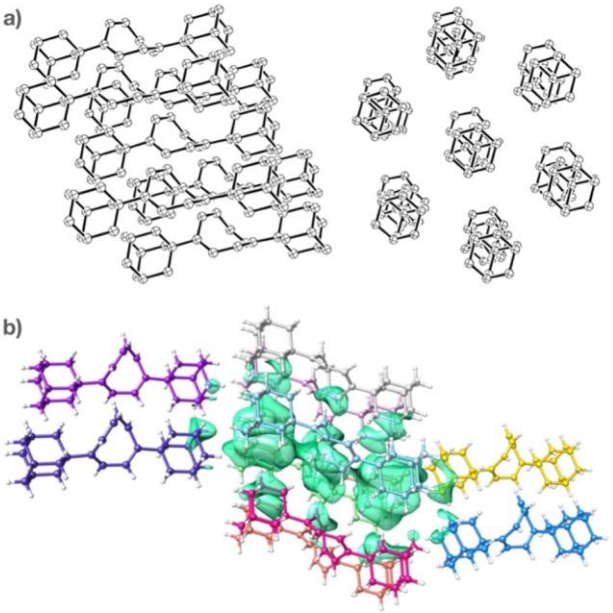

Figure 2. (a) "Beehive" structure of solid-state **1,4-di-Ad-COT**, showing packing of the asymmetric unit cell. Hydrogens and the unresolved COT enantiomer are omitted for clarity. Ellipsoids drawn at 55% probability. (b) Computed dispersion interaction density plot at the HFLD* level on a cluster model based on the experimental crystal structure. The density isosurface value was set to 0.01 kcal mol^{-1} bohr^{-3}.

increases with increasing alkyl substitution: The valence bond shift barrier for COT is 13.7 kcal mol^{-1} at 263 K, 17.3 kcal mol^{-1} for **1,4-di-Me-COT** at 325 K,[39,40] and 22.6 kcal mol^{-1} **1,6-di-*t*Bu-COT** at 298 K.[24] This is also supported by our recent findings on silyl-substituted COT balances.[41] Hence, we allowed the isomer mixtures to equilibrate for at least 1 h at each temperature inside the NMR spectrometer by initially warming the sample to the highest possible temperature for a given solvent and decreasing it in 5−10 °C steps immediately thereafter. The resulting experimental enthalpies and Gibbs free energies at 333 K are summarized and compared with our computational results including implicit solvation in Figure 3.

Figure 3 demonstrates that the folded **1,6-di-R-COT** isomers are preferred in the gas phase and in all employed solvents. Remarkably, the experimental ΔG^{333}_{exp} are very similar across the substituents and solvents. The computations mirror this very well, with deviations between experimental and computed free energies that are typically within 0.1 kcal mol^{-1}. The purely electronic energies do not agree with these findings, as they steadily increase with an increasing size of R and solvent chain length. Hence, it is quite clear that the balance of enthalpic and entropic effects plays a key role in the equilibration.

Indeed, our computations suggest that the relative energy between folded and unfolded structures in solution is determined by a delicate balance of various contributions that show a non-trivial dependence on the system size, such as rotational/vibrational entropy and non-electrostatic solvation effects. For example, the folded conformers show higher vibrational frequencies and hence lower vibrational entropies. This effect originates from the fact that their equilibrium geometries are stabilized by non-covalent $\sigma-\sigma$ interactions that are absent in the unfolded conformers. Accordingly, the net

https://doi.org/10.1021/jacs.2c13301
J. Am. Chem. Soc. 2023, 145, 2093−2097

Journal of the American Chemical Society pubs.acs.org/JACS Communication

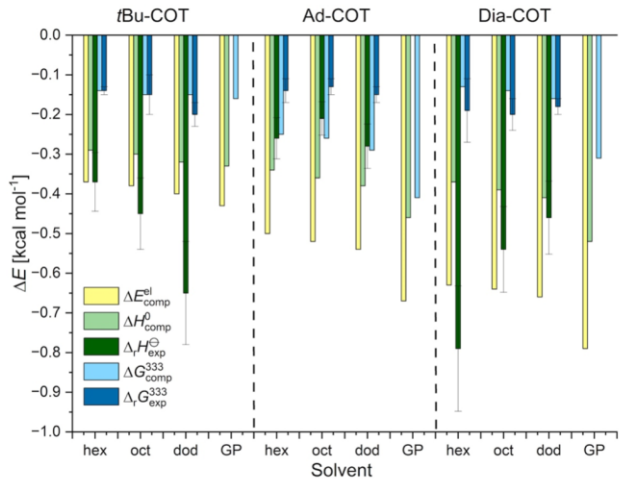

Figure 3. Experimental enthalpies $\Delta H^{\ominus}_{exp}$ and Gibbs free energies ΔG^{333}_{exp} for the equilibration of the **1,4-/1,6-di-R-COT** isomers (R = *t*Bu, Ad, Dia) and comparison with computed r^{2}SCAN-3c values. Error bars for experimental enthalpy are estimated to be 20%; error bars of Gibbs free enthalpy are calculated based on formula S13 in the SI. The computational protocol was validated using state-of-the-art DLPNO-CCSD(T) computations,[43,44] as detailed in the SI. Solvation effects were incorporated in all cases using the SMD model. The yellow bars are the computed electronic energies ΔE^{el}; GP denotes the gas phase. For the computational details, see below and the SI.

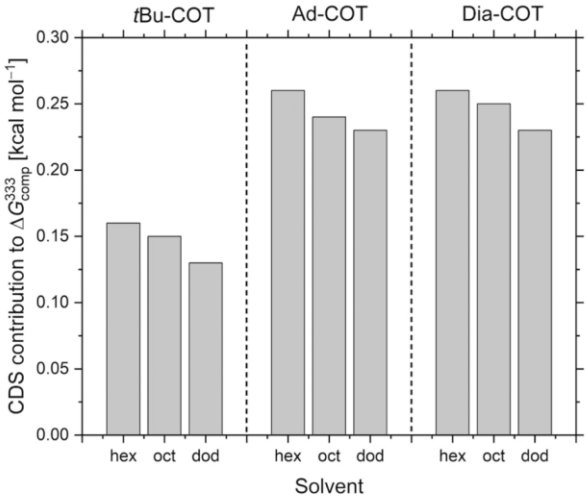

Figure 4. Cavity-dispersion solvent-structure contribution to the computed free energies ΔG^{333}_{comp} for the equilibration of the **1,4-/1,6-di-R-COT** isomers (R = *t*Bu, Ad, Dia) at the r^{2}SCAN-3c/SMD level.

effect of the vibrational entropy contribution is to preferentially stabilize unfolded conformers. This effect increases with the system size and the degrees of freedom. In contrast, rotational entropy follows the opposite trend. To a large extent, this effect originates from the fact that the rotational entropy depends on the point group of the molecule, and folded and unfolded conformers have different symmetry properties (see the SI for further details). In addition, the trend of the experimental ΔG^{333}_{exp} values is also in line with the notion that some compensation of dispersion interactions occurs for larger, more polarizable molecules because of larger solvent displacement.[42]

Within the SMD model, this effect is accounted for by the "cavity-dispersion solvent-structure" term, which incorporates all non-electrostatic contributions to the solvation free energy, such as solute−solvent dispersion interactions. In contrast to LD interactions, this term preferentially stabilizes the "unfolded" isomers (Figure 4), and it increases with substituent size. However, this effect is not large enough to fully compensate the differential stabilization provided by LD interactions, and hence the folded conformers remain more stable in all solvents.

Experimentally, we also estimated the enthalpies of equilibration, $\Delta H^{\ominus}_{exp}$, by means of van't Hoff plots. These measurements assume temperature-independent enthalpies and entropies, which limits the accuracy of our $\Delta H^{\ominus}_{exp}$ estimates.[45,46] In addition, they are extremely sensitive to the number of data points, a fact that is limited by the solubility of the COT derivatives and by the boiling point of the solvents. Hence, we estimated for all slopes an error of roughly 20%. Interestingly, $\Delta H^{\ominus}_{exp}$ increases with solvent chain length for R = *t* Bu, stays constant for R = Ad, and decreases for R = Dia. These trends are only partially followed by the computations, for which ΔH^{333}_{comp} continuously increases with solvent chain length. Considering how challenging the calculation and experimental measurement of enthalpies are for these systems, it is not possible at this point to assess the origin of these deviations. In particular, **1,4-/1,6-di-Dia-COT** show very poor solubility around 25−40 °C in *n*-hexane, resulting in only three useful data points for the van't Hoff plot. This might explain why the experimental enthalpy is unusually high for this system. However, it is comforting to see that the experimental and computed ΔG values agree remarkably well, and that the sign of ΔH is reproduced for all systems.

To shed light on the nature of explicit solute−solvent interactions in these systems, we computationally investigated **1,4-/1,6-di-Dia-COT** in *n*-dodecane using a hybrid implicit/explicit approach (see SI section S12 on explicit solvation). Thorough conformational sampling was performed at the r^{2}SCAN-3c level on cluster models with varying numbers of solvent molecules, in order to determine the low-energy structures for each isomer. Remarkably, the model system with ten solvent molecules yields an electronic energy difference between folded and unfolded conformers of −0.9 kcal mol^{-1}, which is reasonably close to the value obtained using the purely implicit solvation scheme (−0.7 kcal mol^{-1}). The most stable structure obtained for each isomer is shown in Figure 5.

Importantly, irrespective of the number of solvent molecules used, our results unambiguously demonstrate that, for both isomers, there is a clear preference for the solvent molecules aligning parallel to the solute, which is consistent with the crystal structure for **1,4-di-Ad-COT** (Figure 2).

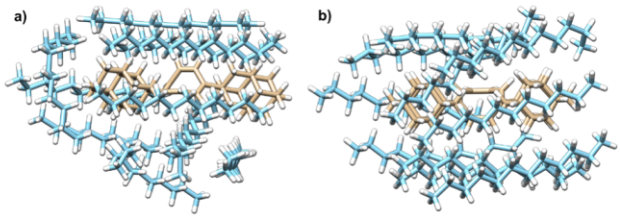

Figure 5. Energetically lowest-lying explicitly solvated (with ten *n*-dodecane molecules) structures: (a) **1,4-di-Dia-COT** and (b) **1,6-di-Dia-COT**. The most stable conformer found from the conformational sampling was further optimized using the r^{2}SCAN-3c method,[47] as implemented in ORCA 5.0,[48−50] without geometric constraints.

https://doi.org/10.1021/jacs.2c13301
J. Am. Chem. Soc. 2023, 145, 2093−2097

Our results demonstrate that the relative stabilities of molecular balances in solution are determined by a delicate balance of intramolecular LD forces, solute−solvent interactions, and entropy effects, which partially counteract each other. Quite remarkably, intramolecular LD effects are so significant that they always make the sterically more crowded 1,6-isomer more stable than the 1,4-isomer. However, other effects effectively limit the relative stabilization provided by DEDs with increasingly bulky substituents.

■ ASSOCIATED CONTENT

Supporting Information

The Supporting Information is available free of charge at https://pubs.acs.org/doi/10.1021/jacs.2c13301.

Comparison with previous measurements, X-ray data, as well as synthetic and computational details (PDF)

Accession Codes

CCDC 2172397 contains the supplementary crystallographic data for this paper. These data can be obtained free of charge via www.ccdc.cam.ac.uk/data_request/cif, or by emailing data_request@ccdc.cam.ac.uk, or by contacting The Cambridge Crystallographic Data Centre, 12 Union Road, Cambridge CB2 1EZ, UK; fax: +44 1223 336033.

■ AUTHOR INFORMATION

Corresponding Authors

Peter R. Schreiner − *Institute of Organic Chemistry, Justus Liebig University, 35392 Giessen, Germany;* orcid.org/0000-0002-3608-5515; Email: prs@uni-giessen.de

Giovanni Bistoni − *Max-Planck-Institut für Kohlenforschung, 45470 Mülheim an der Ruhr, Germany; Dipartmento di Chimica, Biologia e Biotechnologie, Università Degli Studi Di Perugia, 06123 Perugia, Italy;* orcid.org/0000-0003-4849-1323; Email: giovanni.bistoni@unipg.it

Authors

Jan M. Schümann − *Institute of Organic Chemistry, Justus Liebig University, 35392 Giessen, Germany*

Lukas Ochmann − *Institute of Organic Chemistry, Justus Liebig University, 35392 Giessen, Germany;* orcid.org/0000-0002-9207-0975

Jonathan Becker − *Institute of Analytical and Inorganic Chemistry, Justus Liebig University, 35392 Giessen, Germany*

Ahmet Altun − *Max-Planck-Institut für Kohlenforschung, 45470 Mülheim an der Ruhr, Germany;* orcid.org/0000-0001-8818-9925

Ingolf Harden − *Max-Planck-Institut für Kohlenforschung, 45470 Mülheim an der Ruhr, Germany;* orcid.org/0000-0002-3265-678X

Complete contact information is available at: https://pubs.acs.org/10.1021/jacs.2c13301

Notes

The authors declare no competing financial interest.

■ ACKNOWLEDGMENTS

This work was supported by the priority program "Control of London Dispersion in Molecular Chemistry" (SPP1807) of the Deutsche Forschungsgemeinschaft. We thank Heike Hausmann for performing the NMR measurements and Christof Barth for LDI-MS measurements. J.M.S. thanks Marcel A. Strauss, Lars Rummel, and Henrik F. König for fruitful discussions.

■ REFERENCES

(1) Yang, L. X.; Adam, C.; Nichol, G. S.; Cockroft, S. L. How much do van der Waals dispersion forces contribute to molecular recognition in solution? *Nat. Chem.* **2013**, *5* (12), 1006−1010.

(2) Schweighauser, L.; Strauss, M. A.; Bellotto, S.; Wegner, H. A. Attraction or Repulsion? London Dispersion Forces Control Azobenzene Switches. *Angew. Chem., Int. Ed.* **2015**, *54* (45), 13436−13439.

(3) Adam, C.; Yang, L. X.; Cockroft, S. L. Partitioning Solvophobic and Dispersion Forces in Alkyl and Perfluoroalkyl Cohesion. *Angew. Chem., Int. Ed.* **2015**, *54* (4), 1164−1167.

(4) Liptrot, D. J.; Guo, J. D.; Nagase, S.; Power, P. P. Dispersion Forces, Disproportionation, and Stable High-Valent Late Transition Metal Alkyls. *Angew. Chem., Int. Ed.* **2016**, *55* (47), 14766−14769.

(5) Pollice, R.; Bot, M.; Kobylianskii, I. J.; Shenderovich, I. G.; Chen, P. Attenuation of London Dispersion in Dichloromethane Solutions. *J. Am. Chem. Soc.* **2017**, *139* (37), 13126−13140.

(6) Liptrot, D. J.; Power, P. P. London dispersion forces in sterically crowded inorganic and organometallic molecules. *Nat. Rev. Chem.* **2017**, *1* (1), 0004.

(7) Pollice, R.; Chen, P. A Universal Quantitative Descriptor of the Dispersion Interaction Potential. *Angew. Chem., Int. Ed.* **2019**, *58* (29), 9758−9769.

(8) Strauss, M. A.; Wegner, H. A. Molecular Systems for the Quantification of London Dispersion Interactions. *Eur. J. Org. Chem.* **2019**, *2019* (2−3), 295−302.

(9) Strauss, M. A.; Wegner, H. A. London Dispersion in Alkane Solvents. *Angew. Chem., Int. Ed.* **2021**, *60* (2), 779−786.

(10) Ngola, S. M.; Dougherty, D. A. Evidence for the importance of polarizability in biomimetic catalysis involving cyclophane receptors. *J. Org. Chem.* **1996**, *61* (13), 4355−4360.

(11) Warmuth, R.; Kerdelhue, J.-L.; Sanchez Carrera, S.; Langenwalter, K. J.; Brown, N. Rate Acceleration through Dispersion Interactions: Effect of a Hemicarcerand on the Transition State of Inner Phase Decompositions of Diazirines. *Angew. Chem., Int. Ed.* **2002**, *41* (1), 96−99.

(12) Berkessel, A.; Adrio, J. A. Dramatic acceleration of olefin epoxidation in fluorinated alcohols: Activation of hydrogen peroxide by multiple H-bond networks. *J. Am. Chem. Soc.* **2006**, *128* (41), 13412−13420.

(13) Wende, R. C.; Seitz, A.; Niedek, D.; Schuler, S. M. M.; Hofmann, C.; Becker, J.; Schreiner, P. R. The Enantioselective Dakin-West Reaction. *Angew. Chem., Int. Ed.* **2016**, *55* (8), 2719−2723.

(14) Procházková, E.; Kolmer, A.; Ilgen, J.; Schwab, M.; Kaltschnee, L.; Fredersdorf, M.; Schmidts, V.; Wende, R. C.; Schreiner, P. R.; Thiele, C. M. Uncovering Key Structural Features of an Enantioselective Peptide-Catalyzed Acylation Utilizing Advanced NMR Techniques. *Angew. Chem., Int. Ed.* **2016**, *55* (51), 15754−15759.

(15) Lu, G.; Liu, R. Y.; Yang, Y.; Fang, C.; Lambrecht, D. S.; Buchwald, S. L.; Liu, P. Ligand-Substrate Dispersion Facilitates the Copper-Catalyzed Hydroamination of Unactivated Olefins. *J. Am. Chem. Soc.* **2017**, *139* (46), 16548−16555.

(16) Eschmann, C.; Song, L.; Schreiner, P. R. London Dispersion Rather than Steric Hindrance Determines the Enantioselectivity of the Corey-Bakshi-Shibata Reduction. *Angew. Chem., Int. Ed.* **2021**, *60* (9), 4823−4832.

(17) Singha, S.; Buchsteiner, M.; Bistoni, G.; Goddard, R.; Fürstner, A. A New Ligand Design Based on London Dispersion Empowers Chiral Bismuth-Rhodium Paddlewheel Catalysts. *J. Am. Chem. Soc.* **2021**, *143* (15), 5666−5673.

(18) Rummel, L.; Domanski, M. H. J.; Hausmann, H.; Becker, J.; Schreiner, P. R. London Dispersion Favors Sterically Hindered Diarylthiourea Conformers in Solution. *Angew. Chem., Int. Ed.* **2022**, *61* (29), No. e202204393.

(19) Rösel, S.; Quanz, H.; Logemann, C.; Becker, J.; Mossou, E.; Canadillas-Delgado, L.; Caldeweyher, E.; Grimme, S.; Schreiner, P. R. London Dispersion Enables the Shortest Intermolecular Hydrocarbon H···H Contact. *J. Am. Chem. Soc.* **2017**, *139* (22), 7428−7431.
(20) Rösel, S.; Balestrieri, C.; Schreiner, P. R. Sizing the role of London dispersion in the dissociation of all-*meta tert*-butyl hexaphenylethane. *Chem. Sci.* **2017**, *8* (1), 405−410.
(21) Rösel, S.; Becker, J.; Allen, W. D.; Schreiner, P. R. Probing the Delicate Balance between Pauli Repulsion and London Dispersion with Triphenylmethyl Derivatives. *J. Am. Chem. Soc.* **2018**, *140* (43), 14421−14432.
(22) Stennett, C. R.; Bursch, M.; Fettinger, J. C.; Grimme, S.; Power, P. P. Designing a Solution-Stable Distannene: The Decisive Role of London Dispersion Effects in the Structure and Properties of $\{Sn(C_6H_2\text{-}2,4,6\text{-}Cy_3)_2\}_2$ (Cy = Cyclohexyl). *J. Am. Chem. Soc.* **2021**, *143* (51), 21478−21483.
(23) Rummel, L.; Schümann, J. M.; Schreiner, P. R. Hexaphenylditetrels - When Longer Bonds Provide Higher Stability. *Chem.—Eur. J.* **2021**, *27* (55), 13699−13702.
(24) Schümann, J. M.; Wagner, J. P.; Eckhardt, A. K.; Quanz, H.; Schreiner, P. R. Intramolecular London Dispersion Interactions Do Not Cancel in Solution. *J. Am. Chem. Soc.* **2021**, *143* (1), 41−45.
(25) Contreras-García, J.; Johnson, E. R.; Keinan, S.; Chaudret, R.; Piquemal, J.-P.; Beratan, D. N.; Yang, W. NCIPLOT: A Program for Plotting Noncovalent Interaction Regions. *J. Chem. Theory Comput.* **2011**, *7* (3), 625−632.
(26) Lefebvre, C.; Rubez, G.; Khartabil, H.; Boisson, J. C.; Contreras-Garcia, J.; Henon, E. Accurately extracting the signature of intermolecular interactions present in the NCI plot of the reduced density gradient versus electron density. *Phys. Chem. Chem. Phys.* **2017**, *19* (27), 17928−17936.
(27) Grimme, S. Density functional theory with London dispersion corrections. *WIREs Comput. Mol. Sci.* **2011**, *1* (2), 211−228.
(28) Schreiner, P. R.; Chernish, L. V.; Gunchenko, P. A.; Tikhonchuk, E. Y.; Hausmann, H.; Serafin, M.; Schlecht, S.; Dahl, J. E. P.; Carlson, R. M. K.; Fokin, A. A. Overcoming lability of extremely long alkane carbon-carbon bonds through dispersion forces. *Nature* **2011**, *477*, 308−311.
(29) Fokin, A. A.; Chernish, L. V.; Gunchenko, P. A.; Tikhonchuk, E. Y.; Hausmann, H.; Serafin, M.; Dahl, J. E. P.; Carlson, R. M. K.; Schreiner, P. R. Stable Alkanes Containing Very Long Carbon-Carbon Bonds. *J. Am. Chem. Soc.* **2012**, *134* (33), 13641−13650.
(30) Wagner, J. P.; Schreiner, P. R. London Dispersion in Molecular Chemistry—Reconsidering Steric Effects. *Angew. Chem., Int. Ed.* **2015**, *54* (42), 12274−12296.
(31) London, F. Zur Theorie und Systematik der Molekularkräfte. *Z. Phys.* **1930**, *63* (3−4), 245−279.
(32) Haynes, W. M.; Lide, D. R.; Bruno, T. J. *Handbook of Chemistry and Physics*, 97th ed.; CRC Press: Cleveland, OH, 2016−2017; p 84.
(33) Paquette, L. A.; Hefferon, G. J.; Samodral, R.; Hanzawa, Y. Bond fixation in annulenes. 14. Synthesis of and bond shifting equilibrium between 1,4- and 1,6-di-tert-butylcyclooctatetraenes. *J. Org. Chem.* **1983**, *48* (8), 1262−1266.
(34) Ochmann, L.; Kessler, M. L.; Schreiner, P. R. Alkylphosphinites as Synthons for Stabilized Carbocations. *Org. Lett.* **2022**, *24* (7), 1460−1464.
(35) Strating, J.; Zwanenburg, B.; Wagenaar, A.; Udding, A. C. Evidence for the expulsion of bis-CO from bridged alfa-diketones. *Tetrahedron Lett.* **1969**, *10*, 125−128.
(36) Altun, A.; Neese, F.; Bistoni, G. HFLD: A Nonempirical London Dispersion-Corrected Hartree-Fock Method for the Quantification and Analysis of Noncovalent Interaction Energies of Large Molecular Systems. *J. Chem. Theory Comput.* **2019**, *15* (11), 5894−5907.
(37) Altun, A.; Neese, F.; Bistoni, G. Open-Shell Variant of the London Dispersion-Corrected Hartree-Fock Method (HFLD) for the Quantification and Analysis of Noncovalent Interaction Energies. *J. Chem. Theory Comput.* **2022**, *18* (4), 2292−2307.
(38) Altun, A.; Neese, F.; Bistoni, G. Effect of electron correlation on intermolecular interactions: A pair natural orbitals coupled cluster based local energy decomposition study. *J. Chem. Theory Comput.* **2019**, *15* (1), 215−228.
(39) Anderson, J. E.; Kirsch, P. A. Molecular structures determined by intramolecular attractive steric interactions. Dynamic NMR and molecular mechanics investigation of 1,6-dimethylcyclo-octatetraene. *J. Chem. Soc., Perkin Trans. 2* **1990**, No. 6, 885−889.
(40) Anderson, J. E.; Kirsch, P. A. Structural equilibria determined by attractive steric interactions. 1, 6-Dialkylcyclooctatetraenes and their bond-shift and ring inversion investigated by dynamic NMR spectroscopy and molecular mechanics calculations. *J. Chem. Soc., Perkin Trans. 2* **1992**, No. 11, 1951−1957.
(41) König, H. F.; Rummel, L.; Hausmann, H.; Becker, J.; Schümann, J. M.; Schreiner, P. R. Gauging the Steric Effects of Silyl Groups with a Molecular Balance. *J. Org. Chem.* **2022**, *87* (7), 4670−4679.
(42) Hunter, C. A. Quantifying intermolecular interactions: Guidelines for the molecular recognition toolbox. *Angew. Chem., Int. Ed.* **2004**, *43* (40), 5310−5324.
(43) Altun, A.; Neese, F.; Bistoni, G. Extrapolation to the Limit of a Complete Pair Natural Orbital Space in Local Coupled-Cluster Calculations. *J. Chem. Theory Comput.* **2020**, *16* (10), 6142−6149.
(44) Riplinger, C.; Pinski, P.; Becker, U.; Valeev, E. F.; Neese, F. Sparse maps—A systematic infrastructure for reduced-scaling electronic structure methods. II. Linear scaling domain based pair natural orbital coupled cluster theory. *J. Chem. Phys.* **2016**, *144* (2), 024109.
(45) Biedermann, F.; Schneider, H.-J. Experimental Binding Energies in Supramolecular Complexes. *Chem. Rev.* **2016**, *116* (9), 5216−5300.
(46) Liu, L.; Guo, Q.-X. Isokinetic Relationship, Isoequilibrium Relationship, and Enthalpy-Entropy Compensation. *Chem. Rev.* **2001**, *101* (3), 673−696.
(47) Grimme, S.; Hansen, A.; Ehlert, S.; Mewes, J.-M. r2SCAN-3c: A "Swiss army knife" composite electronic-structure method. *J. Chem. Phys.* **2021**, *154* (6), 064103.
(48) Neese, F. The ORCA program system. *WIREs Comput. Mol. Sci.* **2012**, *2* (1), 73−78.
(49) Neese, F. Software update: the ORCA program system, version 4.0. *WIREs Comput. Mol. Sci.* **2018**, *8* (1), 1327.
(50) Neese, F. Software update: The ORCA program system—Version 5.0. *WIREs Comput. Mol. Sci.* **2022**, *12* (5), 1606.

https://doi.org/10.1021/jacs.2c13301
J. Am. Chem. Soc. 2023, 145, 2093−2097

3. Further LD related Publications

3.1 Gauging the Steric Effects of Silyl Groups with a Molecular Balance

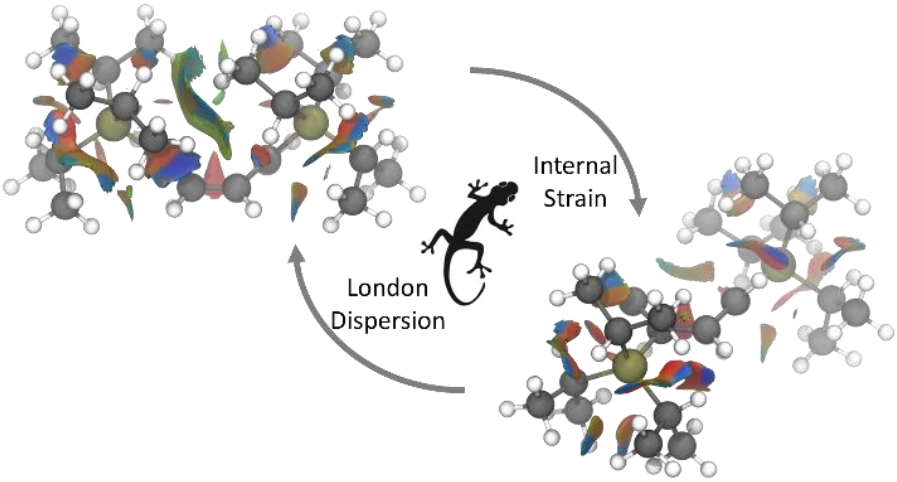

Abstract: *We present an experimental and computational study of a cyclooctatetraene (COT)-based molecular balance disubstituted with commonly used silyl groups. Such groups often serve as protecting groups and are typically considered innocent bystanders. Our motivation here is to determine the actual steric effects of such groups by employing a molecular balance. While in the unfolded 1,4valence isomer the silyl groups are far apart ($d_{\sigma-\sigma} \geq 5.15$ Å), the folded 1,6-isomer is affected greatly by noncovalent interactions due to close σ−σ contacts ($d_{\sigma-\sigma} \leq 2.58$ Å). In order to investigate the thermodynamic equilibrium between the 1,6- and 1,4-valence isomers, we employed temperature-dependent nuclear magnetic resonance measurements. Additionally, we assessed the nature of attractive and repulsive interactions in 1,6-disilyl-COT derivatives via a combination of local energy decomposition analysis (LED) and symmetry-adapted perturbation theory (SAPT) at the DLPNO-CCSD(T)/def2-TZVP and sSAPT0/aug-cc-pVDZ levels of theory. We identified London dispersion interactions as the main contributor to the molecular stability of the folded states, whereas Pauli exchange repulsion and a resulting internal strain favor the unfolded diastereomer.*

Reference:

Gauging the Steric Effects of Silyl Groups with a Molecular Balance. - Henrik F. König, Lars Rummel, Heike Hausmann, Jonathan Becker, Jan M. Schümann, and Peter R. Schreiner, *J. Org. Chem.* **2022**, *87* (7), 4670-4679. **DOI:** 10.1021/acs.joc.1c03103

JOC The Journal of Organic Chemistry

pubs.acs.org/joc Article

Gauging the Steric Effects of Silyl Groups with a Molecular Balance

Henrik F. König,[§] Lars Rummel,[§] Heike Hausmann, Jonathan Becker, Jan M. Schümann, and Peter R. Schreiner*

Cite This: J. Org. Chem. 2022, 87, 4670–4679 Read Online

ACCESS | Metrics & More | Article Recommendations | Supporting Information

ABSTRACT: We present an experimental and computational study of a cyclooctatetraene (COT)-based molecular balance disubstituted with commonly used silyl groups. Such groups often serve as protecting groups and are typically considered innocent bystanders. Our motivation here is to determine the actual steric effects of such groups by employing a molecular balance. While in the unfolded 1,4-valence isomer the silyl groups are far apart ($d_{\sigma-\sigma} \geq 5.15$ Å), the folded 1,6-isomer is affected greatly by noncovalent interactions due to close $\sigma-\sigma$ contacts ($d_{\sigma-\sigma} \leq 2.58$ Å). In order to investigate the thermodynamic equilibrium between the 1,6- and 1,4-valence isomers, we employed temperature-dependent nuclear magnetic resonance measurements. Additionally, we assessed the nature of attractive and repulsive interactions in 1,6-disilyl-COT derivatives via a combination of local energy decomposition analysis (LED) and symmetry-adapted perturbation theory (SAPT) at the DLPNO-CCSD(T)/def2-TZVP and sSAPT0/aug-*cc*-pVDZ levels of theory. We identified London dispersion interactions as the main contributor to the molecular stability of the folded states, whereas Pauli exchange repulsion and a resulting internal strain favor the unfolded diastereomer.

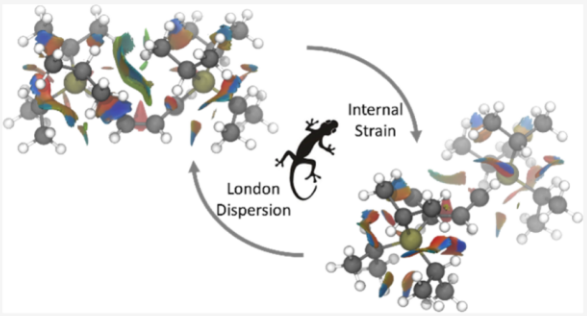

INTRODUCTION

Silyl groups often are conveniently employed to transform, for example, "reactive" hydroxyl groups to "unreactive" silyl ethers.[1,2] These groups enjoy great popularity due to their commercial availability, simple attachment, as well as mild and selective detachment procedures. Such silyl-protecting groups are commonly chosen on the basis of their stability under typically neutral or basic reaction conditions. The bulkiness of silyl-protecting groups is mostly considered only with regards to selective cleavability.[3] The use of abbreviations such as TPS (triphenylsilyl) further obfuscates the spatial demand of such groups. However, attaching bulky silyl-protecting groups to a flexible backbone can significantly alter conformational preferences and hence the stereoelectronic properties of a system. This is highlighted by so-called "super-armed" glycosyl donors, for which exclusive protection with bulky silyl ethers enforces an all-axial conformation.[4,5] As a consequence, this results in a reactivity increase by more than an order of magnitude in comparison to the benzylated derivatives.[4,5] Clearly, bulkiness is an important feature of the most frequently utilized silyl-protecting groups, but this fact is often not given much attention. Consequently, only a few efforts have been made to quantify the steric demand of such groups.[6−8]

In recent years, the role of London dispersion (LD) interactions[9−12] as a decisive structural factor for conformational preferences and transition structures emerged in a variety of molecular systems.[13−19] Because LD interactions are approximately additive pairwise interactions, it is clear that large alkyl and silyl groups must be more than just providers of steric bulk. While LD interactions between alkyl groups, allegedly, are capable of facilitating labile compounds such as hexaphenylethane[20−23] or coupled diamondoids[24] by offering intramolecular stabilization, the effects of commonly utilized silyl groups have not been studied in detail. Apart from intramolecular noncovalent interactions, intermolecular stabilization via silyl groups, that is, in transition structures, can be of great importance. Hartwig et al.[25] already demonstrated the impact of trimethylsilyl (TMS) as a dispersion energy donor group[26] (DED[11,27]) in hydroboration reactions. Here, the TMS groups increased reaction rates by binding the substrate more efficiently. With the aim to utilize silyl groups as variable steric directing groups, we chose a cyclooctatetraene (COT)-based molecular balance to gauge the size and potential of commonly used silyl groups to act as DEDs.

A systematic study of the di-*tert*-butyl-substituted COT molecular balance in various solvents highlighted the attractive nature of LD interactions.[28] The disubstituted COT system, initially presented by Streitwieser et al.[29] using di-*tert*-butyl

Received: December 22, 2021
Published: March 16, 2022

https://doi.org/10.1021/acs.joc.1c03103
J. Org. Chem. 2022, 87, 4670–4679

The Journal of Organic Chemistry pubs.acs.org/joc Article

Scheme 1. Equilibrium of 1,4- and 1,6-Disilyl Substituted Cyclooctatetraene

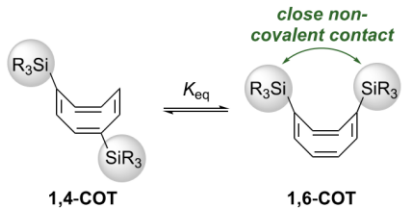

substituents and its folding mechanism (a double-bond valence shift and ring inversion[30,31]), has been studied both experimentally[32−34] and computationally.[35,36] All studies confirmed the sterically more hindered 1,6-di-*tert*-butyl COT to be the preferred valence isomer in solution and in the gas phase.

We chose the COT system to enforce close $\sigma-\sigma$ contacts in the 1,6-disilyl-COT (Scheme 1) valence isomer. On the other hand, the 1,4-disilyl-COT does not display close contacts between the silyl groups. An analysis of the equilibrium between 1,6- and 1,4-disilyl-COT should offer insights into the attractive and repulsive nature between the silyl groups. While di-*tert*-butyl substituted COT prefers the folded isomer *independent* of the solvent, bulky silyl groups are expected to disfavor this valence isomer due to an increasing number of repulsive contacts.[28] Therefore, our system is suitable to gauge the relative bulkiness of various silyl groups.

RESULTS AND DISCUSSION

We utilized the COT molecular balance substituted with trimethylsilyl[37] (TMS), triethylsilyl (TES), *tert*-butyldimethylsilyl[38] (TBDMS), tri-*iso*-propylsilyl[39] (TIPS), tri-*iso*-butylsilyl (TIBS), tris(trimethylsilyl)silyl (TTMSS), and triphenylsilyl[40,41] (TPS).

We adopted modified literature procedures[37−41] to synthesize the disilyl COT derivatives (Scheme 2). We gathered single-crystal X-ray structural data for di-TIPS-COT (Scheme 2) and di-TTMSS-COT (see Supporting Information). Both compounds crystallize in the unfolded valence isomer form, thereby maximizing intermolecular alkyl−alkyl interactions. In solution, di-TIPS-COT equilibrates between both diastereomers. The thermodynamic equilibria were subjected to van't Hoff analyses utilizing temperature-dependent nuclear magnetic resonance (NMR) measurements to dissect the isomerization enthalpies (ΔH_{eq}) and entropies (ΔS_{eq}).

NMR samples were equilibrated for 16 h at 40 °C prior to the experiment (Figure 1) and measured in the temperature range of 313−373 K (steps of 10 K; for details, see Supporting Information). All COT balances show linear regressions with $R^2 > 0.97$. As the folding equilibrium of di-*tert*-butyl substituted COT varies with the NMR solvent in a range from $K_{eq} = 1.18-2.13$, toluene was chosen for temperature-dependent measurements, as it lies in the middle of the solvent bias range ($K_{eq} = 1.55$).[28]

We also analyzed the noncovalent interactions between the silyl groups computationally utilizing the well-established B3LYP[42,43] functional excluding and including LD interactions with the Becke−Johnson (BJ) damped dispersion D3 correction of Grimme et al.[27,44] This provides an estimate of the LD correction. To validate this method, we compared our results with those computed using the M06-2X[45] and ωB97X-D[46] functional combinations. Ahlrich's def2-TZVPP basis set[47] was used for all computations. Because all methods show the same trend, the B3LYP-D3(BJ)/def2-TZVPP-optimized geometries were utilized as the basis for DLPNO-CCSD(T)/def2-TZVP single-point energy computations[48,49] (see Supporting Information). This approach has demonstrated good agreement with experimental data for COT molecular balances.[28] The rate-determining double-bond valence shift barrier was computationally estimated to be around 24 kcal mol^{-1} for alkyl-substituted silyl groups, which is similar to that of di-*tert*-butyl COT.[28] In contrast, the activation barrier for di-TPS-COT was estimated to be around 35 kcal mol^{-1}, that is, thermally out of reach for our experimental parameters (see Supporting Information).

While the silyl groups are even more demanding in size than a *tert*-butyl substituent (with van der Waals Volume of around 101 Å^3, Scheme 3 and Supporting Information), the equilibria between 1,6- and 1,4-disilyl-COT were assumed to shift markedly toward the unfolded balance. Figure 2 displays the experimental enthalpies ΔH_{eq} (black markings) and the computed values (red markings). While computations suggest that the di-TMS-COT is nearly thermoneutral ($\Delta H_{eq} \approx 0$ kcal mol^{-1}), larger silyl groups shift the equilibrium toward 1,4-disilyl-COT. The computed increase in energy for the equilibrium depicted in Figure 2 between di-TBDMS-, di-TES-, di-TIPS-, and di-TTMSS-COT ranges from 0.3 to 1.4 kcal mol^{-1}, favoring 1,4-disilyl-COT. The computational assessment and the experimental data agree within ±0.6 kcal mol^{-1} with an experimental error smaller than 0.13 kcal mol^{-1}. The experimentally determined enthalpy value for di-TMS-COT is with $\Delta H_{eq} = -0.6$, only 0.1 kcal mol^{-1} higher in energy than the di-*tert*-butyl substituted COT.[28] While di-TTMSS-COT is completely in favor of 1,4-disilyl-COT and therefore cannot be measured, the di-TIPS-COT equilibrium shows the highest enthalpy ($\Delta H_{eq} = 1.7$ kcal mol^{-1}). Interestingly, di-TIBS-COT does not follow the expected pattern that a larger van der Waals surface or volume introduces more steric hindrance into the system. Both the computational and

Scheme 2. Synthetic Procedure for the Preparation of Disilyl COT Derivatives (Left) and Single Crystal X-ray Structure of di-TIPS COT (Bottom Right, Bond Distances in Å)[a]

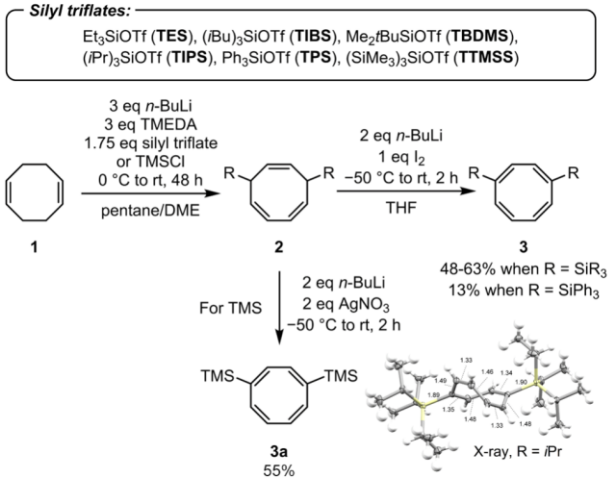

[a]Thermal ellipsoid plot of the molecular structure obtained by single-crystal X-ray diffraction was drawn at 50% probability level.

https://doi.org/10.1021/acs.joc.1c03103
J. Org. Chem. 2022, 87, 4670−4679

The Journal of Organic Chemistry pubs.acs.org/joc Article

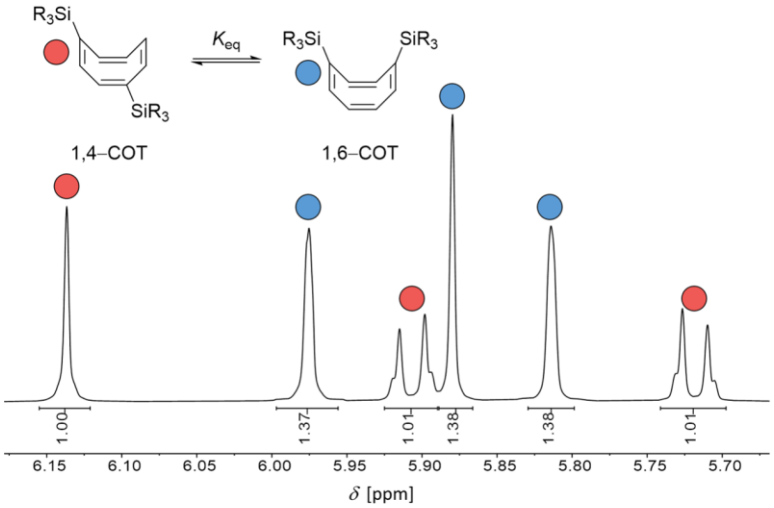

Figure 1. ^{1}H NMR spectra (600 MHz) and signal assignment of the equilibrium between 1,4- (red) and 1,6-di-TMS (blue) COT at 40 °C.

Scheme 3. Comparison of van der Waals Surfaces and Volumes of Tri-substituted Silyl Groups (Optimized with the Silane Geometry) at the B3LYP-D3/def2-TZVPP Level of Theory

Structure	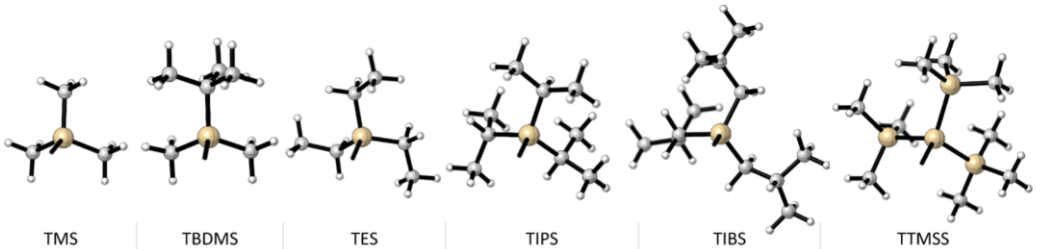					
Abbreviation	TMS	TBDMS	TES	TIPS	TIBS	TTMSS
Van der Waals Surface [Å^2]	127.8	171.1	173.3	219.2	295.7	340.2
Van der Waals Volume [Å^3]	109.2	155.5	151.5	199.6	285.2	328.8

experimental values give a ΔH_{eq} as high as di-TBDMS- and di-TES-COT ($\Delta H_{eq} \approx 0.8$ kcal mol^{-1}). Therefore, an additional source of stabilization must be present.

Three questions arise from the data collected:

1. What is the origin of the stabilization of the folded di-TMS-COT?
2. Why do larger silyl groups not show similar behavior?
3. Why does di-TIBS-COT not follow that trend?

To answer the first question, we focused on the noncovalent interactions between the interacting groups. By utilizing homodesmotic equations,[50,51] we extracted the magnitude of the LD interactions due to close $\sigma-\sigma$ contacts between the silyl groups in 1,6-disilyl-COT. Including and excluding LD interactions via Grimme's D3(BJ) correction results in an LD correction estimate, which we take, in a first approximation, as a measure of the dispersion energy. This seems reasonable, as we are comparing similar groups in the same molecular system where absolute magnitudes are less important than relative measures for comparison.

The analysis reveals large LD contributions between the silyl groups (Figure 3). Whereas the DFT computations excluding LD (red bars) demonstrate the general assumption that large substituents repel each other due to steric hindrance, including LD (blue bars) suggests the opposite trend. The magnitude of LD interactions (green bars) increases with the size of the silyl groups. Therefore, the largest alkyl substituent (TTMSS) stabilizes 1,6-disilyl-COT by around $\Delta E_{disp} = -5.0$ kcal mol^{-1}. Only di-TIBS-COT deviates from the general trend observed.

For better energy estimates of the intramolecular LD interactions, we performed local energy decomposition[52−54] (LED) analyses as implemented in ORCA.[55] Thereby, we separated each balance into three molecular fragments (F1, F2, and F3) according to Figure 4 and dissected the interaction energy into its main parts. Because this process involves bond splitting, the resulting radical fragment interactions involve large electrostatic interactions. As a consequence, we can only isolate an energy term for LD interactions between F2 and F3.

Apart from di-TIBS substituted COT, the results of this analysis (Figure 4) fit qualitatively to the results of the homodesmotic equation (Figure 3). While in both cases the magnitude of intramolecular LD interactions increases from di-TMS- to di-TTMSS-COT, di-TIBS-COT is the strongest dispersion energy donor (DED) group within the LED analysis. On the other hand, di-TMS-COT benefits the least from stabilizing LD interactions. Nevertheless, it is the only case favoring 1,6-disilyl-COT. Counteracting repulsive interactions do not outweigh the LD stabilization in di-TMS-COT. The strong stabilizing contacts between two TIBS groups translate into a measurable shift in the equilibrium as well. In comparison to di-TMS-COT, the interaction is not prominent

https://doi.org/10.1021/acs.joc.1c03103
J. Org. Chem. 2022, 87, 4670−4679

The Journal of Organic Chemistry pubs.acs.org/joc Article

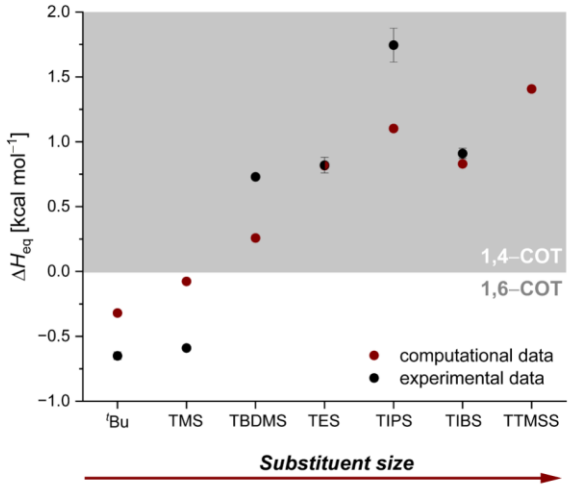

Figure 2. Enthalpies for the equilibrium of 1,4- and 1,6-disilyl substituted cyclooctatetraene. Experimental data (black markings) were derived from van't Hoff analyses. Computations (red markings) at the DLPNO-CCSD(T)/def2-TZVP//B3LYP-D3/def2-TZVPP level of theory. The silyl groups were ordered according to increasing van der Waals surface. All datapoints within the shaded area favor 1,4-disilyl-COT. Data for ^{t}Bu was extracted from the work of Schümann et al.[28]

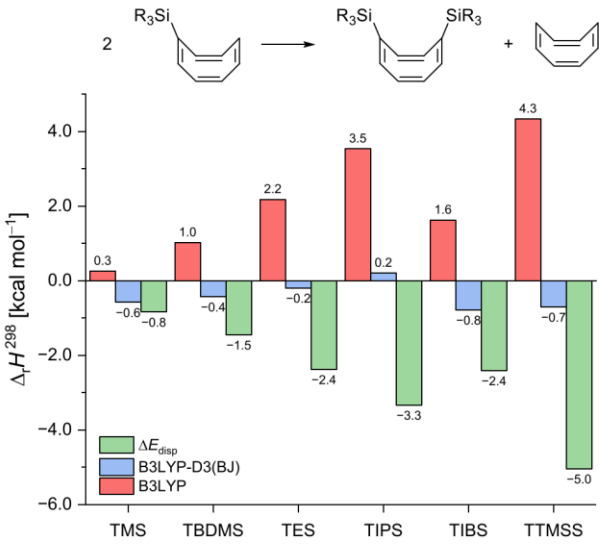

Figure 3. Homodesmotic equation and reaction enthalpies ($\Delta_r H^{298}$) in kcal mol^{-1} at B3LYP(D3(BJ))/def2-TZVPP.

enough to favor 1,6-disilyl-COT. Because larger groups favor 1,4-disilyl-COT, destabilizing interactions must counteract LD.

To answer the second question, we aimed at isolating the contributions of Pauli repulsion for 1,4- and 1,6-disilyl-COT. We employed symmetry-adapted perturbation theory[56] (SAPT) at the sSAPT0/aug-*cc*-pVDZ level of theory utilizing a scaled protocol according to Parker et al.[57] To isolate interactions between the silyl groups, we employed B3LYP-D3/def2-TZVPP optimized structures, removed the COT backbone, and saturated the radical sites.[58] The total interaction energy E_{tot} can then be decomposed into its main components (Figure 5). Whereas the inductive energy E_{ind} (yellow markings) and the electrostatic energy E_{elst} (blue markings) terms marginally stabilize 1,6-disilyl-COT, the main

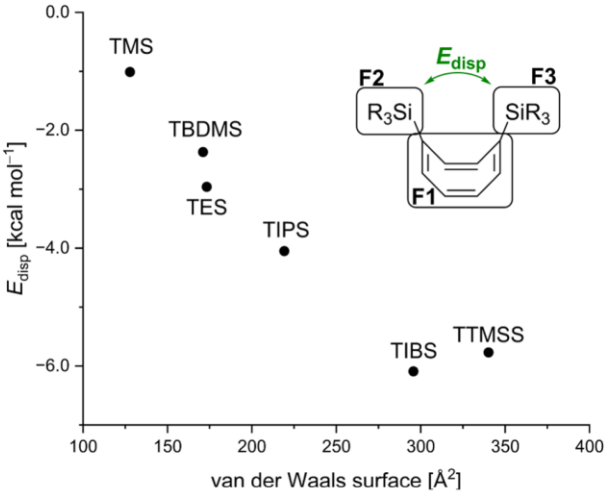

Figure 4. LED analysis of two silyl groups in their 1,6-disilyl-substituted cyclooctatetraene geometry at DLPNO-CCSD(T)/def2-TZVP//B3LYP-D3(BJ)/def2-TZVPP.

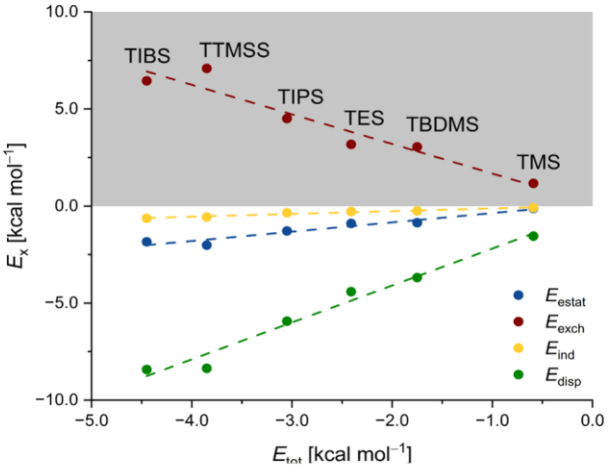

Figure 5. sSAPT analysis of two silyl groups in geometries of the respective 1,6-COT derivative at sSAPT0/aug-*cc*-pVDZ. The dashed lines are used as a guide to the eye.

contributors to the total interaction energy are LD interactions E_{disp} (green markings) and Pauli exchange repulsion E_{exch} (red markings). While 1,4-disilyl-COT is hardly influenced by repulsive interactions, the close $\sigma-\sigma$ contacts in 1,6-disilyl-COT result in significant Pauli repulsion (Figure 5). The latter is, however, largely offset by LD interactions for all studied derivatives and hence cannot be the decisive factor for the shift in folding equilibria. In particular, di-TIBS-COT benefits from stabilizing LD interactions coupled with fewer steric constraints than di-TTMSS-COT. Therefore, flexible alkyl groups align more efficiently and optimize the balance between attractive and repulsive contacts.

The SAPT analysis does not directly yield an explanation for our findings, and the origin of increasing destabilization must lie elsewhere. When assessing optimized 1,6-disilyl-COT structures, we noticed significant deviations in the geometric parameters of the respective COT backbone with differing silyl groups, that is, the dihedral angle α (Figure 6). Consequently, we carried out a strain analysis, with the aim of capturing ring strain introduced in both the COT scaffold and the silyl

https://doi.org/10.1021/acs.joc.1c03103
J. Org. Chem. 2022, 87, 4670−4679

The Journal of Organic Chemistry pubs.acs.org/joc Article

groups. To account for the ring strain, we utilized the B3LYP-D3/def2-TZVPP optimized structures, split off the substituents attached to Si, and saturated the compound with H to give a strained disilane COT. Next, the single-point energies of these compounds were compared to a disilane COT optimized at the same level of theory. Additionally, we utilized the optimized structures, removed the COT molecular backbone, and saturated the radical sites to give the corresponding strained silanes. Again, the difference in energy between strained silanes and geometry optimized compounds was taken into account (for details, see Supporting Information).

Figure 6 displays the sum of strain energy ΔE_{strain} exerted on the ring due to the substituents of the corresponding di-silyl substituted COT derivative and van der Waals strain introduced in the silyl groups due to repulsive contacts (see Supporting Information for details). While the incorporation of six methyl groups does not affect ΔE_{strain} (0.0 kcal mol^{-1} for di-TMS-COT), the introduction of bulkier substituents leads to a rise in strain up to 1.9 kcal mol^{-1} for di-TTMSS-COT. For smaller and flexible silyl substituents up to TIBS ΔE_{strain} is mostly comprised of strain from the silyl substituents (see Supporting Information). The influence of ring strain increases significantly for bulkier and rigid substituents (TIPS and TTMSS). The strain energy is a result of the attenuation of Pauli repulsion between both silyl groups. By increasing the distance between substituents the release in repulsive interaction energy is directly exerted on the COT molecular backbone. Because LD decreases slower with respect to the distance (r^{-6}) in comparison to Pauli repulsion (r^{-12}), the ratio of both energy components is optimized.[9,10]

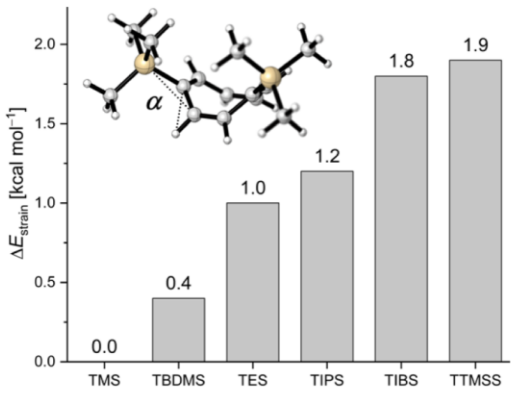

Figure 6. Strain energy ΔE_{strain} for disilyl-substituted cyclooctatetraene. The energy values correspond to the relative strain between 1,4- and 1,6-disilyl-substituted cyclooctatetraene.

By mapping the obtained experimental data to parameters capturing steric bulk, such as A-values,[7,8,59] solvolysis rates,[6] and Tolman's steric parameter θ,[60,61] the suitability of disilyl COTs to gauge the steric size of silyl groups can be further rationalized. While θ resembles an empirical measure, it is nevertheless often used to assess the steric demand of ligands. Figure 7 showcases the correlation between θ and ΔG_{eq} values of the disilyl COT balances. Because of the strong correlation observed, it is possible to predict θ from computed or experimental ΔG_{eq} values. For instance, TIBS has recently found use as a protecting group in organic synthesis but has not been characterized within the framework of steric parameters. According to the data collected (Figure 7), we can determine θ = 144° for the TIBS group (red marking), which is in accordance with Tolman's parameter for P(^{i}Bu)$_3$ (θ = 143°).[60] Similar correlations of ΔG_{eq} to steric parameters such as *A*-values and solvolysis rates are observed (see Supporting Information).

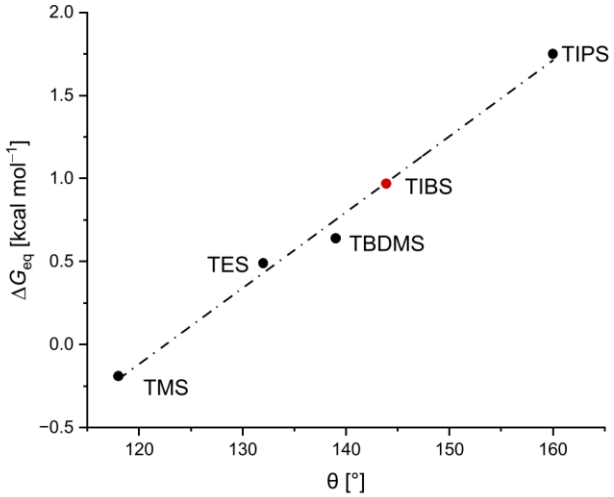

Figure 7. Correlation of experimental free energy values (ΔG_{eq}) of the COT molecular balances and Tolman's steric parameter. The dashed line is derived from linear regression of the black data points. The red marking was calculated according to a linear regression as a guide to the eye.

CONCLUSIONS

We prepared a variety of 1,4- and 1,6-disilyl-substituted cyclooctatetraene structures and conducted temperature-dependent NMR measurements to determine equilibrium parameters. By comparing the thus obtained ΔH_{eq} values to computed thermochemical data ($\Delta_r H^{298}$, and ΔE_{strain}), we were able to pinpoint LD interactions as a key factor affecting the folding equilibria. The main interaction energy component that counteracts LD is Pauli exchange repulsion, while the induced strain is a mechanism to either attenuate repulsion or optimize LD. With the exception of di-TMS-COT, ring strain overcompensates the stabilizing contribution of LD interactions in the folded 1,6-isomer. Hence, the equilibrium shifts toward the unfolded 1,4-isomer as bulkier silyl groups are installed.

Our experimentally determined ΔG_{eq} values correlate well with steric parameters for silyl groups known from the literature. The ring strain observed in the 1,6-valence isomers can be interpreted as a "fingerprint" of the respective group. This renders the COT molecular balance system suitable for gauging the relative bulkiness of silyl and, in the future, other groups.

LD interactions turn out to play a key role in stabilizing the folded 1,6-isomers. This is particularly evident from LED and SAPT analyses (vide infra). Without the LD contributions, the equilibria are predicted to favor the unfolded 1,4-isomer much more strongly than what is observed experimentally.

While the incorporation of bulky substituents directly attached to Si (TMS, TBDMS, TIPS, and TTMSS) results in a linear correlation between the actual size (van der Waals surface, Scheme 3) and the apparent relative bulkiness (ΔG_{eq} and ΔH_{eq}, Figure 2) of silyl groups, a remote substitution

https://doi.org/10.1021/acs.joc.1c03103
J. Org. Chem. 2022, 87, 4670−4679

The Journal of Organic Chemistry pubs.acs.org/joc Article

pattern as in di-TIBS-COT stabilizes the folded 1,6-valence isomer via LD interactions.

EXPERIMENTAL SECTION

General Information. Thin-layer chromatography was carried out using PolyGram SIL G/UV_{254} plates with detection via UV λ = 254 nm and by staining with a 10 wt % ethanolic phosphomolybdic acid (PMA) stain solution. All chemicals were commercially obtained from Acros Organics, TCI, and Sigma-Aldrich and used without further purification. Anhydrous solvents were purchased from Acros Organics. Unless otherwise noted, all reactions were carried out under standard Schlenk conditions employing N_2 as the inert gas. Standard NMR spectra were obtained using Bruker Avance II 400 MHz and Bruker Avance III HD 400 MHz (^{13}C spectra) spectrometers. Temperature-dependent NMR experiments were carried out with a Bruker Avance III HD 600 MHz spectrometer. High-resolution mass spectra were obtained with a Bruker micrOTOF mass spectrometer. For temperature-dependent measurements, NMR samples were equilibrated for 16 h at 40 °C prior to the experiment utilizing an IKA ICC basic eco 8 immersion circulator.

Temperature-Dependent NMR Experiments. After sample transfer from the thermostat to the NMR spectrometer, equilibration was continued for another hour in the spectrometer before the first spectrum (40 °C) was recorded. Spectra were recorded in 10 °C steps. From 60 °C onward, the equilibration period before measurement was reduced to 30 min.

Synthetic Procedures. *Triphenylsilyl Triflate (4).* Triphenylsilyl triflate was prepared according to a modified literature procedure.[62] To a stirred suspension of 3.592 g (14 mmol) of AgOTf in 30 mL of DCM was added a solution of 4.428 g (15 mmol) triphenylsilyl chloride in 20 mL of DCM at room temperature. After complete addition, the reaction mixture was stirred under the exclusion of light at room temperature for another 12 h. The mixture was then filtered to remove AgCl, yielding a clear colorless filtrate. The filtrate was then concentrated under reduced pressure to yield 6.032 g of a colorless solid, which was used without further purification in the preparation of di(TPS)cyclooctatetraene **3g**.

Tris(trimethylsilyl)silyl Triflate (5). Tris(trimethylsilyl)silyl silane (4.63 mL, 15 mmol) was diluted with 7 mL of *n*-pentane. Afterward, 1.25 mL (14 mmol, 0.95 equiv) of trifluoromethanesulfonic acid was added dropwise (gas formation) and the resulting mixture was stirred for 1 h at room temperature. The resulting solution was used without further purification in the preparation of di(TTMSS)-cyclooctatetraene **3f**.

Tri(isobutyl)silyl Triflate (6). Triisobutylsilane 3.87 mL (15 mmol) was diluted in 5 mL of *n*-pentane. Afterward, 1.23 mL (14 mmol, 0.95 equiv) of trifluoromethanesulfonic acid was added dropwise (gas formation) and the resulting mixture was stirred for 1 h at room temperature. The resulting solution was used without further purification in the preparation of di(TIBS)cyclooctatetraene **3c**.

5,8-Di(silyl)cycloocta-1,3,6-trienes (2).[37−41] 5,8-Di(silyl)-cycloocta-1,3,6-trienes were prepared according to the following general procedure: to a stirred solution of 0.98 mL (8.0 mmol) of 1,5-cyclooctadiene in 10 mL of *n*-pentane was added 9.60 mL (24 mmol, 3.0 equiv) of a *n*-butyllithium solution (2.5 M in hexanes) at 0 °C. Afterward, 3.60 mL (24 mmol, 3.0 equiv) of TMEDA was added dropwise and the yellow solution was kept stirring at 0 °C for 15 min. The cooling bath was removed thereafter, and stirring was continued at room temperature for 48 h. To the then orange mixture was added 20 mL of DME, and stirring was continued for another 15 min at room temperature. The mixture was then filtered to yield a deep red filtrate that was cooled to −50 °C and treated with 1.75 equiv of the corresponding silyl triflate or silyl chloride. After 30 min at −50 °C, the reaction mixture was quenched with 20 mL of a saturated aqueous $NaHCO_3$ solution. Phases were separated, and the aqueous phase was extracted with *n*-hexane (3 × 50 mL). The combined organic phases were dried over anhydrous $MgSO_4$, filtered, and concentrated under reduced pressure to yield the corresponding crude products as either off-white oils or solids. Purification was carried out by filtering through a pad of silica eluting with *n*-hexane or a 10:1 mixture of *n*-hexane and ethyl acetate (5,8-di(TPS)cycloocta-1,3,6-triene **2g**). Because of their instability, the 5,8-di(silyl)cycloocta-1,3,6-triene **2** precursors were used immediately in the next synthetic step.

Di(TMS)cyclooctatetraene (3a). 1.264 g (5.0 mmol) of 5,8-di(TMS)cycloocta-1,3,6-triene was dissolved in 20 mL of THF and cooled to −50 °C. While stirring, 4.45 mL (11 mmol, 2.2 equiv) of 2.5 M *n*-butyllithium in hexanes was added dropwise. After stirring for 15 min at −50 °C, the reaction mixture was allowed to reach 0 °C by replacing the liquid nitrogen−acetone cooling bath with an ice-water cooling bath. Stirring of the solution was continued for 2 h at 0 °C. The now deep red solution was brought to −30 °C, and 1.712 g (10 mmol, 2.0 equiv) of silver nitrate was added in small portions. The reaction mixture was stirred for a further 16 h at room temperature before quenching was carried out with 20 mL of water. Phases were separated, and the aqueous phase was extracted with *n*-hexane (3 × 50 mL). The combined organic phases were dried over anhydrous $MgSO_4$, filtered, and concentrated under reduced pressure to yield the crude product as an off-white solid. The crude product was purified by crystallization using methanol at −25 °C, yielding 1.093 g (4.4 mmol, 55% over two steps) of **3a** as a colorless solid.

^1H NMR (400 MHz, $CDCl_3$), 1,4-**3a**: δ 6.11 (s, 2H), 5.99−5.84 (m, 2H), 5.73 (q, J = 2.8 Hz, 2H), 0.07 (s, 18H).

^1H NMR (400 MHz, $CDCl_3$), 1,6-**3a**: δ 5.99−5.84 (m, 6H), 0.08 (s, 18H).

$^{13}C\{^1H\}$ NMR (100 MHz, $CDCl_3$): δ 149.3, 148.8, 139.6, 138.4, 134.2, 132.9, 132.3, 129.3, −1.4, −1.6.

HRMS (APCI-TOF) m/z: $[M + H]^+$ calcd for $C_{14}H_{24}Si_2$, 249.1494; found, 249.1487.

Di(silyl)cyclooctatetraenes (3).[37−41] With the exception of di-(trimethylsilyl)cyclooctatetraene **3a**, all cyclooctatetraenes were prepared according to the following general procedure: a 0.25 M solution of the corresponding 5,8-di(silyl)cycloocta-1,3,6-triene **2** in THF was prepared and cooled to −50 °C. While stirring, 2.2 equiv of *n*-butyllithium (2.5 M in hexanes) was added dropwise. After stirring for 15 min at −50 °C, the reaction mixture was allowed to reach 0 °C by replacing the liquid nitrogen−acetone cooling bath with an ice-water cooling bath. Stirring of the deep red solution was continued for 2 h at 0 °C before cooling the solution to −30 °C. Upon complete addition of 1.1 equivalents of elemental iodine at −30 °C in small portions, the color of the solution faded completely. The reaction mixture was stirred for another 15 min before quenching was carried out with 20 mL of a saturated aqueous Na_2SO_3 solution. Phases were separated, and the aqueous phase was extracted with *n*-hexane (3 × 50 mL). The combined organic phases were dried over anhydrous $MgSO_4$, filtered, and concentrated under reduced pressure to yield the corresponding crude products as either off-white oils or solids. The di(silyl)cyclooctatetraenes were purified either by trituration with cold methanol (−20 °C) or by silica flash column chromatography eluting with *n*-hexane or a 10:1 mixture of *n*-hexane and ethyl acetate (di(TPS)cyclooctatetraene **3g**).

Di(TES)cyclooctatetraene (3b). 3.16 mL (14 mmol, 1.75 equiv) of triethylsilyl triflate was utilized according to the general procedure described above for the preparation of 5,8-di(silyl)cycloocta-1,3,6-trienes (**2**). 1.686 g (5.0 mmol) of 5,8-di(TES)cycloocta-1,3,6-triene **2b** was obtained as a colorless oil. Compound **2b** was dissolved in 20 mL of THF and subsequently treated as in the general procedure for the preparation of di(silyl)cyclooctatetraenes (**3**) described above. 4.43 mL (11 mmol) of 2.5 M *n*-butyllithium in hexanes and 1.404 g (5.5 mmol) of elemental iodine were utilized for the preparation of di(TES)cyclooctatetraene (**3b**). After purification by flash column chromatography, 1.408 g (4.2 mmol, 53%) of **3b** was obtained as a colorless oil.

^1H NMR (400 MHz, $CDCl_3$), 1,4-**3b**: δ 6.09 (s, 2H), 5.96−5.79 (m, 2H), 5.69 (q, J = 2.8 Hz, 2H), 0.98−0.89 (m, 18H), 0.65−0.52 (m, 12H).

^1H NMR (400 MHz, $CDCl_3$), 1,6-**3b**: δ 5.96−5.79 (m, 6H), 0.98−0.89 (m, 18H), 0.65−0.52 (m, 12H).

$^{13}C\{^1H\}$ NMR (100 MHz, $CDCl_3$): δ 146.0, 145.2, 141.2, 139.9, 135.0, 132.9, 132.6, 128.8, 7.6, 7.5, 3.1, 3.0.

https://doi.org/10.1021/acs.joc.1c03103
J. Org. Chem. 2022, 87, 4670−4679

HRMS (APCI-TOF) m/z: $[M + H]^+$ calcd for $C_{20}H_{36}Si_2$, 333.2434; found, 333.2427.

*Di(TIBS)cyclooctatetraene (**3c**).* Tri(isobutyl)silyl triflate (**6**) was utilized according to the general procedure described above for the preparation of 5,8-di(silyl)cycloocta-1,3,6-trienes (**2**). 2.495 g (5.0 mmol) of 5,8-di(TIBS)cycloocta-1,3,6-triene **2c** was obtained as a colorless oil. Compound **2c** was dissolved in 20 mL of THF and subsequently treated as in the general procedure for the preparation of di(silyl)cyclooctatetraenes (**3**) described above. 4.40 mL (11 mmol) of 2.5 M *n*-butyllithium in hexanes and 1.385 g (5.5 mmol) of elemental iodine were utilized for the preparation of di(TES)-cyclooctatetraene (**3b**). After purification by flash column chromatography, 2.085 g (4.2 mmol, 52%) of **3c** was obtained as a colorless oil.

^{1}H NMR (400 MHz, $CDCl_3$), 1,4-**3c**: δ 6.05 (s, 2H), 5.93 (q, J = 2.7 Hz, 2H), 5.65 (q, J = 2.8 Hz, 2H), 1.86−1.74 (m, 6H), 0.96−0.90 (m, 36H), 0.69−0.54 (m, 12H).

^{1}H NMR (400 MHz, $CDCl_3$), 1,6-**3c**: δ 5.99 (s, 2H), 5.85 (s, 2H), 5.84 (s, 2H), 1.86−1.74 (m, 6H), 0.96−0.90 (m, 36H), 0.69−0.54 (m, 12H).

^{13}C{^{1}H} NMR (100 MHz, $CDCl_3$): δ 147.5, 146.6, 141.4, 140.3, 135.3, 132.9, 132.9, 129.2, 26.9, 26.8, 26.8, 26.7, 24.9, 24.9, 24.1, 23.7.

HRMS (APCI-TOF) m/z: $[M + H]^+$ calcd for $C_{32}H_{60}Si_2$, 501.4312; found, 501.4308.

*Di(TBDMS)cyclooctatetraene (**3d**).* 3.22 mL (14 mmol) of *tert*-butyldimethylsilyl triflate was utilized according to the general procedure described above for the preparation of 5,8-di(silyl)-cycloocta-1,3,6-trienes (**2**). 2.821 g (5.6 mmol) of 5,8-di(TBDMS)-cycloocta-1,3,6-triene **2d** was obtained as a colorless solid. Compound **2d** was dissolved in 22 mL of THF and subsequently treated as in the general procedure for the preparation of di(silyl)cyclooctatetraenes (**3**) described above. 4.93 mL (12 mmol) of 2.5 M *n*-butyllithium in hexanes and 1.570 g (6.2 mmol) of elemental iodine were utilized for the preparation of di(TBDMS)cyclooctatetraene (**3d**). After purification by trituration with cold methanol, 2.523 g (5.0 mmol, 63%) of **3d** was obtained as a colorless solid.

^{1}H NMR (400 MHz, $CDCl_3$), 1,4-**3d**: δ 6.10 (s, 2H), 6.01−5.84 (m, 2H), 5.68 (q, J = 2.8 Hz, 2H), 0.90 (s, 18H), 0.08−0.01 (m, 12H).

^{1}H NMR (400 MHz, $CDCl_3$), 1,6-**3d**: δ 6.01−5.84 (m, 6H), 0.89 (s, 18H), 0.08−0.01 (m, 12H).

^{13}C{^{1}H} NMR (100 MHz, $CDCl_3$): δ 146.6, 145.9, 141.8, 140.9, 136.0, 133.2, 132.9, 128.8, 27.0, 27.0, 17.4, 17.2, −5.6, −5.7, −5.7, −6.2.

HRMS (APCI-TOF) m/z: $[M + H]^+$ calcd for $C_{20}H_{36}Si_2$, 333.2434; found, 333.2428.

*Di(TIPS)cyclooctatetraene (**3e**).* 3.76 mL (14 mmol) of triisopropylsilyl triflate was utilized according to the general procedure described above for the preparation of 5,8-di(silyl)-cycloocta-1,3,6-trienes (**2**). 2.113 g (5.0 mmol) of 5,8-di(TIPS)-cycloocta-1,3,6-triene **2e** was obtained as a colorless solid. Compound **2e** was dissolved in 20 mL of THF and subsequently treated as in the general procedure for the preparation of di(silyl)cyclooctatetraenes (**3**) described above. 4.43 mL (11 mmol) of 2.5 M *n*-butyllithium in hexanes and 1.412 g (5.5 mmol) of elemental iodine were utilized for the preparation of di(TIPS)cyclooctatetraene (**3e**). After purification by trituration with cold methanol, 1.650 g (4.0 mmol, 50%) of **3e** was obtained as a colorless solid.

^{1}H NMR (400 MHz, $CDCl_3$), 1,4-**3e**: δ 6.11 (s, 2H), 6.03−5.83 (m, 2H), 5.67 (q, J = 2.8 Hz, 2H), 1.15−1.01 (m, 42H).

^{1}H NMR (400 MHz, $CDCl_3$), 1,6-**3e**: δ 6.03−5.83 (m, 6H), 1.15−1.01 (m, 42H).

^{13}C{^{1}H} NMR (100 MHz, $CDCl_3$): δ 144.3, 142.6, 142.2, 141.9, 136.6, 133.5, 132.8, 128.5, 19.0, 19.0, 18.8, 18.7, 11.4, 11.2.

HRMS (APCI-TOF) m/z: $[M + H]^+$ calcd for $C_{26}H_{48}Si_2$, 417.3373; found, 417.3368.

*Di(TTMSS)cyclooctatetraene (**3f**).* Tris(trimethylsilyl)silyl triflate (**5**) was utilized according to the general procedure described above for the preparation of 5,8-di(silyl)cycloocta-1,3,6-trienes (**2**). 2.872 g (4.8 mmol) of 5,8-di(TTMSS)cycloocta-1,3,6-triene **2f** was obtained as a colorless solid. Compound **2f** was dissolved in 19 mL of THF and subsequently treated as in the general procedure for the preparation of di(silyl)cyclooctatetraenes (**3**) described above. 4.22 mL (10 mmol) of 2.5 M *n*-butyllithium in hexanes and 1.328 g (5.3 mmol) of elemental iodine were utilized for the preparation of di(TTMSS)-cyclooctatetraene (**3f**). After purification by trituration with cold methanol, 2.295 g (3.8 mmol, 48%) of **3f** was obtained as a colorless solid.

^{1}H NMR (400 MHz, $CDCl_3$), 1,4-**3f**: δ 6.01 (s, 2H), 5.89 (q, J = 2.8 Hz, 2H), 5.59 (q, J = 2.8 Hz, 2H), 0.21−0.17 (m, 54H).

^{13}C{^{1}H} NMR (100 MHz, $CDCl_3$): δ 142.2, 141.4, 138.2, 126.9, 1.5.

HRMS (APCI-TOF) m/z: $[M + H]^+$ calcd for $C_{26}H_{60}Si_8$, 597.2927; found, 597.2924.

*Di(TPS)cyclooctatetraene (**3g**).* Triphenylsilyl triflate (**4**) was utilized according to the general procedure described above for the preparation of 5,8-di(silyl)cycloocta-1,3,6-trienes (**2**). 1.391 g (2.2 mmol) of 5,8-di(TPS)cycloocta-1,3,6-triene **2g** was obtained as a colorless solid. Compound **2g** was dissolved in 9 mL of THF and subsequently treated as in the general procedure for the preparation of di(silyl)cyclooctatetraenes (**3**) described above. 1.96 mL (4.9 mmol) of 2.5 M *n*-butyllithium in hexanes and 0.631 g (2.5 mmol) of elemental iodine were utilized for the preparation of di(TPS)-cyclooctatetraene (**3g**). After purification by flash column chromatography (10:1 *n*-hexane and ethyl acetate), 0.638 g (1.0 mmol, 13%) of **3g** was obtained as a colorless solid.

^{1}H NMR (400 MHz, CD_2Cl_2), 1,4-**3g**: δ 7.61−7.25 (m, 30H), 6.24 (s, 2H), 6.10 (q, J = 2.8 Hz, 2H), 5.91−5.84 (m, 2H).

^{1}H NMR (400 MHz, CD_2Cl_2), 1,6-**3g**: δ 7.61−7.25 (m, 30H), 6.24 (s, 2H), 5.96 (s, 2H), 5.91−5.84 (m, 2H).

^{13}C{^{1}H} NMR (100 MHz, CD_2Cl_2): δ 147.2, 146.2, 143.6, 143.4, 136.7, 136.7, 135.9, 134.3, 134.1, 134.0, 133.6, 130.8, 130.0, 129.9, 128.3, 128.1.

HRMS (APCI-TOF) m/z: $[M + H]^+$ calcd for $C_{44}H_{37}Si_2$, 621.2434; found, 621.2427.

Computational Details. To compute the LD interactions, we utilized multiple tools recognized in the literature. We started our investigation with a conformer search in the gas-phase using the Conformer-Rotamer Ensemble Sampling Tool (crest) developed by Grimme et al.[63] The results for 1,6- and 1,4-disilyl-COT (the conformers lowest in energy) were further optimized with Gaussian16[64] in the gas phase using B3LYP,[42,43] B3LYP-D3(BJ),[27,44] M06-2X,[45] and ωB97X-D[46] in conjunction with the def2-SVPP and def2-TZVPP basis sets.[47] Hereby, the highest possible symmetry was employed (C_2 for 1,4-disilyl-COT and C_s/C_1 for 1,6-disilyl-COT). All structures were characterized as minima on the potential energy hypersurface. Additionally, single-point energy computations at the DLPNO-CCSD(T)/def2-TZVP level of theory[48,49] were performed on the B3LYP-D3(BJ)/def2-TZVPP optimized geometries. Tables S23−S28 summarize the results of the thermochemical analyses.

Homodesmotic (error-balancing) equations[50,51] were performed to estimate the strength of the intramolecular LD interactions. As described above, the crest program was utilized to identify all conformers lowest in energy, which were then optimized in the gas phase using B3LYP/def2-TZVPP including (GD3BJ) and excluding LD interactions. The dispersion energy was computed according to the following equation

$$E_{disp} = \sum E(\text{product}) - \text{D3(BJ)} - \sum E(\text{starting material}) - \text{D3(BJ)} - \sum E(\text{product}) - \sum E(\text{starting material})$$

Figures S13−S18 summarize the results of the homodesmotic equations.

A local energy decomposition[52−54] (LED) analysis was performed by using the Orca program[55] version 4.2.1. The B3LYP-D3(BJ)/def2-TZVPP-optimized geometries were utilized, and the molecules were split into fragments (F1−F3), which are defined in detail in the Supporting Information. The LED analysis was performed at DLPNO-CCSD(T)/def2-TZVP utilizing tight pair natural orbital

https://doi.org/10.1021/acs.joc.1c03103
J. Org. Chem. 2022, 87, 4670−4679

(TightPNO) settings. Tables S29−S34 summarize the results of the LED analyses of all silyl COT derivatives.

Finally, a scaled Symmetry-Adapted Perturbation Theory[56] (sSAPT) analysis was performed using the PSI4 program.[65,66] In order to isolate the interactions between the silyl groups, the molecular backbone of the COT balance was removed and the groups were saturated with hydrogens. A nonrelaxed dimer scan was performed at the sSAPT0/aug-*cc*-pVDZ level of theory. The empirical recipe for scaled SAPT0 was utilized in order to improve the performance according to Parker et al.[57] Tables S35−S40 and Figures S19−S24 summarize the results of the sSAPT analysis.

Visualizations of noncovalent interactions (NCI-plots[67]) were plotted as a reduced density gradient in regions of low electron density. The B3LYP-D3(BJ)/def2-TZVPP-optimized geometries were utilized for the visualization of noncovalent interactions. All plots were generated with NCIPLOT[68] and visualized with VMD.[69] The density cut-off of the reduced density gradient ($\rho(r)$ = −0.2 to +0.2 a.u.) and the color scale data range (−2 to +2 a.u.) were kept consistent throughout all NCI plots. Thereby, red isosurfaces indicate strongly repulsive interactions, green isosurfaces correspond to weak noncovalent contacts, and blue isosurfaces indicate strongly attractive interactions. Figures S25−S30 show all visualizations of 1,6- and 1,4-disilyl-COT.

■ ASSOCIATED CONTENT

Supporting Information

The Supporting Information is available free of charge at https://pubs.acs.org/doi/10.1021/acs.joc.1c03103.

^{1}H NMR and ^{13}C{^{1}H} NMR data for all molecular balances; error estimation for experimental data; single-crystal X-ray diffraction data; HRMS data; and computational details (PDF)

XYZ files for 1,6- and 1,4-cyclooctatetraene (ZIP)

Accession Codes

CCDC 2124606−2124607 contain the supplementary crystallographic data for this paper. These data can be obtained free of charge via www.ccdc.cam.ac.uk/data_request/cif, or by emailing data_request@ccdc.cam.ac.uk, or by contacting The Cambridge Crystallographic Data Centre, 12 Union Road, Cambridge CB2 1EZ, UK; fax: +44 1223 336033.

■ AUTHOR INFORMATION

Corresponding Author

Peter R. Schreiner − *Institute of Organic Chemistry, Justus Liebig University, 35392 Giessen, Germany;* orcid.org/0000-0002-3608-5515; Email: prs@uni-giessen.de

Authors

Henrik F. König − *Institute of Organic Chemistry, Justus Liebig University, 35392 Giessen, Germany;* orcid.org/0000-0002-4246-6744

Lars Rummel − *Institute of Organic Chemistry, Justus Liebig University, 35392 Giessen, Germany;* orcid.org/0000-0002-3772-2109

Heike Hausmann − *Institute of Organic Chemistry, Justus Liebig University, 35392 Giessen, Germany*

Jonathan Becker − *Institute of Inorganic and Analytical Chemistry, Justus Liebig University, 35392 Giessen, Germany*

Jan M. Schümann − *Institute of Organic Chemistry, Justus Liebig University, 35392 Giessen, Germany;* orcid.org/0000-0001-7494-5603

Complete contact information is available at: https://pubs.acs.org/10.1021/acs.joc.1c03103

Author Contributions

[§]H.F.K. and L.R. contributed equally to this work.

Notes

The authors declare no competing financial interest.

■ ACKNOWLEDGMENTS

This work was supported by the priority program "Control of London Dispersion in Molecular Chemistry" (SPP1807) of the Deutsche Forschungsgemeinschaft.

■ DEDICATION

This paper is dedicated to the memory of Andrew Streitwieser who taught us so much about organic chemistry.

■ REFERENCES

(1) Greene, T. W.; Wuts, P. G. *Protective Groups in Organic Synthesis*; Wiley, 1991.

(2) Schelhaas, M.; Waldmann, H. Protecting Group Strategies in Organic Synthesis. *Angew. Chem., Int. Ed.* **1996**, *35*, 2056−2083.

(3) Nelson, T. D.; Crouch, R. D. Selective Deprotection of Silyl Ethers. *Synthesis* **1996**, *1996*, 1031−1069.

(4) Pedersen, C. M.; Marinescu, L. G.; Bols, M. Conformationally armed glycosyl donors: reactivity quantification, new donors and one pot reactions. *Chem. Commun.* **2008**, *21*, 2465−2467.

(5) Bols, M.; Pedersen, C. M. Silyl-protective groups influencing the reactivity and selectivity in glycosylations. *Beilstein J. Org. Chem.* **2017**, *13*, 93−105.

(6) Shimizu, N.; Naohide, T.; Sigefumi, Y.; Takahiko, I. Prediction of Structural Effects of Trialkylsilyl Groups on Reactivity toward Nucleophilic Displacement at Silicon. *Chem. Lett.* **1993**, *22*, 1807−1810.

(7) Eliel, E. L.; Satici, H. Conformational analysis of cyclohexyl silyl ethers. *J. Org. Chem.* **1994**, *59*, 688−689.

(8) Marzabadi, C. H.; Anderson, J. E.; Gonzalez-Outeirino, J.; Gaffney, P. R. J.; White, C. G. H.; Tocher, D. A.; Todaro, L. J. Why Are Silyl Ethers Conformationally Different from Alkyl Ethers? Chair−Chair Conformational Equilibria in Silyloxycyclohexanes and Their Dependence on the Substituents on Silicon. The Wider Roles of Eclipsing, of 1,3-Repulsive Steric Interactions, and of Attractive Steric Interactions. *J. Am. Chem. Soc.* **2003**, *125*, 15163−15173.

(9) London, F. Zur Theorie und Systematik der Molekularkräfte. *Z. Phys.* **1930**, *63*, 245−279.

(10) London, F. The General Theory of Molecular Forces. *Trans. Faraday Soc.* **1937**, *33*, 8b−26.

(11) Wagner, J. P.; Schreiner, P. R. London Dispersion in Molecular Chemistry—Reconsidering Steric Effects. *Angew. Chem., Int. Ed.* **2015**, *54*, 12274−12296.

(12) Liptrot, D. J.; Power, P. P. London dispersion forces in sterically crowded inorganic and organometallic molecules. *Nat. Chem. Rev.* **2017**, *1*, 0004.

(13) Schweighauser, L.; Strauss, M. A.; Bellotto, S.; Wegner, H. A. Attraction or Repulsion? London Dispersion Forces Control Azobenzene Switches. *Angew. Chem., Int. Ed.* **2015**, *54*, 13436−13439.

(14) Procházková, E.; Kolmer, A.; Ilgen, J.; Schwab, M.; Kaltschnee, L.; Fredersdorf, M.; Schmidts, V.; Wende, R. C.; Schreiner, P. R.; Thiele, C. M. Uncovering Key Structural Features of an Enantioselective Peptide-Catalyzed Acylation Utilizing Advanced NMR Techniques. *Angew. Chem., Int. Ed.* **2016**, *55*, 15754−15759.

(15) Hwang, J.; Li, P.; Smith, M. D.; Shimizu, K. D. Distance-Dependent Attractive and Repulsive Interactions of Bulky Alkyl Groups. *Angew. Chem., Int. Ed.* **2016**, *55*, 8086−8089.

(16) Lu, G.; Liu, R. Y.; Yang, Y.; Fang, C.; Lambrecht, D. S.; Buchwald, S. L.; Liu, P. Ligand−Substrate Dispersion Facilitates the Copper-Catalyzed Hydroamination of Unactivated Olefins. *J. Am. Chem. Soc.* **2017**, *139*, 16548−16555.

https://doi.org/10.1021/acs.joc.1c03103
J. Org. Chem. 2022, 87, 4670−4679

(17) Pollice, R.; Bot, M.; Kobylianskii, I. J.; Shenderovich, I.; Chen, P. Attenuation of London Dispersion in Dichloromethane Solutions. *J. Am. Chem. Soc.* **2017**, *139*, 13126−13140.
(18) Eschmann, C.; Song, L.; Schreiner, P. R. London Dispersion Interactions Rather than Steric Hindrance Determine the Enantioselectivity of the Corey−Bakshi−Shibata Reduction. *Angew. Chem., Int. Ed.* **2021**, *60*, 4823−4832.
(19) Singha, S.; Buchsteiner, M.; Bistoni, G.; Goddard, R.; Fürstner, A. A New Ligand Design Based on London Dispersion Empowers Chiral Bismuth−Rhodium Paddlewheel Catalysts. *J. Am. Chem. Soc.* **2021**, *143*, 5666−5673.
(20) Gomberg, M. Triphenylmethyl, ein Fall von dreiwerthigem Kohlenstoff. *Ber. Dtsch. Chem. Ges.* **1900**, *33*, 3150−3163.
(21) Gomberg, M.; Carbon, A. I. O. T. An Instance of Trivalent Carbon: Triphenylmethyl. *J. Am. Chem. Soc.* **1900**, *22*, 757−771.
(22) Grimme, S.; Schreiner, P. R. Steric Crowding Can Stabilize a Labile Molecule: Solving the Hexaphenylethane Riddle. *Angew. Chem., Int. Ed.* **2011**, *50*, 12639−12642.
(23) Rösel, S.; Balestrieri, C.; Schreiner, P. R. Sizing the role of London dispersion in the dissociation of all-meta tert-butyl hexaphenylethane. *Chem. Sci.* **2017**, *8*, 405−410.
(24) Schreiner, P. R.; Chernish, L. V.; Gunchenko, P. A.; Tikhonchuk, E. Y.; Hausmann, H.; Serafin, M.; Schlecht, S.; Dahl, J. E. P.; Carlson, R. M. K.; Fokin, A. A. Overcoming lability of extremely long alkane carbon−carbon bonds through dispersion forces. *Nature* **2011**, *477*, 308−311.
(25) Xi, Y.; Su, B.; Qi, X.; Pedram, S.; Liu, P.; Hartwig, J. F. Application of Trimethylgermanyl-Substituted Bisphosphine Ligands with Enhanced Dispersion Interactions to Copper-Catalyzed Hydroboration of Disubstituted Alkenes. *J. Am. Chem. Soc.* **2020**, *142*, 18213−18222.
(26) Grimme, S.; Huenerbein, R.; Ehrlich, S. On the Importance of the Dispersion Energy for the Thermodynamic Stability of Molecules. *ChemPhysChem* **2011**, *12*, 1258−1261.
(27) Grimme, S.; Ehrlich, S.; Goerigk, L. Effect of the damping function in dispersion corrected density functional theory. *J. Comput. Chem.* **2011**, *32*, 1456−1465.
(28) Schümann, J. M.; Wagner, J. P.; Eckhardt, A. K.; Quanz, H.; Schreiner, P. R. Intramolecular London Dispersion Interactions Do Not Cancel in Solution. *J. Am. Chem. Soc.* **2021**, *143*, 41−45.
(29) Miller, M. J.; Lyttle, M. H.; Streitwieser, A., Jr tert-Butyl-substituted cyclooctatetraenes. *J. Org. Chem.* **1981**, *46*, 1977−1984.
(30) Wenthold, P. G.; Hrovat, D. A.; Borden, W. T.; Lineberger, W. C. Transition-State Spectroscopy of Cyclooctatetraene. *Science* **1996**, *272*, 1456−1459.
(31) Castaño, O.; Palmeiro, R.; Frutos, L. M.; Luisandrés, J. Role of bifurcation in the bond shifting of cyclooctatetraene. *J. Comput. Chem.* **2002**, *23*, 732−736.
(32) Lyttle, M. H.; Streitwieser, A., Jr; Kluttz, R. Q. Unusual equilibrium between 1, 4-and 1, 6-di-tert-butylcyclooctatetraenes. *J. Am. Chem. Soc.* **1981**, *103*, 3232−3233.
(33) Paquette, L. A.; Hefferon, G. J.; Samodral, R.; Hanzawa, Y. Bond fixation in annulenes. 14. Synthesis of and bond shifting equilibrium between 1, 4-and 1, 6-di-tert-butylcyclooctatetraenes. *J. Org. Chem.* **1983**, *48*, 1262−1266.
(34) Anderson, J. E.; Kirsch, P. A. Structural equilibria determined by attractive steric interactions. 1,6-Dialkylcyclooctatetraenes and their bond-shift and ring inversion investigated by dynamic NMR spectroscopy and molecular mechanics calculations. *J. Chem. Soc., Perkin Trans. 1* **1992**, *2*, 1951−1957.
(35) Allinger, N. L.; Frierson, M.; Van-Catledge, F. A. The importance of van der Waals attractions in determining the equilibrium between 1, 4-and 1, 6-dialkylcyclooctatetraenes. *J. Am. Chem. Soc.* **1982**, *104*, 4592−4593.
(36) Tosi, C. A quantum mechanical study of the equilibrium between 1,4- and 1,6-dialkylcyclooctatetraenes. *J. Comput. Chem.* **1984**, *5*, 248−251.
(37) Burton, N. C.; Cloke, F. G. N.; Joseph, S. C. P.; Karamallakis, H.; Sameh, A. A. Trimethylsilyl derivatives of cyclooctatetraene. *J. Organomet. Chem.* **1993**, *462*, 39−43.
(38) Parry, J. S.; Coles, S. J.; Hursthouse, M. B. Synthesis and Characterization of the First Sandwich Complex of Trivalent Thorium: A Structural Comparison with the Uranium Analogue. *J. Am. Chem. Soc.* **1999**, *121*, 6867−6871.
(39) Summerscales, O. T.; Cloke, F. G. N.; Hitchcock, P. B.; Green, J. C.; Hazari, N. Reductive Cyclotetramerization of CO to Squarate by a U(III) Complex: The X-ray Crystal Structure of $[(U(\eta\text{-}C_8H_6\{Si^iPr_3\text{-}1,4\}_2)(\eta\text{-}C_5Me_4H)]_2(\mu\text{-}\eta^2\text{:}\ \eta^2\text{-}C_4O_4)$. *J. Am. Chem. Soc.* **2006**, *128*, 9602−9603.
(40) Lorenz, V.; Schmiege, B. M.; Hrib, C. G.; Ziller, J. W.; Edelmann, A.; Blaurock, S.; Evans, W. J.; Edelmann, F. T. Unprecedented Bending and Rearrangement of f-Element Sandwich Complexes Induced by Superbulky Cyclooctatetraenide Ligands. *J. Am. Chem. Soc.* **2011**, *133*, 1257−1259.
(41) Lorenz, V.; Liebing, P.; Rausch, J.; Blaurock, S.; Hrib, C. G.; Hilfert, L.; Edelmann, F. T. Preparation and crystal structures of silyl-substituted potassium cyclooctatetraenides. *J. Organomet. Chem.* **2018**, *857*, 38−44.
(42) Lee, C.; Yang, W.; Parr, R. G. Development of the Colle-Salvetti correlation-energy formula into a functional of the electron density. *Phys. Rev. B: Condens. Matter Mater. Phys.* **1988**, *37*, 785−789.
(43) Becke, A. D. Density-functional thermochemistry. III. The role of exact exchange. *J. Chem. Phys.* **1993**, *98*, 5648−5652.
(44) Grimme, S.; Antony, J.; Ehrlich, S.; Krieg, H. A consistent and accurate ab initio parametrization of density functional dispersion correction (DFT-D) for the 94 elements H-Pu. *J. Chem. Phys.* **2010**, *132*, 154104.
(45) Zhao, Y.; Truhlar, D. G. The M06 suite of density functionals for main group thermochemistry, thermochemical kinetics, noncovalent interactions, excited states, and transition elements: two new functionals and systematic testing of four M06-class functionals and 12 other functionals. *Theor. Chem. Acc.* **2008**, *120*, 215−241.
(46) Chai, J.-D.; Head-Gordon, M. Long-range corrected hybrid density functionals with damped atom−atom dispersion corrections. *Phys. Chem. Chem. Phys.* **2008**, *10*, 6615−6620.
(47) Schäfer, A.; Huber, C.; Ahlrichs, R. Fully optimized contracted Gaussian basis sets of triple zeta valence quality for atoms Li to Kr. *J. Chem. Phys.* **1994**, *100*, 5829−5835.
(48) Riplinger, C.; Neese, F. An efficient and near linear scaling pair natural orbital based local coupled cluster method. *J. Chem. Phys.* **2013**, *138*, 034106.
(49) Liakos, D. G.; Sparta, M.; Kesharwani, M. K.; Martin, J. M. L.; Neese, F. Exploring the Accuracy Limits of Local Pair Natural Orbital Coupled-Cluster Theory. *J. Chem. Theory Comput.* **2015**, *11*, 1525−1539.
(50) Wheeler, S. E.; Houk, K. N.; Schleyer, P. v. R.; Allen, W. D. A Hierarchy of Homodesmotic Reactions for Thermochemistry. *J. Am. Chem. Soc.* **2009**, *131*, 2547−2560.
(51) Wagner, J. P.; Schreiner, P. R. London Dispersion Decisively Contributes to the Thermodynamic Stability of Bulky NHC-Coordinated Main Group Compounds. *J. Chem. Theory Comput.* **2016**, *12*, 231−237.
(52) Schneider, W. B.; Bistoni, G.; Sparta, M.; Saitow, M.; Riplinger, C.; Auer, A. A.; Neese, F. Decomposition of Intermolecular Interaction Energies within the Local Pair Natural Orbital Coupled Cluster Framework. *J. Chem. Theory Comput.* **2016**, *12*, 4778−4792.
(53) Altun, A.; Neese, F.; Bistoni, G. Effect of Electron Correlation on Intermolecular Interactions: A Pair Natural Orbitals Coupled Cluster Based Local Energy Decomposition Study. *J. Chem. Theory Comput.* **2019**, *15*, 215−228.
(54) Altun, A.; Saitow, M.; Neese, F.; Bistoni, G. Local Energy Decomposition of Open-Shell Molecular Systems in the Domain-Based Local Pair Natural Orbital Coupled Cluster Framework. *J. Chem. Theory Comput.* **2019**, *15*, 1616−1632.
(55) Neese, F. The ORCA program system. *Wiley Interdiscip. Rev.: Comput. Mol. Sci.* **2012**, *2*, 73−78.

https://doi.org/10.1021/acs.joc.1c03103
J. Org. Chem. 2022, 87, 4670−4679

(56) Szalewicz, K. Symmetry-adapted perturbation theory of intermolecular forces. *Wiley Interdiscip. Rev.: Comput. Mol. Sci.* **2012**, *2*, 254−272.
(57) Parker, T. M.; Burns, L. A.; Parrish, R. M.; Ryno, A. G.; Sherrill, C. D. Levels of symmetry adapted perturbation theory (SAPT). I. Efficiency and performance for interaction energies. *J. Chem. Phys.* **2014**, *140*, 094106.
(58) Hwang, J.; Li, P.; Smith, M. D.; Warden, C. E.; Sirianni, D. A.; Vik, E. C.; Maier, J. M.; Yehl, C. J.; Sherrill, C. D.; Shimizu, K. D. Tipping the Balance between S-π and O-π Interactions. *J. Am. Chem. Soc.* **2018**, *140*, 13301−13307.
(59) Solel, E.; Ruth, M.; Schreiner, P. R. London Dispersion Helps Refine Steric A-Values: Dispersion Energy Donor Scales. *J. Am. Chem. Soc.* **2021**, *143*, 20837−20848.
(60) Tolman, C. A. Steric effects of phosphorus ligands in organometallic chemistry and homogeneous catalysis. *Chem. Rev.* **1977**, *77*, 313−348.
(61) Panek, J. S.; Prock, A.; Eriks, K.; Giering, W. P. Addition of carbenium ions to allylsilanes: interpretation of kinetic data via the quantitative analysis of ligand effects. *Organometallics* **1990**, *9*, 2175−2176.
(62) Weicker, S. A.; Stephan, D. W. Activation of Carbon Dioxide by Silyl Triflate-Based Frustrated Lewis Pairs. *Chem.—Eur. J.* **2015**, *21*, 13027−13034.
(63) Pracht, P.; Bohle, F.; Grimme, S. Automated exploration of the low-energy chemical space with fast quantum chemical methods. *Phys. Chem. Chem. Phys.* **2020**, *22*, 7169−7192.
(64) Frisch, M. J.; Trucks, G. W.; Schlegel, H. B.; Scuseria, G. E.; Robb, M. A.; Cheeseman, J. R.; Scalmani, G.; Barone, V.; Petersson, G. A.; Nakatsuji, H.; Li, X.; Caricato, M.; Marenich, A. V.; Bloino, J.; Janesko, B. G.; Gomperts, R.; Mennucci, B.; Hratchian, H. P.; Ortiz, J. V.; Izmaylov, A. F.; Sonnenberg, J. L.; Ding, F.; Lipparini, F.; Egidi, F.; Goings, J.; Peng, B.; Petrone, A.; Henderson, T.; Ranasinghe, D.; Zakrzewski, V. G.; Gao, J.; Rega, N.; Zheng, G.; Liang, W.; Hada, M.; Ehara, M.; Toyota, K.; Fukuda, R.; Hasegawa, J.; Ishida, M.; Nakajima, T.; Honda, Y.; Kitao, O.; Nakai, H.; Vreven, T.; Throssell, K.; Montgomery, J. A., Jr.; Peralta, J. E.; Ogliaro, F.; Bearpark, M. J.; Heyd, J. J.; Brothers, E. N.; Kudin, K. N.; Staroverov, V. N.; Keith, T. A.; Kobayashi, R.; Normand, J.; Raghavachari, K.; Rendell, A. P.; Burant, J. C.; Iyengar, S. S.; Tomasi, J.; Cossi, M.; Millam, J. M.; Klene, M.; Adamo, C.; Cammi, R.; Ochterski, J. W.; Martin, R. L.; Morokuma, K.; Farkas, O.; Foresman, J. B.; Fox, D. J. *Gaussian 16*, Rev. C. 01; Wallingford, CT, 2016.
(65) Turney, J. M.; Simmonett, A. C.; Parrish, R. M.; Hohenstein, E. G.; Evangelista, F. A.; Fermann, J. T.; Mintz, B. J.; Burns, L. A.; Wilke, J. J.; Abrams, M. L.; Russ, N. J.; Leininger, M. L.; Janssen, C. L.; Seidl, E. T.; Allen, W. D.; Schaefer, H. F.; King, R. A.; Valeev, E. F.; Sherrill, C. D.; Crawford, T. D. Psi4: an open-source ab initio electronic structure program. *Wiley Interdiscip. Rev.: Comput. Mol. Sci.* **2012**, *2*, 556−565.
(66) Parrish, R. M.; Burns, L. A.; Smith, D. G. A.; Simmonett, A. C.; DePrince, A. E.; Hohenstein, E. G.; Bozkaya, U.; Sokolov, A. Y.; Di Remigio, R.; Richard, R. M.; Gonthier, J. F.; James, A. M.; McAlexander, H. R.; Kumar, A.; Saitow, M.; Wang, X.; Pritchard, B. P.; Verma, P.; Schaefer, H. F.; Patkowski, K.; King, R. A.; Valeev, E. F.; Evangelista, F. A.; Turney, J. M.; Crawford, T. D.; Sherrill, C. D. Psi4 1.1: An Open-Source Electronic Structure Program Emphasizing Automation, Advanced Libraries, and Interoperability. *J. Chem. Theory Comput.* **2017**, *13*, 3185−3197.
(67) Johnson, E. R.; Keinan, S.; Mori-Sánchez, P.; Contreras-García, J.; Cohen, A. J.; Yang, W. Revealing Noncovalent Interactions. *J. Am. Chem. Soc.* **2010**, *132*, 6498−6506.
(68) Contreras-García, J.; Johnson, E. R.; Keinan, S.; Chaudret, R.; Piquemal, J.-P.; Beratan, D. N.; Yang, W. NCIPLOT: A Program for Plotting Noncovalent Interaction Regions. *J. Chem. Theory Comput.* **2011**, *7*, 625−632.
(69) Humphrey, W.; Dalke, A.; Schulten, K. VMD: Visual molecular dynamics. *J. Mol. Graph. Model.* **1996**, *14*, 33−38.

https://doi.org/10.1021/acs.joc.1c03103
J. Org. Chem. 2022, 87, 4670−4679

3.2 Hexaphenylditetrels – When longer Bonds Provide Higher Stability

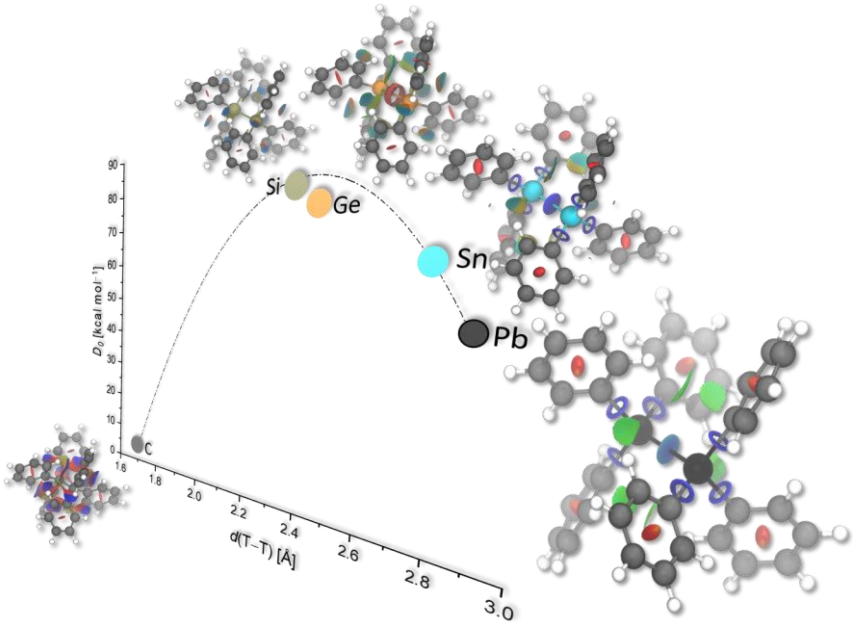

Abstract: *We present a computational analysis of hexaphenylethane derivatives with heavier tetrels comprising the central bond. In stark contrast to parent hexaphenylethane, the heavier tetrel derivatives can readily be prepared. In order to determine the origin of their apparent thermodynamic stability against dissociation as compared to the carbon case, we employed local energy decomposition analysis (LED) and symmetry-adapted perturbation theory (SAPT) at the DLPNO-CCSD(T)/def2-TZVP and sSAPT0/def2-TZVP levels of theory. We identified London dispersion (LD) interactions as the decisive factor for the molecular stability of heavier tetrel derivatives. This stability is made possible owing to the longer (than C–C) central bonds that move the phenyl groups out of the heavily repulsive regime so they can optimally benefit from LD interactions.*

Reference: Hexaphenylditetrels – When Longer Bonds Provide Higher Stability – L. Rummel, J. M. Schümann, and P. R. Schreiner, *Chem. Eur. J.* **2021**, *27*, 13699-13702. **DOI:** 10.1002/chem.202102271

Highlight: Hexaphenylditetrels – When Longer Bonds Provide Higher Stability, *Chemistry Views* **2021**

(https://www.chemistryviews.org/details/ezine/11318599/When_Longer_Bonds_Provide_Higher_Stability/)

Check for updates

Chemistry–A European Journal | Communication
doi.org/10.1002/chem.202102271

Chemistry Europe
European Chemical Societies Publishing

VIP Hexaphenylditetrels – When Longer Bonds Provide Higher Stability

Lars Rummel[+],[a] Jan M. Schümann[+],[a] and Peter R. Schreiner*[a]

Abstract: We present a computational analysis of hexaphenylethane derivatives with heavier tetrels comprising the central bond. In stark contrast to parent hexaphenylethane, the heavier tetrel derivatives can readily be prepared. In order to determine the origin of their apparent thermodynamic stability against dissociation as compared to the carbon case, we employed local energy decomposition analysis (LED) and symmetry-adapted perturbation theory (SAPT) at the DLPNO-CCSD(T)/def2-TZVP and sSAPT0/def2-TZVP levels of theory. We identified London dispersion (LD) interactions as the decisive factor for the molecular stability of heavier tetrel derivatives. This stability is made possible owing to the longer (than C–C) central bonds that move the phenyl groups out of the heavily repulsive regime so they can optimally benefit from LD interactions.

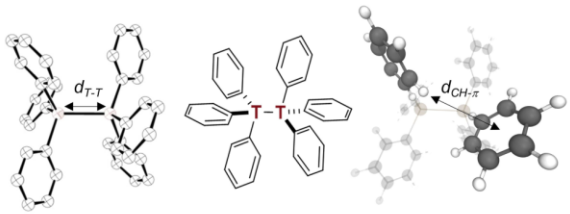

$d_{T\text{-}T}$ /Å	1T	$d_{CH\text{-}\pi}$ /Å
n.a. (1.70)	1C	n.a. (2.50)
n.a. (1.98)	1CSi	n.a. (2.63/2.98)
2.38 (2.35)	1Si	3.06 (3.04)
2.44 (2.44)	1Ge	3.23 (3.18)
2.77 (2.76)	1Sn	3.87 (3.68)
2.83 (2.88)	1Pb	3.71 (3.91)

Figure 1. S_6-symmetric hexaphenylditetrel structure **1T** (center), X-ray structure (left), and corresponding computed hexaphenylditetrel structure with highlighted $d_{CH-\pi}$ contact at B3LYP-D3(BJ)/def2-TZVP (right). First numbers are experimental distances, numbers in parentheses correspond to the computations.

While long sought-after hexaphenylethane[1] (**1C**, Figure 1, the letter T designates the tetrel) remains elusive[2] (trityl radicals dimerize in a head-to-tail fashion),[3] its higher tetrel congeners with T=CSi,[4] Si,[5] Ge,[6] Sn,[7] and Pb[8] have been known for a long time. What makes the latter stable under ambient conditions even though the higher tetrel-tetrel single bond energies decrease rapidly as one goes down group 14?

The Pb–Pb bond dissociation energy (BDE) of hexamethyldiplumbane is 22.5 kcal mol^{-1} lower than that of the central C–C bond in "hexamethylethane" (2,2,3,3-tetramethylbutane, BDE = 77.1 ± 1.0 kcal mol^{-1}),[9] in line with the expectations of bond energies down a group in the periodic table.[10] The opposite is observed for hexaphenylditetrels **1T** and parent **1C** has not been reported experimentally. Only some highly substituted derivatives utilizing dispersion energy donors[11] (DED) such as *t*butyl groups in the all-*meta* positions of **1C** can be observed,[2b,12] thereby emphasizing the notion of stabilizing London dispersion (LD) interactions.[13] As the higher tetrel derivatives do not need additional DED groups to be isolable, but intrinsically have higher T–T BDEs than **1C**, one asks what makes these compounds stable toward central T–T bond dissociation. Note that some derivatives with T=Sn are extraordinarily stable, even up to 235 °C.[14] The first equilibrium measurement of a **1Sn** derivative was with the phenyl groups equipped with 2,4,6-trimethyl and triethyl substituents. The onset of dissociation as measured through the presence of EPR signals of the "hetero-Gomberg-type" radicals was found at 180 and 100 °C for these derivatives, respectively.[15]

Even though there is no physical basis, there is a well-accepted principle in organic chemistry that longer bonds are assumed to be weaker and therefore dissociate more easily.[16] While this simple diatomic model-derived concept has been investigated and confirmed for large series of molecules, it cannot explain the discrepancy in thermodynamic stabilities of the hexaphenylditetrels **1T**. Especially for large structures (i.e., far beyond diatomics), the transferability of this concept is questionable.[17] Prominent examples are the phosphine-metal dissociation energies of Grubbs catalysts with sterically demanding N-heterocyclic carbene ligands[18] and 2-(1-diamantyl)-[121]tetramantane with a bond length of 1.71 Å but a sizeable BDE of around +36 kcal mol^{-1}.[19]

As studies highlight that the noncovalent van-der-Waals benzene dimers are stabilized by LD interactions,[20] we hypothesized that such interactions may be responsible for the

[a] L. Rummel,[+] J. M. Schümann,[+] Prof. Dr. P. R. Schreiner
Institute of Organic Chemistry
Justus Liebig University
Heinrich-Buff-Ring 17, 35392 Giessen (Germany)
E-mail: prs@uni-giessen.de

[+] These authors contributed equally to this work.

Supporting information for this article is available on the WWW under https://doi.org/10.1002/chem.202102271

Part of a Special Collection on Noncovalent Interactions.

Chemistry–A European Journal | Communication doi.org/10.1002/chem.202102271 | Chemistry Europe European Chemical Societies Publishing

stabilities of the higher **1T** structures as well. But why does this apparently not provide sufficient stabilization for **1C**?

We began our computational study with the crystal structure geometries for gas phase optimizations. Following the theoretical treatment of Rösel et al.[2b] we utilized the well-established B3LYP[21] and M06-2X[22] functionals for direct comparisons with existing data and because they are commonly employed. Ahlrich's def2-TZVP basis set[23] was used for all computations. B3LYP was used with the Becke-Johnson (BJ) damped dispersion D3 correction of Grimme et al.[24] First and foremost, the optimized structures are in good agreement with the experimental structures (Figure 1 and Figures S2–S5, Table S10). All phenyl moieties are arranged in an off-set T-shape manner with CH–π contacts with the opposite trityl group. The computed dimerization energy of the triphenylmethyl radical is endergonic ($\Delta G^{298}_{dim} = +11.8$ kcal mol^{-1}) and agrees with the results of previous studies.[2b] Both the B3LYP-D3(BJ) and M06-2X results show the same trends. Due to a lack of experimental dissociation energies for the unsubstituted **1T**, we validated our method by comparing dissociation energies of H_3T–TH_3 as well as Me_3T–TMe_3 that agree well with experimental values within their error bounds (Tables S1–S3, Figure S1).

Whereas the carbon-based hexaphenylditetrel readily dissociates into its monomers ($\Delta G^{298}_{dim} > 0$), the higher tetrel derivatives all display $\Delta G^{298}_{dim} < 0$ up to -70 kcal mol^{-1} (Figure 2). The reason behind the dissociation of **1C** can only be explained by Pauli (exchange) repulsion that has a very steep distance dependence, outweighing LD interactions, in line with the notion of excessive steric hindrance. Due to close intramolecular contacts of the aromatic moieties, hexaphenylethane **1C** cannot persist at 298 K (the computed shortest contact $d_{CH-\pi}$ in **1C** is around 2.5 Å). However, as higher tetrels display significantly longer central bonds, this leads to an increase of the CH–π contact distances (the computed $d_{CH-\pi}$ in **1Si** is around 3.1 Å, Figure 1). In comparison, the CH–π distance in the crystal lattice of benzene at 270 K is around 2.9 Å.[25]

To investigate the origin of the somewhat counterintuitive stabilities of the higher tetrel congeners, we visualized all intramolecular interactions using non-covalent interaction plots (NCI plots, Figure 3) for T = C vs. Pb.[26] Hereby, strongly attractive and repulsive interactions are visualized as blue and red isosurfaces, respectively. Green areas indicate weak molecular contacts predominantly evoked by LD interactions.

A comparison of the NCI-plots reveals strong repulsions (red) and strong attractions (blue) but no "weak" interactions (green) in **1C** between the two molecular halves. The opposite is observed for **1Pb** (with the same drawing cut-offs) that clearly shows a green isosurface orthogonal to the central bond, emanating from the phenyl substituents.

Another approach for assessing the LD contributions is through splitting the central tetrel bond and analyzing the interactions between the two resulting fragments via a Local Energy Decomposition (LED) analysis[27] as implemented in ORCA (Version 4.1.2).[28] As a consequence of this approach, two radical fragments interact at short range, resulting in large electrostatic interactions. Hence, in this analysis we focus only on the magnitude of the LD interactions evoked by three phenyl-phenyl CH–π contacts (Figure 4). According to this analysis, **1C** benefits from the highest LD contribution, while all higher congeners are LD-stabilized by a remarkably similar amount around 20 ± 5 kcal mol^{-1} for T ≠ C. That is, the instability of **1C** is not due to an insufficient LD stabilization but must lie in the massive growth of steric repulsion at short distance (see above). Vice versa, the lengthening of the central T–T bonds reduces Pauli repulsion more than dispersion so that an overall stabilization results.

In addition to the LED analysis, we utilized a homodesmotic equation[29] (Figure 5) to determine the overall relative thermodynamic stabilities of **1T**. Thereby, we aimed at isolating the amount of LD due to the three pairwise phenyl-phenyl contacts excluding the central tetrel interactions through calculating $\Delta\Delta E_{disp} = \Delta G$ (B3LYP-D3(BJ))-ΔG (B3LYP).

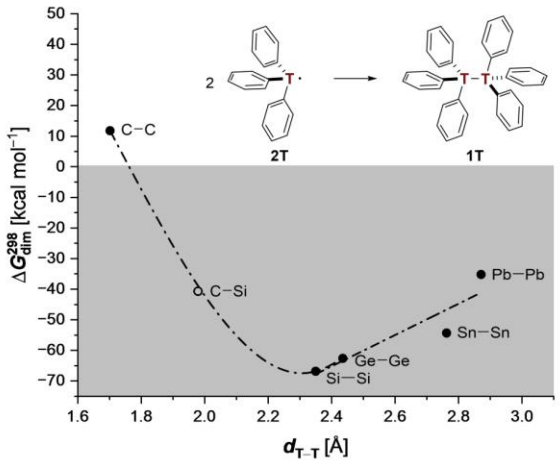

Figure 2. Correlation of distance d_{T-T} [Å] of the central tetrel bond with the computed Gibbs free energies ΔG^{298}_{dim} [kcal mol^{-1}] for the depicted dimerization reaction. Computations at the B3LYP-D3(BJ)/def2-TZVP level of theory. The dashed line is used to guide the eye.

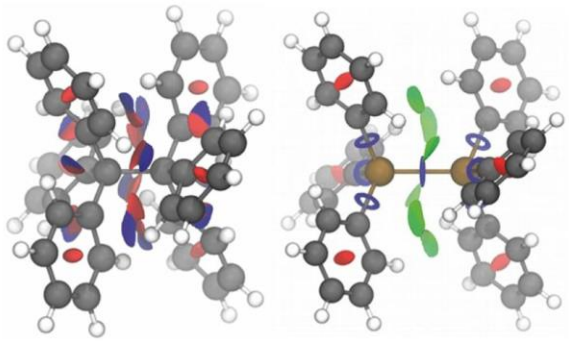

Figure 3. Non-covalent interaction (NCI) plots of hexaphenylethane **1C** (left) and the hexaphenyldiplumbane **1Pb** compound (right) at the B3LYP-D3(BJ)/def2-TZVP level of theory. Isosurfaces are colored on a blue-green-red scale according to an isovalue s(ρ) of 0.2, ranging from $\rho(r) = -2$ a.u. to $+2$ a.u. Blue indicates strong attractive interactions, green corresponds to weak NCI, and red indicates strong repulsion.

Chemistry–A European Journal | Communication doi.org/10.1002/chem.202102271 | Chemistry Europe European Chemical Societies Publishing

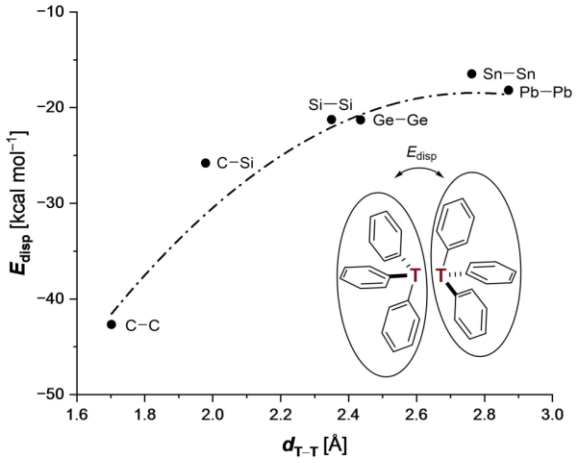

Figure 4. LED analysis of two trityl monomer singlet radicals in their dimer geometry at DLPNO-CCSD(T)/def2-TZVP//B3LYP-D3(BJ)/def2-TZVP. The dashed line is used to guide the eye.

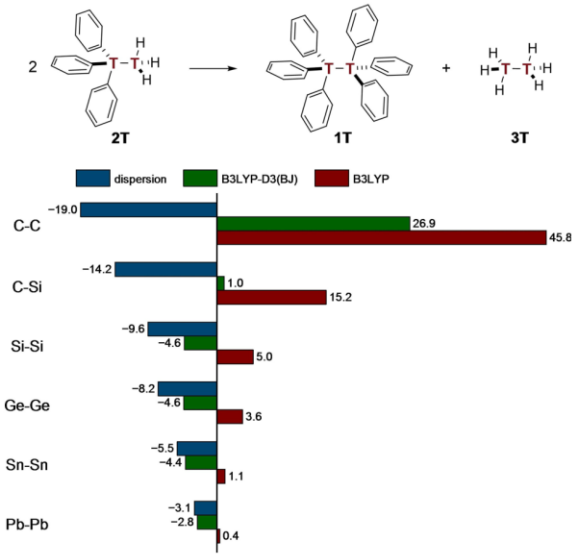

Figure 5. Homodesmotic equation with free energies (ΔG_{298}) given in kcal mol^{-1} at the B3LYP-D3(BJ)/def2-TZVP level of theory.

The DFT computations not including LD suggest that the presence of all six phenyl groups within one molecule (**1T**) is highly unfavorable relative to distributing them across two triphenylditetrels **2T**. This picture would support the widespread notion of the predominance of steric hindrance. The elongation of the central tetrel bond entails a rapid decrease in repulsive energy from ~46 kcal mol^{-1} in **1C** to only 0.4 kcal mol^{-1} in **1Pb**. Additionally, inclusion of LD, estimated from the value of the D3 correction, stabilizes all structures. Even though **1C** is stabilized most, LD cannot outbalance the strong repulsions, leading to an overall thermodynamically unstable structure. As repulsion reduces upon central bond elongation, all other tetrel derivatives beyond **1C** are stabilized overall. Whereas mixed **1CSi** is thermo-neutral in terms of LD and electron-electron repulsion, higher tetrel derivatives are stable due to LD that falls off less rapidly than Pauli repulsion. Consequently, LD interactions are most effective in the tetrel derivative with the longest bond (**1Pb**) where the total energy for this equation is comprised of 90% LD interactions.

As most recently demonstrated by Herbert and Carter-Fenk,[20c] LD interactions and Pauli repulsion are the dominant factor in the noncovalent dimerization process of two benzene molecules, with the electrostatic component essentially being sidelined.[20a,b,27a,30] Within the series of hexaphenylditetrels the phenyl moieties adopt an off-set T-shaped geometry to optimized these two dominant interactions. This supports our findings since **1Si** is the most stable hexaphenylditetrel with an off-set CH–π distance of 3.1 Å. In order to qualitatively evaluate the dispersion energy deriving from phenyl moieties, we also employed a symmetry-adapted perturbation theory (SAPT) analysis.[31] The scaled protocol was utilized to improve performance of the SAPT computations according to Parker et al.[32] Hereby, we focus on the interaction between benzene dimers.[33] We took the B3LYP-D3(BJ)/def2-TZVP optimized geometries, removed the tetrels, and saturated the resulting phenyl radicals with hydrogen atoms in order to avoid open-shell configurations[34] (Figure 6). The total interaction energy (black) shows an energy minimum at a central bond distance d_{Si-Si} of around 2.3 Å. The carbon derivative with a d_{C-C} of 1.7 Å is again the only thermodynamically unstable **1T** due to the large Pauli exchange repulsion term (red). All other structures are situated within the attractive part of the diagram. While LD interactions (green) are the main attractive component, electrostatics (blue) as well as induction (brown) also favor the dimerization process.

Our findings utilizing various interaction analyses and a homodesmotic equation are well in line with the conceptually simple but very useful r^{-12} repulsive and r^{-6} LD[13a] attractive (12,6)-Lennard-Jones type potential of the noncovalent inter-

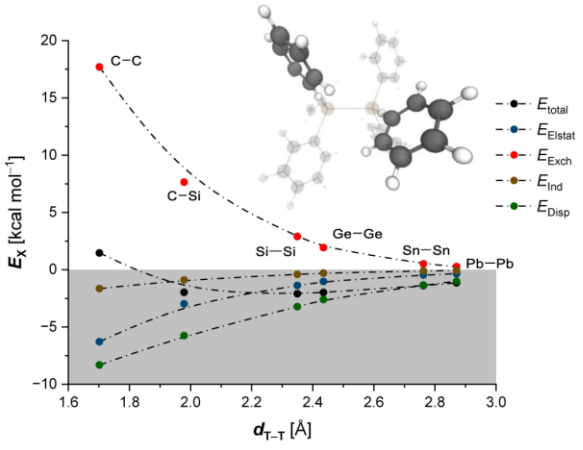

Figure 6. sSAPT analysis of two benzene monomers in geometry of the hexaphenylditetrels, d_{T-T} corresponds to the central tetrel bond. Computations at the sSAPT0/def2-TZVP level of theory.

Chemistry–A European Journal | Communication doi.org/10.1002/chem.202102271 | Chemistry Europe European Chemical Societies Publishing

action distance. The much steeper repulsive potential may have led to the general notion in structural chemistry that repulsion may be more important overall, which is not true. As a consequence, hexaphenyldisilane (**1Si**) is the most stable parent hexaphenylditetrel derivative.

As we demonstrate here, there is a fine interplay of attraction and repulsion in molecular structures; naturally, that is why they are called "equilibrium structures." As repulsion decreases rapidly with distance, LD is the most important stabilizing factor. The often invoked principle that longer bonds are to be weaker[16] does not have to be true[35] in the presence of additional interactions around the bonds in question. In the cases shown here this means that depending on the length of the central tetrel bond the phenyl groups can have a stabilizing or destabilizing effect on the structures. Hence, the high stability of the compounds with longer bonds is made possible through the assistance of LD interactions of the phenyl groups.

Acknowledgments

This work was supported by the priority program "Control of London Dispersion in Molecular Chemistry" (SPP1807) of the Deutsche Forschungsgemeinschaft. We thank Dennis Gerbig for technical assistance and Bastian Bernhardt for fruitful discussions. Open Access funding enabled and organized by Projekt DEAL.

Conflict of Interest

The authors declare no conflict of interest.

Keywords: bond dissociation energy · bond strength · C–H-π-interactions · London dispersion · Pauli repulsion

[1] a) M. Gomberg, *Ber. Dtsch. Chem. Ges.* **1900**, *33*, 3150–3163; b) M. Gomberg, *J. Am. Chem. Soc.* **1900**, *22*, 757–771.
[2] a) S. Grimme, P. R. Schreiner, *Angew. Chem. Int. Ed.* **2011**, *50*, 12639–12642; *Angew. Chem.* **2011**, *123*, 12849–12853; b) S. Rösel, C. Balestrieri, P. R. Schreiner, *Chem. Sci.* **2017**, *8*, 405–410.
[3] a) P. Jacobson, *Ber. Dtsch. Chem. Ges.* **1905**, *38*, 196–199; b) H. Lankamp, W. T. Nauta, C. MacLean, *Tetrahedron Lett.* **1968**, *9*, 249–254.
[4] A. Brook, H. Gilman, L. Miller, *J. Am. Chem. Soc.* **1953**, *75*, 4759–4765.
[5] a) W. Schlenk, J. Renning, G. Racky, *Ber. Dtsch. Chem. Ges.* **1911**, *44*, 1178–1182; b) H. Gilman, G. Dunn, *J. Am. Chem. Soc.* **1951**, *73*, 5077–5079; c) T. Bernert, B. Winkler, Y. Krysiak, L. Fink, M. Berger, E. Alig, L. Bayarjargal, V. Milman, L. Ehm, P. W. Stephens, N. Auner, H.-W. Lerner, *Cryst. Growth Des.* **2014**, *14*, 2937–2944.
[6] a) G. T. Morgan, H. D. K. Drew, *J. Chem. Soc. Trans.* **1925**, *127*, 1760–1768; b) P. Selwood, *J. Am. Chem. Soc.* **1939**, *61*, 3168–3169; c) M. Dräger, L. Ross, *Z. Anorg. Allg. Chem.* **1980**, *460*, 207–216.
[7] a) E. Krause, R. Becker, *Ber. Dtsch. Chem. Ges.* **1920**, *53*, 173–190; b) H. Morris, W. Byerly, P. Selwood, *J. Am. Chem. Soc.* **1942**, *64*, 1727–1729; c) H. Preut, H. J. Haupt, F. Huber, *Z. Anorg. Allg. Chem.* **1973**, *396*, 81–89; d) H. Piana, U. Kirchgäßner, U. Schubert, *Chem. Ber.* **1991**, *124*, 743–751; e) D. Dakternieks, F. Sheen Kuan, A. Duthie, E. R. T. Tiekink, *Main Group Met. Chem.* **2001**, *24*, 65–66; f) J. O. Bauer, *Main Group Met. Chem.* **2020**, *43*, 1–6.
[8] a) E. Krause, G. G. Reißaus, *Ber. Dtsch. Chem. Ges.* **1922**, *55*, 888–902; b) R. Preckel, P. Selwood, *J. Am. Chem. Soc.* **1940**, *62*, 2765–2766; c) H. Preut, H. Haupt, F. Huber, *Z. Anorg. Allg. Chem.* **1972**, *388*, 165–168; d) H. Preut, F. Huber, *Z. Anorg. Allg. Chem.* **1976**, *419*, 92–96.
[9] W. M. Haynes, *Handbook of Chemistry and Physics*, 97th ed. CRC Press., Cleveland, Ohio, **2016–2017**, p. 84.
[10] G. Frenking, S. Shaik, *The Chemical Bond: Chemical Bonding Across the Periodic Table*, Vol. 2, John Wiley & Sons, **2014**.
[11] S. Grimme, R. Huenerbein, S. Ehrlich, *ChemPhysChem* **2011**, *12*, 1258–1261.
[12] a) M. Stein, W. Winter, A. Rieker, *Angew. Chem. Int. Ed.* **1978**, *17*, 692–694; *Angew. Chem.* **1978**, *90*, 737–738; b) B. Kahr, D. Van Engen, K. Mislow, *J. Am. Chem. Soc.* **1986**, *108*, 8305–8307; c) S. Rösel, J. Becker, W. D. Allen, P. R. Schreiner, *J. Am. Chem. Soc.* **2018**, *140*, 14421–14432.
[13] a) F. London, *Z. Phys.* **1930**, *63*, 245–279; b) F. London, *Trans. Faraday Soc.* **1937**, *33*, 8b–26; c) J. P. Wagner, P. R. Schreiner, *Angew. Chem. Int. Ed.* **2015**, *54*, 12274–12296; *Angew. Chem.* **2015**, *127*, 12446–12471; d) D. J. Liptrot, P. P. Power, *Nat. Chem. Rev.* **2017**, *1*, 0004.
[14] E. J. Bulten, H. A. Budding, J. G. Noltes, *J. Organomet. Chem.* **1970**, *22*, C5-C6.
[15] a) H. U. Buschhaus, W. P. Neumann, *Angew. Chem. Int. Ed.* **1978**, *17*, 59–59; *Angew. Chem.* **1978**, *90*, 74–74; b) H.-U. Buschhaus, W. P. Neumann, T. Apoussidis, *Liebigs Ann. Chem.* **1981**, *1981*, 1190–1197.
[16] A. A. Zavitsas, *J. Phys. Chem. A* **2003**, *107*, 897–898.
[17] P. R. Schreiner, L. V. Chernish, P. A. Gunchenko, E. Y. Tikhonchuk, H. Hausmann, M. Serafin, S. Schlecht, J. E. P. Dahl, R. M. K. Carlson, A. A. Fokin, *Nature* **2011**, *477*, 308–311.
[18] Y. Zhao, D. G. Truhlar, *Org. Lett.* **2007**, *9*, 1967–1970.
[19] A. A. Fokin, L. V. Chernish, P. A. Gunchenko, E. Y. Tikhonchuk, H. Hausmann, M. Serafin, J. E. P. Dahl, R. M. K. Carlson, P. R. Schreiner, *J. Am. Chem. Soc.* **2012**, *134*, 13641–13650.
[20] a) M. O. Sinnokrot, C. D. Sherrill, *J. Phys. Chem. A* **2006**, *110*, 10656–10668; b) S. E. Wheeler, *J. Am. Chem. Soc.* **2011**, *133*, 10262–10274; c) K. Carter-Fenk, J. M. Herbert, *Chem. Sci.* **2020**, *11*, 6758–6765.
[21] a) A. D. Becke, *J. Chem. Phys.* **1993**, *98*, 5648–5652; b) C. Lee, W. Yang, R. Parr, *Phys. Rev. B* **1988**, *37*, 785–789.
[22] a) Y. Zhao, D. G. Truhlar, *Theor. Chem. Acc.* **2008**, *120*, 215–241; b) D. Josa, J. Rodríguez-Otero, E. M. Cabaleiro-Lago, M. Rellán-Piñeiro, *Chem. Phys. Lett.* **2013**, *557*, 170–175.
[23] A. Schäfer, C. Huber, R. Ahlrichs, *J. Chem. Phys.* **1994**, *100*, 5829–5835.
[24] a) S. Grimme, J. Antony, S. Ehrlich, H. Krieg, *J. Chem. Phys.* **2010**, *132*, 154104; b) S. Grimme, S. Ehrlich, L. Goerigk, *J. Comput. Chem.* **2011**, *32*, 1456–1465.
[25] a) E. G. Cox, J. A. S. Smith, *Nature* **1954**, *173*, 75–75; b) E. G. Cox, D. W. J. Cruickshank, J. A. S. Smith, *Proc. R. Soc. London Ser. A* **1958**, *247*, 1–21.
[26] a) E. R. Johnson, S. Keinan, P. Mori-Sánchez, J. Contreras-García, A. J. Cohen, W. Yang, *J. Am. Chem. Soc.* **2010**, *132*, 6498–6506; b) J. Contreras-García, E. R. Johnson, S. Keinan, R. Chaudret, J.-P. Piquemal, D. N. Beratan, W. Yang, *J. Chem. Theory Comput.* **2011**, *7*, 625–632.
[27] a) W. B. Schneider, G. Bistoni, M. Sparta, M. Saitow, C. Riplinger, A. A. Auer, F. Neese, *J. Chem. Theory Comput.* **2016**, *12*, 4778–4792; b) A. Altun, F. Neese, G. Bistoni, *J. Chem. Theory Comput.* **2018**, *15*, 215–228; c) A. Altun, M. Saitow, F. Neese, G. Bistoni, *J. Chem. Theory Comput.* **2019**, *15*, 1616–1632.
[28] a) F. Neese, *WIREs Comput. Mol. Sci.* **2012**, *2*, 73–78; b) F. Neese, *WIREs Comput. Mol. Sci.* **2018**, *8*, e1327.
[29] a) S. E. Wheeler, K. N. Houk, P. v. R. Schleyer, W. D. Allen, *J. Am. Chem. Soc.* **2009**, *131*, 2547–2560; b) J. P. Wagner, P. R. Schreiner, *J. Chem. Theory Comput.* **2016**, *12*, 231–237.
[30] M. Linnemannstöns, J. Schwabedissen, A. A. Schultz, B. Neumann, H.-G. Stammler, R. J. F. Berger, N. W. Mitzel, *Chem. Commun.* **2020**, *56*, 2252–2255.
[31] K. Szalewicz, *WIREs Comput. Mol. Sci.* **2012**, *2*, 254–272.
[32] T. M. Parker, L. A. Burns, R. M. Parrish, A. G. Ryno, C. D. Sherrill, *J. Chem. Phys.* **2014**, *140*, 094106.
[33] C. D. Sherrill, *Acc. Chem. Res.* **2013**, *46*, 1020–1028.
[34] J. Hwang, P. Li, M. D. Smith, C. E. Warden, D. A. Sirianni, E. C. Vik, J. M. Maier, C. J. Yehl, C. D. Sherrill, K. D. Shimizu, *J. Am. Chem. Soc.* **2018**, *140*, 13301–13307.
[35] M. Kaupp, B. Metz, H. Stoll, *Angew. Chem. Int. Ed.* **2000**, *39*, 4607–4609; *Angew. Chem.* **2000**, *112*, 4780–4782.

Manuscript received: June 25, 2021
Version of record online: August 6, 2021

"Give me insights, not numbers"

Charles Coulson